INFORMATION TO USERS

This manuscript has been reproduced from the microfilm master. UMI films the text directly from the original or copy submitted. Thus, some thesis and dissertation copies are in typewriter face, while others may be from any type of computer printer.

The quality of this reproduction is dependent upon the quality of the copy submitted. Broken or indistinct print, colored or poor quality illustrations and photographs, print bleedthrough, substandard margins, and improper alignment can adversely affect reproduction.

In the unlikely event that the author did not send UMI a complete manuscript and there are missing pages, these will be noted. Also, if unauthorized copyright material had to be removed, a note will indicate the deletion.

Oversize materials (e.g., maps, drawings, charts) are reproduced by sectioning the original, beginning at the upper left-hand corner and continuing from left to right in equal sections with small overlaps.

Photographs included in the original manuscript have been reproduced xerographically in this copy. Higher quality 6" x 9" black and white photographic prints are available for any photographs or illustrations appearing in this copy for an additional charge. Contact UMI directly to order.

COMPUTER AIDED REVERSE ENGINEERING OF
HUMAN TISSUES AND STRUCTURES

By

Kevin Dennis Creehan

B.S., Allegheny College, 1997

M.S. in I.E., University of Pittsburgh, 1999

Submitted to the Graduate Faculty

of the school of Engineering

in partial fulfillment of

the requirements for the degree of

Doctor

of

Philosophy

University of Pittsburgh

2001

The author grants permission
to reproduce single copies

Signed

COMMITTEE SIGNATURE PAGE

This dissertation was presented

by

Kevin Dennis Creehan

It was defended on

October 3, 2001

and approved by

(Signature)_____

Committee Chairperson

Bopaya Bidanda, Professor of Industrial Engineering

(Signature)_____

Committee Member

Jayant Rajgopal, Associate Professor of Industrial Engineering

(Signature)_____

Committee Member

Bartholomew Nnaji, Professor of Manufacturing Engineering

(Signature)_____

Committee Member

Harvey Wolfe, Professor of Industrial Engineering

(Signature)_____

Committee Member

Richard Debski, Assistant Professor of Orthopedic Surgery

ii

ACKNOWLEDGEMENTS

This dissertation is dedicated to my family. Without their unwavering support, its completion would have never been possible.

ABSTRACT

Signature _____

Bopaya Bidanda

COMPUTER AIDED REVERSE ENGINEERING OF HUMAN TISSUES AND STRUCTURES

Kevin Dennis Creehan, Ph.D.

University of Pittsburgh

In the past, collecting accurate geometric data of human body parts has been extremely difficult due to the flexibility of the items and their oddly shaped structures. Until the recent advancement of digitizing technologies, acquiring data points within small levels of precision has been nearly impossible. The rapid advancement of computer technology has given rise to numerous automated reverse engineering methods that utilize a broad range of technologies to acquire data. These technologies provide extremely precise three-dimensional geometric information of nearly any item. The objective of this study is to extend the applications of reverse engineering technology from manufacturing industries to the biomedical industry. By obtaining nearly exact

iv

geometric data of human body tissues and structures, in a high-speed and inexpensive manner, potentially groundbreaking research becomes possible for applications in injury rehabilitation, injury prevention, and strengthening. The primary advantage provided by scanning technologies is an improved quality of data. The completed objective of the research was to standardize the process of reverse engineering by developing detailed methodologies for reverse engineering human tissues and by developing algorithms to repair inevitable small data errors.

DESCRIPTORS

Reverse engineering	Repair algorithm
Digitizing	Traveling salesman problem
Laser scanning	Bezier curve
Human tissue	Scanning methodology

TABLE OF CONTENTS

vii

LIST OF FIGURES

x

LIST OF TABLES

1.0 INTRODUCTION

1.1 Problem Overview

Reverse engineering, the process by which an existing item is identically reproduced, becomes necessary when a physical prototype exists but accurate geometric data of the part does not. In order to recreate the existing part, a computerized (CAD) model of the part must be drawn or otherwise acquired. This CAD file provides the coordinates of multiple points on the product surface, which is then used to develop the drawing of the product for redesign or manufacturing. This data may then be analyzed within the CAD program, used to create a three-dimensional reconstruction of the part, or exported to a machine capable of rebuilding the new design, such as rapid prototyping equipment. Although the automatic regeneration of the CAD model without the time-consuming use of CAD software is merely a single step in the reverse engineering process, it has become the focus of the reverse engineering community due to the ongoing pursuit to acquire more accurate three-dimensional data in a faster and less expensive manner.

Collecting accurate geometric data of human tissues is complicated by the flexibility of the items and their numerous curves and odd shapes. Inexact data can be obtained using simple calipers, but the time required to gather the data becomes extensive and the results become susceptible to inevitable human error. Until the recent advancement of digitizing technologies, acquiring data points within small levels of precision has been nearly impossible.

1

Digitizing, or scanning, is the term used to describe the process of gathering information about an undefined three-dimensional surface. It is used in several fields of study, wherever there is a need to reproduce a complex free form shape.

The rapid advancement of computer technology has given rise to numerous automated reverse engineering methods that utilize a broad range of technologies to acquire data. These technologies provide extremely precise three-dimensional geometric information of nearly any item. Two of these technologies, contact scanning and laser scanning, have become increasingly popular in several manufacturing industries due to their speed, accuracy, and relatively low cost.

The objective of this research is to extend the applications of the innovative laser scanning technology from manufacturing industries to the biomedical industry. By obtaining high precision geometric data of human body parts, such as bones, tendons, and ligaments, in a high-speed and inexpensive manner, potentially groundbreaking research becomes possible for applications in injury rehabilitation, injury prevention, and strengthening. Previous applications of reverse engineering technologies in the biomedical community have dealt largely with prosthetic design and plastic surgery. This study would expand this research to include the aforementioned musculoskeletal applications.

1.2 Importance of This Problem

The medical community has used medical imaging techniques, such as Computed Tomography (CT), Magnetic Resonance Imaging (MRI), and Ultrasound Scanning (US)

2

for many years now. Similar to the contact and laser scanning processes, each of these methods provides cross-sectional images of the scanned human body part. But unlike the scanning processes, the aforementioned medical imaging techniques provide significant detail of the interior of the part. This quality explains why these technologies have been so important to the medical industry for so long, as they are capable of scanning living patients.

There is no debate concerning the relevance or significance of these medical imaging technologies. However, despite the advantages that the medical community has seen from these techniques, from a medical research standpoint, significant benefits would arise from the ability to easily obtain geometric data from these accurate new reverse engineering techniques.

The primary advantage provided by scanning technologies would be improved quality of the data. Laser scanning technologies are known to obtain repeatable results accurate to within 0.001 inch, a figure topped by only the contact scanning reverse engineering technology, a significantly faster method that has disadvantages with respect to its ability to scan all axes of any item, and the coordinate measuring technology, a similar contact method that would be inappropriate to use in this case due to its inferior speed and lack of flexibility.

Secondly, the time investment for the researcher and clinical practitioner would be greatly reduced. Using either of these scanning technologies requires very little user intervention until the data analysis stage. Conversely, once the CT or MRI is complete, the task of obtaining accurate geometric data just begins. Software that automatically

3

converts these medical images to an acceptable CAD package format, although they have improved significantly in recent years, sometimes has difficulty deciphering the borders of the body part in question due to the density of the surrounding tissues. In this case, the researcher must then go back to the CT or MRI images and manually obtain the point data by digitizing the outline of the structure. Manual digitizing leads to inaccuracy due to inevitable human error as well as the unnecessary additional time spent by the researcher.

Thirdly, the use of a scanner would reduce the current need for three-dimensional reconstruction software as reconstruction algorithms are already built into the scanning software programs. Currently, when a scan from a medical imaging technique is completed, the data is input to a software package that translates the two-dimensional slice data into a three-dimensional representation of the item. Significant research continues to be performed in this rapidly expanding topic of computer science to improve the existing reconstruction algorithms so that physicians and researchers have a better ability to see an accurate picture of their patients' troubles. However, because the use of medical imaging technologies on deceased specimens is unnecessary, as they can be dissected, the use of reconstruction software will also be unnecessary because the laser scanning technology will provide the medical researcher with an accurate three-dimensional representation that can be exported to many data file types, including CAD software.

And finally, the use of a scanning technology will usually provide a less expensive alternative to the medical imaging counterparts. The most intrusive barrier for

4

medical researchers is often the cost of using medical imaging techniques. High local demand with system availability in short supply will significantly increase the cost of using such systems. Also, operating costs are much lower for reverse engineering systems because they generally use standard electric current, have low maintenance costs, and do not require a licensed operator. Should the medical imaging services be as inexpensive and easy to use as the contact scanning or laser scanning technology, the need for implementing the scanning technologies into the medical industry would be significantly reduced. The problems posed by the other obstacles could be solved as the technology to obtain accurate surface data improves. Nevertheless, the cost of medical imaging remains significantly high compared to that of scanning technologies, which creates an opportunity for this technology to assist the medical research field.

1.3 Example of Research Importance

Shoulder injuries in athletics, especially throwing sports, are a rather common occurrence. The assessment and evaluation of shoulder problems requires a systematic approach that must be both comprehensive and efficient. The evaluation of shoulder injuries in athletes is a complex process that relies on accurate diagnosis before proper treatment can be successful. It is one of the most difficult areas of the body to assess given its complicated composition and structure and the considerable demands placed on it in overhand athletics [63]*.

---

* Bracketed references refer to the bibliography.

5

The shoulder joint actually consists of four joints: the scapulothoracic, sternoclavicular, acromioclavicular, and glenohumeral. The ball-and-socket joint is made up of three bones (scapula, humerus, and clavicle) and several major ligaments including: the glenohumeral, coracohumeral, coracoacromial, coracoclavicular, and acromioclavicular [40]. The complex joints are able to provide an extraordinary range of movements, but all at a substantially increased risk for injury [63]. For example, a National Collegiate Athletic Association study of the injuries suffered in intercollegiate competition showed that shoulder injuries accounted for the highest number of baseball injuries each year between 1985 and 1999 [45, 66]. Thus, increased diagnostic ability and rehabilitation knowledge could assist in limiting the rehabilitation time required for these numerous injuries, and would impact a large segment of the athletic population.

The primary goal of the researchers is to study joint motion, including the effects of the static and dynamic restraints at the glenohumeral joint [44]. The laboratory utilizes a shoulder testing apparatus, which has been developed over the past several years, to examine joint motion. In its use, "simulated muscle forces are used to produce joint motion through hydraulic cylinders while tendon excursions and six degree-of-freedom joint motions are recorded using a magnetic tracking device [44]." Other ongoing work in the laboratories includes the examination of the structural properties of the superior glenohumeral and coracohumeral ligaments, mechanical properties of the long head of the biceps tendon, and the examination of the length and orientation changes of the ligament at the glenohumeral joint. Further, the research has grown to include measurement and evaluation of strain in the glenohumeral ligaments during passive and

6

active motion and the determination of the different structures to joint stability during active motion using the shoulder testing apparatus [44].

Applications of this research to that at Musculoskeletal Research Center, such as the examination of the structural properties of the shoulder ligaments, and the examination of the length and orientation changes of the ligament at the glenohumeral joint are significant. Successful completion of this research will substantially benefit research in these areas, which in turn will benefit those rehabilitating shoulder injuries. The availability of extremely precise geometric data would allow these researchers to develop highly accurate virtual models of these shoulder structures and their motions. With these accurate models, the researchers could perform shoulder-testing procedures virtually, enabling them to add forces to the virtual model that would be unsafe or impossible to simulate on living specimens.

1.4 Research Overview

The goal of the research herein is to develop guidelines and methodologies for scanning human body parts that will assist medical researchers and reverse engineers alike. In order to do so completely and thoroughly, the research was conducted in the following three-step manner.

The first challenge of this study was to develop a thorough taxonomy of human tissues and structures based on traits such as shape, texture, tissue type, and curvature, which may affect the scanning parameters. Although two human body parts may be functionally very different, they may have similar characteristics with respect to scanning

7

parameters and thus should be scanned in very similar ways. As such, the guidelines for a medical researcher to follow need not be customized to each body part, but rather to each classification, or part family, with only occasional instructions for specific members of the category.

Once the taxonomy of body parts was complete, the research focused on developing a strict methodology for scanning each category. These methodologies detail the best manner in which the parts may be scanned, including the optimal scanning parameters and part configuration, with respect to the scan quality and speed, while also detailing potential trouble areas that may lead to poor scan quality or speed.

Finally, this research evaluated different techniques to repair an imperfect laser scan, such as interpolation algorithms that have been created by computer scientists investigating three-dimensional reconstruction. Several factors may adversely affect the quality of a laser scan. Generally, errors of this nature are not detected until the entire scanning process is complete and the editing process has begun. If an error has occurred, the researcher should not be forced to discard the entire scan, unless this problem is so large that it has terribly affected a large percentage of the scan. Rather, the researcher should have the ability to repair those imperfect portions of the scan, thus saving the time and costs of an additional scan. Significant research has been performed in this area with focus on three-dimensional reconstruction. Thus, the challenge for this project would be in identifying or developing the most appropriate algorithm, or set of algorithms, for the laser scanning data gathering process.

8

1.5 Contribution of the Research

Successful completion of this research project would impact the medical community primarily by providing access to substantially improved data quality, but also by reducing significantly the imaging cost and three-dimensional reconstruction time and cost associated with medical imaging. The use of scanning technologies will provide extremely precise three-dimensional geometric information for human tissues, such as bones, tendons, and ligaments, from which three-dimensional physical models may be created via rapid prototyping or three-dimensional reconstructions may be created by one of many software programs and reconstruction methods.

Access to improved data quality and excessive cost stemming from increased demand for medical imaging machinery has proven to be major obstacles for developing three-dimensional reconstructions of human tissues and structures. This research will confront the task of improving the access to high-quality data.

Significant study has been performed to determine the best practices for using medical imaging equipment to obtain the most accurate data. However, the random error associated with the medical imaging scanners themselves and the accompanying human digitization, which have been shown to range between five and ten thousandths of an inch, far exceed those obtained using advanced reverse engineering equipment, whose random error values are generally less than one thousandth of an inch [50,53]. Clearly the disadvantage of the reverse engineering systems is the inability to obtain internal data of the scanned item, and thus the inability to scan living patients. However, in the cases of medical research where data is collected from cadaver parts, and dissection is feasible,

9

the increased data quality available through reverse engineering technologies would be an attractive alternative to the current systems in use.

Costs of medical imaging vary based on the particular protocol used and the part of the body being scanned. These imaging methods are commonly used for diagnosis of various clinical symptoms rather than for medical research purposes. The tremendous utilization of medical imaging devices for clinical purposes and the initial overhead cost of the equipment leads to high imaging costs for research. Further, these are the costs for only a series of two-dimensional images, and do not include the additional cost of generating a three-dimensional reconstruction upon completion of the scan. These excessive scanning costs are unnecessary for many medical research applications, and their reduction could provide an enormous savings for many research applications. Use of reverse engineering scanning technologies for medical research purposes could be the first step in reducing these enormous costs.

This research provides the medical research and reverse engineering fields of study with a set of structured methodologies for using laser-scanning equipment. From an engineering perspective, this primary contribution details an application of reverse engineering by part family, rather than through the more typical job shop approach that requires developing application-specific methods using very general instructions and substantial operator influence. The factors presented in this methodology include part mounting and orientation, geometric considerations such as concavity, expected scan duration, and optimal parameter settings such as the scanning range and horizontal and vertical point spacing. Because these technologies are not widely used among medical

10

researchers, their future research burden will be reduced once more research applications of this technology are realized.

Additionally, this research provides guidelines, or a structured methodology, for all potential users of these scanners. At present, no structured methodology based on part families exists on any level for geometric data acquisition scanning equipment. All users of this equipment, such as those in the manufacturing community, could examine these methodologies and apply them to their specific need. For example, at present, each user relies on experience to determine scanning parameters that may or may not be optimal. This research will provide a framework for decision making for all researchers that would reduce or limit the human intervention in the scanning process that is considered essential today.

Finally, this research contributes to efforts made in repairing imperfect scan data. Imperfections occur throughout the data in every laser scan application for many reasons. Currently, visual estimation and user experiences are used to realign points that appear to be incorrect. By viewing point data from adjacent layers, the editor of the imperfect scanning data estimates the appropriate location of the stray point and replaces it based only on his or her experiences with the part itself and other editing tasks that they have performed in the past. The human element of this process can be reduced. This research develops a set of algorithms that, among other possible scanning imperfections, approximates the appropriate location of stray or missing points and relocates them by using several algorithms that have been developed herein or by researchers studying optimization, neural networks, and three-dimensional reconstruction.

11

1.6 Background

The environment in which this research was performed was relatively inexperienced with respect to scanning technologies in the biomedical community. The most significant amount of research had been performed with respect to CT or MRI data for geometric data acquisition, and most of this research had focused on potential applications to rapid prototyping (RP), or on creating a more accurate three-dimensional reconstruction. These technologies lend themselves to the RP industry because most RP technologies build the prototype in an additive, layer-by-layer construction, which is very similar to the manner in which CT, MRI, and many scanning technologies' data are collected. The challenge facing the RP industry has been to develop a straightforward way to translate CT or MRI data into the standard RP file type, a challenge that has already been solved by the scanning software for these technologies. The majority of recent research in the area of CT and MRI data with respect to rapid prototyping and reverse engineering has focused around this challenge. In fact, the popularity of rapid prototyping in the medical industry has blossomed to the point where several conferences have been held to promote its recent advancements and entice new research.

Also, several software packages, for example MedCAD by Materialise, have substantially improved their ability to translate medical data into a format easily readable by CAD packages and rapid prototyping systems. The CTM software by Materialise interpolates the medical slice data in very tiny layers, and interfaces directly with most RP systems. Because of this direct interface and its impressive interpolation algorithms, it has the ability to produce accurate models in a very short time. Advancements of this

12

nature have been prevalent throughout the rapid prototyping arena in recent years. The disadvantage of systems such as these is the lower accuracy levels attainable by the CT or MRI machines and thus the computer software, as opposed to scanning systems, which have the capability of finding repeatable geometric data accurate to within 0.001 inch, or better.

While much research has been done in the biomedical community using imaging techniques such as CT and MRI, little research has been conducted with respect to scanning technologies in the biomedical community. Nor has any research been performed to determine a structured methodology for scanning in general. At present, both scanning methods contain a "human element" for determining scan parameters. Each operator uses his/her personal experiences as a basis for parameter decision-making. At present, no structured methodology exists on any level for the use of geometric data acquisition laser scanning equipment.

1.7 Research Methodology

As previously mentioned, the research began by developing a thorough taxonomy of the human body parts that were studied. This taxonomy was not based on functionality, although similar functioning parts were in fact classified together in many cases. Rather, classifications were determined by geometric similarities such as shape, texture, tissue type, and curvature, all of which may affect scanning parameters. At this point a parallel between this research and the applications to other scanning uses may be shown. Although this research focused on the physiological parts, their geometric shapes

13

may be very similar to parts used for manufacturing applications. If so, the manufacturer may utilize the results of this research to implement into their own scanning methodology.

Upon completion of the taxonomy, the research turned to the development of strict methodologies for each classification of parts. Based on the scanning input variables previously noted, and the result variable, scan quality, the new task was to determine the optimal scanning parameters for each class of parts. In order to complete this task, multiple tests were needed for each classification. A statistical design of experiments was developed to determine the proper combinations of factor levels. Because the ranges of values of many of the scanning variables are real numbers, the number of possible levels for each variable was large. As the number of factors increase along with the levels for each factor, the size of the experimental procedure grows exponentially. As a result, the research experimentation procedure required substantial front-end decisions limiting the number of levels observed initially, and a fractional factorial design of experiments limiting the number of experiments needed to develop tangible results. Once the experiments were completed, the data was evaluated to determine the appropriate scanning parameters. From these conclusions, the methodology for each class of parts was derived.

Next, the research turned to the reconstruction of imperfect data files obtained via the laser scanning equipment. While performing the above portion of the research methodology, clues arose in the scanning process that shined light on how and why imperfect data files occur. By analyzing the scanning properties of the part at the time of

14

the imperfect scan, trends or similarities between events of imperfection became evident. In these cases, preventative information was included in the methodologies.

To complete the research, a study was conducted to determine the feasibility of implementing interpolation algorithms into the laser scanning software if the preventative predictors fail or do not exist. For example, there is often considerable doubt whether a point is accurate or astray. At present, the operator determines visually, and sometimes erroneously, if the point is accurate. This portion of the study would examine the possibility that the computer be able to detect and make the user aware of possible stray points based on built-in estimation algorithms. Furthermore, a set of algorithms was developed to facilitate the imperfect scan repair process. These algorithms provide the basis for the proper sequencing of raw data, the elimination of outlier, or stray points, and the insertion of missing points, or filling of holes, based on the location of neighboring data points. These algorithms, coupled with a curve fitting algorithm developed by other research and a comparison algorithm developed herein which compares completed layers of data with neighboring layers as an inspection, provides the capability of repairing imperfect scan data with minimal user intervention.

1.8 Summary of Research

In summary, the primary objective of this research is to standardize the processes of reverse engineering human tissues and structures so that technical expertise of reverse engineering equipment is unnecessary for further research to proceed. To accomplish this objective, two major goals must be completed, which are:

15

- To develop detailed scanning methodologies that describe the digitizing of human tissues based on part families, which are obtained through the development of a thorough taxonomy of the human musculoskeletal system.

- To develop a set of algorithms that quickly repairs the common imperfections of data obtained through the use of the laser scanning process.

2.0 LITERATURE REVIEW

2.1 Reverse Engineering

Reverse engineering, widely noted as an effective cost saving tool, is a systematic approach used to analyze the design of an existing device so that one may derive potential improvements to the device or perform competitive benchmarking to further understand the product [67]. Typically a manufacturing tool, the resulting information contributes to product evolution, either at the subsystem, configuration, component, or parametric levels, that will occur through redesign processes [68].

The origins of reverse engineering are largely unknown. Rather than having been developed at a specific period or moment in time, the concept of reverse engineering arose in an evolutionary manner [29]. It began as a way to "build a better mousetrap." As a design was developed, it would be critically assessed, examined, changed, and thus the design would inevitably be improved [29]. Today reverse engineering is used not as a tool to be employed to an existing problem, but as practical methodology to a new challenge [29].

Ingle [29] defines reverse engineering as "a four-stage process in the development of technical data to support the efficient use of capital resources and to increase productivity." These stages are:

- Data evaluation – visual inspection, dimensional inspection, quality evaluation, possible failure analysis

- Data generation – engineering drawings, technical data package

17

- Design verification – prototyping, model testing, model failure analysis, quality assurance

- Design implementation – prototype delivery, project summaries, economic analysis, final implementation

Wood and Otto [68,69] describe the following ten-step reverse engineering and redesign methodology that focuses on the process steps needed to understand and represent a current product [68].

Figure 2-1 The reverse engineering process as presented by Wood and Otto [68,69]
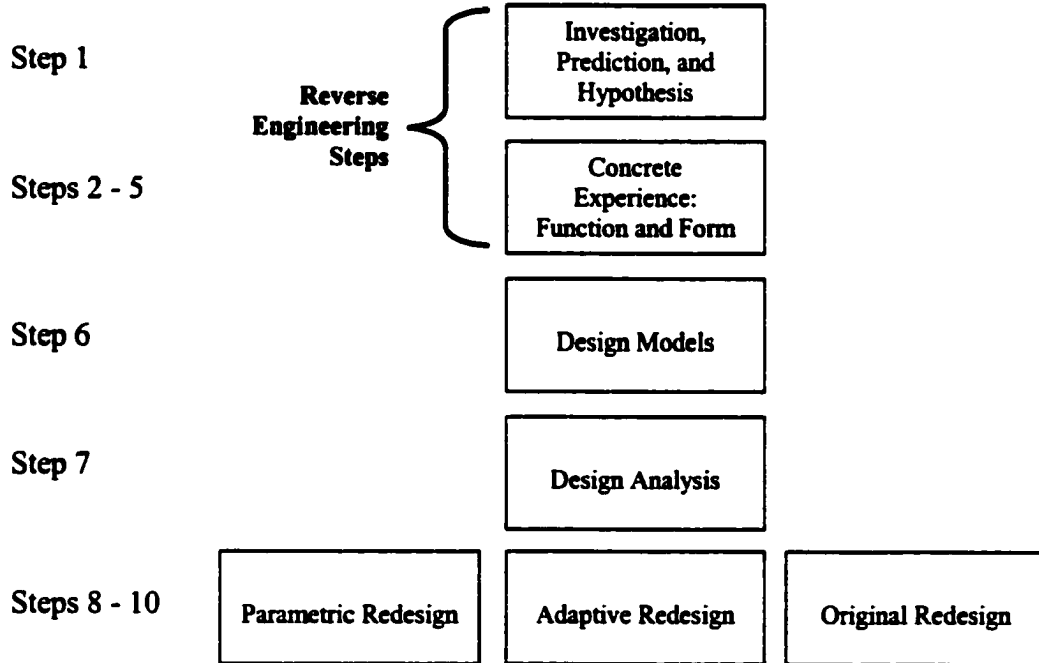
They explain that reverse engineering serves as a starting point in the product redesign process, during which the product is analyzed in terms of its functionality, physical principles, manufacture-ability, and assemble-ability, for the purpose of fully understanding every detail of the product [68]. However, to begin the reverse

18

engineering sequence, accurate geometric data from the surface of the existing part must be obtained [9].

In order to accurately recreate the existing part, a computerized (CAD) model of the part's geometry must be developed in some manner [9,10,11]. This CAD file provides the coordinates of multiple points on the product surface, which, in a manufacturing setting, is used to develop the drawing of the product for redesign or manufacturing. This data may then be analyzed and improved within the CAD program. The improved CAD design, along with other manufacturing information, is then used to create the manufacturing process plan and the Computer Numeric Control (CNC) tool path [11].

There are several different methods that can be employed to collect surface data. These methods can be broadly classified into two categories: contact and non-contact methods [9,10,11]. Contact methods, the more traditional manner of collecting data that has been utilized for several years, requires contact between the surface and a measuring device, usually a probe or stylus. Conversely, newer non-contact methods typically use light, or laser beams, as the main tool for deducing surface information.

Contact methods of reverse engineering have been available for nearly forty years [10]. The first, and still the most popular method of reverse engineering, to be introduced was the coordinate measuring machine (CMM). The CMM measures the surface of the object using a contact probe, a highly sensitive pressure-sensing device that is activated by any contact with an object. The linear distances from three axes to the position of the probe are ascertained, thus giving the x, y, and z coordinates of the surface.

19

Other contact methods of reverse engineering include electromagnetic digitizing and sonic digitizing [11]. Electromagnetic digitizers determine the surface data of non-metallic objects (placed in a magnetic field) by tracing a hand-held stylus containing a magnetic field sensor across the surface of the object. The magnetic field sensor, in conjunction with an electronic unit, detects the position and orientation of the stylus. The sonic digitizer uses sound waves to calculate the position of a point relative to a reference point. Again using a hand-held stylus tracing the surface, an ultrasonic impulse is emitted by the stylus and is detected by four microphones. The times taken to reach each of the four microphones are recorded and the computer calculates the x, y, and z coordinates from these time differences [11].

Non-contact techniques can be further classified into two additional categories: active and passive techniques [10]. Active techniques, organized into two subgroups, structured lighting and spot ranging, recover depth information after a light or ultrasonic source illuminates the object [11]. Structured lighting methods are classified according to the pattern of light that is used to illuminate the object, such as single light beam, single stripe of light, and patterned lighting [11]. Surface information is determined using triangulation procedures. Spot ranging techniques are generalized based on the source used, either optical-based or ultrasonic [10,11]. Both methods cast a beam onto the object surface and then inspect the reflected beam using a sensor that is placed coaxial to the source. The location of the source gives the two coordinate measurements of the surface point while the analysis of the reflected beam gives the third dimension [10,11]. The third coordinate is determined either by calculating the phase difference

20

between the incident and reflected light or by the time taken for the light to reflect back from the surface of the part [10,11]. Typically, it is more accurate to use a method that calculates the phase difference of the incident light rather than one that calculates the time of reflection because this calculation of the time of refection relies on sensitive, accurate timing devices [9].

Passive techniques, which are much less popular than the preceding examples, work with ambient light, and are divided into three categories: range from texture, range from focus, and stereo scanning [10].

Applications of reverse engineering in manufacturing are widespread. There are many instances where an existing part or prototype requires reproduction. Often a new product does not start from a CAD model but rather a prototype is built first [10]. Upon completion, the measurements of the new prototype are taken. Also, design changes are often required to an existing product for which CAD data does not exist. Numerous additional applications of reverse engineering in manufacturing exist and include: the design of large equipment whose measurements can not be taken using metrology, replacement of worn or broken parts for which CAD data is unavailable, and inspection of a produced part compared to its original CAD design [9].

Applications of the reverse engineering process in the biomedical community are similarly popular, although performed with different methods. For years, the medical community has used several non-invasive imaging devices to produce two-dimensional cross-section images of patients. As computer technology has grown software products have been developed that extract three-dimensional images from this data [60]. At this

21

point however, with only a few exceptions such as surgery planning and prosthesis milling, the similarities to a manufacturing-style reverse engineering and redesign methodology typically end. Comparing the current methods used by the medical community to the four reverse engineering and redesign stages described by Ingle [29], one can see a relationship between the manufacturing process Ingle described and the processes the medical community applies.

- Data evaluation – patient examination, preliminary diagnosis, etc.

- Data generation – development of medical image (MRI, CT, US, etc.)

- Design verification – 3-D computerized reconstruction, physical model generation

- Design implementation – final diagnosis, patient treatment, etc.

2.1.1 Contact Scanning

Currently, the best results in terms of accuracy and quality of surface finish are obtained using contact reverse engineering systems. Contact systems have several fundamental advantages over non-contact systems [54]:

- Treatment of surfaces to prevent reflections is not required

- Vertical faces can be accurately scanned

- Data density is not fixed and is automatically controlled by the shape of the component

- Time-consuming manual editing of the data to remove stray points is not required

22

- Post processing for cutting can be faster as surface offsetting may not be required

- Very tiny detail can be accurately replicated

Contact scanners are stand-alone scanning systems with these advantages and are evaluated based on additional qualities that separate themselves from other systems of this type. For example, those systems that require very low probing forces, which provides the ability to accurately scan of delicate materials, and are able to utilize extremely small styli (0.3mm), which allows the scanning of very fine detail, are the most commonly used systems [54]. Other advantages of using the contact scanning systems are their quiet and clean operation and the magnetic breakaway ability of the stylus, which provides damage protection for both the work piece and stylus in a crash situation caused by an improper set up by the user [54].

The ability to define planes and align axes plus a full range of datum functions make complex fixtures unnecessary and allow for rapid job set up. The many options for data capture allow almost any free form shape, no matter how detailed, to be scanned [55].

Contact scanning systems combine output from their scanning probes and axes positions using a purpose built scan control card for data capture. The accompanying software calculates the surface coordinate data point and a new target position to which the machine should move by analyzing the force placed upon the stylus. The stylus then moves to the new position automatically [55].

23

The scanning software packages are used to digitize original models on both CNC machine tools and coordinate measuring machines to produce mold and die cavities, CAM profiles, and templates. Data can be captured using touch-trigger or analog probes. Once the data has been captured, model variants can be produced by mirroring, scaling, rotation, translation and male/female inversion [54].

Some systems maintain a contact pressure of only 12 grams and are able to translate a model into pure data that can then be processed for use by either manufacturing or engineering purposes. Once the scan is complete, the software enables the user to manipulate data and then create an NC program or export the data to any of several CAD output file types [55].

The contact systems' touch-trigger probes can be used to digitize components when fitted to either a CNC machine tool or coordinate measuring machine. The analog probes operate at very high scanning speeds, with greater accuracy and lower contact force than existing tracer probes [54]. This allows better machine finishing of parts, and the ability to scan relatively soft materials. The scanning probes have been developed for the intricate scanning of objects such as coins, watermark dies and jewelry, where fine detail requires the use of very low contact force [54].

The contact scanning technology's flexible scanning solutions can provide the answers to most scanning problems. However, because the scanning stylus does not have the capacity for five-axis data acquisition, some items cannot be entirely scanned. In the biomedical context of this project, this fact presents problems that may need to be solved

24

with another method of data acquisition, such as the non-contact laser scanning technology [55].

2.1.2 Laser Scanning

A rapidly emerging technology designed for accurate geometric data acquisition is laser scanning, whose machines generally utilize the structured lighting technologies described above. Laser scanners, which provide the ability to quickly acquire large amounts of geometric data, measure points on the part surface by computing the position of a laser spot projected onto the surface [14]. The laser scanner casts a beam onto the object surface and then inspects the reflected beam using a sensor that is placed coaxial to the source. The location of the source gives the x and y coordinate measurements of the surface point while the analysis of the reflected beam by a triangulation procedure gives the third dimension [9].

A popular laser scanning system utilizes geometry acquisition technology that does not use imaging optics or sophisticated detector array processors. Rather, it is a linear device with none of the conventional focal length or image processing complexities inherent in other scanning technologies [20].

Mechanically, the laser scanning systems fully integrate both rotation of the scanned part and translation of the source (laser). They utilize a geometric data acquisition method that provides high-resolution measurements across the entire work volume [20]. This method removes any need for additional mechanics to move toward or

25

away from the part, thus removing any risk of destructive contact between the scanner and the part [20].

Figure 2-2 A top-down view of the laser scanning depth coordinate acquisition process
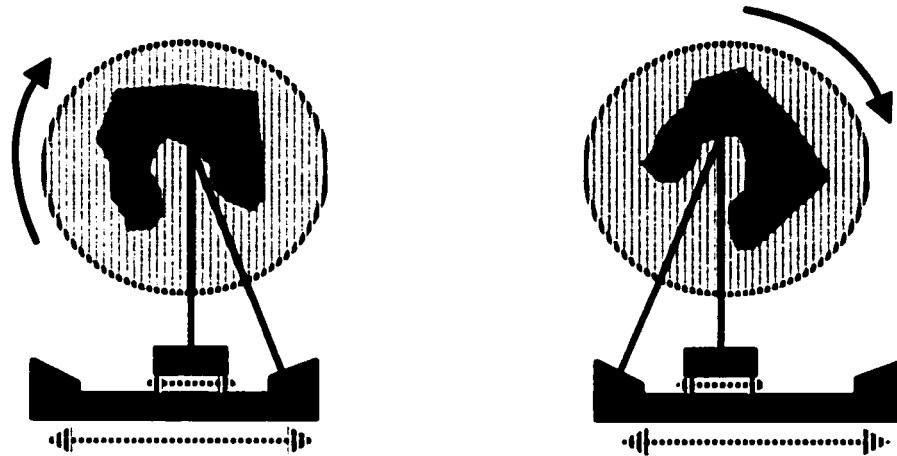
Figure 2-3 The triangle formed between the laser, the scanned part, and the sensors, which provides the geometry to obtain the depth coordinate

26
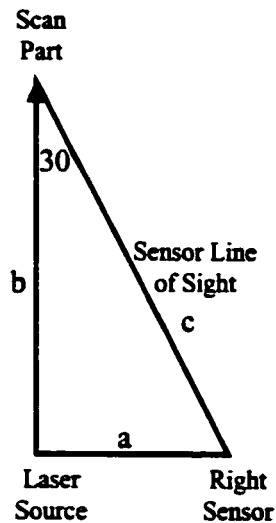
The top-down views of the laser scanner (above) illustrate the functionality of the data acquisition devices, which are composed of two triangulation sensors located on either side of a laser projector, all positioned on a single horizontal plane [20]. The view line of each sensor is fixed to thirty degrees relative to the laser beam. This creates a 30°-60°-90° right triangle between the source, sensor, and part whose dimensions may be easily obtained with minimal information and simple geometric laws. To measure a surface point, the scanner rotates the object so that the point's surface normal is parallel to the laser beam [50]. The laser beam and sensors are then translated horizontally to illuminate the point [50]. Once the laser beam illuminates the desired spot on the piece, the sensors further translate until the view line of one of the sensors intersects the point [50]. Thus, because the horizontal distance (or "a" on the diagram) between the source and the sensor is known, and all three angles of the triangle are known, the depth measurement (or "b") is easily obtained [50]. The location of the source provides the horizontal and vertical coordinates of the illuminated point, and the process outlined above provides the depth coordinate, thus creating the three-dimensional surface data.

When the sensors are placed at the extreme left of the horizontal railing, the view line of the left sensor is in position to measure points at the back of the work volume, while the right sensor is in position to measure points at the front of the work volume. As the sensors move to the right, they both scan the full length of the laser beam in opposite directions across the entire depth of the work volume [20,50]. Thus, the laser scanner has the ability to accurately measure all points within its work volume.

27

The scanning process begins by scanning the bottom layer of the work volume and proceeds upward to each layer in intervals chosen by the user. Therefore, when the scanning process is complete, the data is organized as a collection of the vertical layers [50]. At each section the laser translates horizontally left to right while the object rotates on the platter. By coordinating these motions the computerized scanning algorithm intelligently maneuvers the laser about the object, exposing and recording all portions of the object's surface [20]. The challenge remains in attempting to minimize shadowing effects that occur as a result of concavities in the part and to provide part orientations that optimize measurement [50].

Once the scanning procedure is complete, the resulting data must be analyzed to ensure its accuracy. Presently, the scanning technician performs this analysis manually. Because this machine is operated using a laser rather than a touch probe, occasionally during the scanning process, the scanner will bypass, or miscalculate points. There are a variety of reasons why this occurs; the most common being the scanned piece was not properly "painted" at the given position. (To obtain the most accurate results, the scanned part is coated with a removable layer of white powder or white paint, which helps to provide the brightest possible reflected beam.) Sometimes slight deviations in the data appear to occur randomly. Nevertheless, these aberrations need to be repaired before exporting the file to a solid modeling package. The same software employed during the scanning process is used for the editing procedure [50].

Four basic editing applications should be performed on each scan: scan repair, bridge construction, cap construction, and triangulation. During these four processes,

28

which typically are completed in the order listed above, the scanned computer model is checked, and validated at every level of the vertical axis. Layer by layer, the part is verified, or in some cases reconstructed [50].

The first task of the editing process can be broadly titled as "scan repairs." As previously mentioned, the laser scanner will occasionally miscalculate the distance between it and the scanning surface, or perhaps miss a point all together, for a variety of reasons. The software provides the capability to repair these holes by manual editing, point insertion, and automated smoothing techniques [50]. The replacement of stray or missing points is simplified by the software's ability to display the adjacent layers. Typically, because the distance between these layers is minute, the adjacent layers provide the technician with a precise location to place the stray or missing point. Once the point data of the scanned file has been adjusted to remove data holes and stray points, two tasks, "bridge construction" and "cap construction", are performed to ensure data compatibility with other CAD systems by pinpointing the joining of two contours and the enclosing of a contour [50]. Finally, a "triangulation" procedure is performed to illustrate the three-dimensional data structure by joining the vertical layers together [50]. At this point, the file may be exported to many CAD data file types [50].

The four-axis capability of the laser scanner allows for the acquisition of complex, three-dimensional surface data in one scanning session without having to reset and rescan the part [20]. The laser scanning technology is able to produce accurate geometric data repeatable to less than 0.001 inch [50]. The data is highly compatible with most CAD software programs as well as rapid prototyping machines and Computer

29

Aided Manufacturing (CAM) software, and can be exported as an ASCII file, which was used in the final phase of this project for the validation of the imperfect laser scan repair algorithms [50].

Laser scanning equipment has been used for several medical applications and case studies, but very little research that would be considered similar to that which is performed herein has been conducted [20]. The most similar study was conducted at the University of Texas [33] where researchers used the laser scanning equipment to develop a "digital library" of the human skeleton. The goal of the research, in much the same manner as this research, was to provide broad access to anatomical data to a wide number of disciplines for study and research. To date, this project has completed scanning of all elements of the human skeleton and has proceeded to the chimpanzee and baboon. Although no further significant research has been performed using the different methods of laser scanning, several interesting applications have been performed in the medical industry using these scanning technologies. For example, researchers at the Johns Hopkins University utilize a full-body laser scanner to develop better burn masks to help speed the healing process for burn victims [65]. A full-body laser-scanning machine takes hundreds of quick and painless measurements of a burn patient's face. The data helps doctors design a better fitting mask that limits scarring at the cost of about $1,500 each. Similar research using a full-body laser scanner has developed better oxygen masks for the United States Air Force fighter pilots, better fitting diapers for babies, and better fitting bicycle helmets [39].

30

Among many other researchers in the same area, Curless [17], Curless and Levoy [19], and Kaisto, et al. [32] have studied the data extraction and reconstruction of data obtained through optical triangulation scanners and have found that curved surfaces, discontinuous surfaces, and surfaces of varying reflectance cause systematic distortions of the range data. To solve these problems, they propose an alternate method of data extraction based on analyzing the time evolution of the structured light reflections, a much slower and more equipment dependent process.

Other causes of inconsistency in laser scanning are laser speckles, which introduce noise to the data. Baribeau and Rioux [7] and Dorsch, et al. [21] have studied the effect of speckle on data and have determined that it limits the accuracy of range triangulation. However, the effects of speckle can be reduced through well-known speckle reduction techniques.

2.2 Medical Imaging

The rapidly growing field of medical imaging has become a cornerstone of the health care industry today. The advancement of digital technology, specifically mass data storage and expeditious data acquisition has led to explosive growth in the industry through the development of several new imaging technologies [60]. However, the development of these new techniques has not only improved the quality of health care, but has also contributed to its rising cost [60]. Imaging methods such as Magnetic Resonance Imaging or Computed Tomography can now acquire accurate three-dimensional data with excellent precision, but the cost of these imaging methods can be

31

prohibitive. Costs vary based on the particular protocol used and the part of the body being scanned, as well as the availability of and local demand for the technology.

Bracewell [13] thoroughly describes the physics and mathematics of two-dimensional imaging, which is so complicated and exhaustive that it requires several semesters of study in order to be fully understood.

Collecting extremely accurate geometric data from human body parts is generally difficult due to their complex shapes and the flexibility of soft tissues. In addition, collecting geometric data from organs within a living subject requires a non-invasive imaging technique. Thus, these imaging methods, having these complex abilities, are frequently used for diagnosis of various clinical symptoms despite their considerable expense. Unfortunately however, medical researchers typically use these expensive and less accurate methods on cadaver specimens, adding significant unnecessary costs to their research projects.

2.2.1 Medical Imaging Data Files

The data formats for medical imaging devices, specifically MRI images and CT scans, are extremely similar. Standard formats have been developed and are adhered to in varying degrees. However, some imaging equipment proprietors have developed their own proprietary formats that do not resemble the standard formats [16]. Three types of information are generally present in medical imaging data files [16]:

- Image data, which may be unmodified or compressed
- Patient identification and demographics

32

- Technique information about the exam, series, and slice/image

Although extracting the image information is usually straightforward, the extraction of descriptive information such as geometric details in order to combine images into three-dimensional data sets is more difficult and requires a deep understanding of how the files are constructed [16].

There are three basic families of formats that are popular in use [16]:

- Fixed format, where layout is identical in each file

- Block format, where the header contains pointers to information

- Tag based format, where each item contains its own length

The block format is the a popular type used, though in most cases the header contains only a limited number of pointers to large blocks and the blocks are almost always in the same place and a constant length [16]. Thus, a user can succeed by assuming a fixed format if the specifics of the layout are unknown [16].

The American College of Radiologists (ACR) and the National Electrical Manufacturers Association (NEMA) developed the first standard in 1985, referred to as ACR/NEMA version 1.0, to facilitate multi-vendor connectivity. After several revisions, the standard was re-released as version 2.0 in 1988 [16]. In 1993, the most recent version was released as Standards Publication PS3, but is commonly referred to as DICOM 3 (Digital Imaging Communications in Medicine) [49].

In the ACR/NEMA format, the presentation of the data and the application layers are described in a "message" format, which, along with the ACR/NEMA data dictionary

33

and extension mechanisms, has been adopted by many proprietary formats and other standards [16]. Clunie [16] describes the format as follows:

> "A message consists of a series of 'data elements' each of which contains a piece of information. Each element is described by an 'element name' consisting of a pair of 16 bit unsigned integers ('group number', 'data element number'). The data stream is ordered by ascending group number, and within each group by ascending data number. Each element may occur only once in a message. Even numbered groups describe elements defined by the standard. Odd numbered groups are available for use by vendors or users, but must conform to the same structure as standard elements. Following the (group number, data element number) pair is a length field that is a 32 bit unsigned even integer that describes the number of bytes from the end of the length field to the beginning of the next data element. The last part of a data element is its value, which is defined by the data dictionary to be an ASCII or binary value."

An unwritten standard has developed among the vendors of the equipment to almost universally put the image data at the end of the file [16]. Clunie [16] provides this simple example to illustrate:

> "...if an image is 256 by 256, uncompressed, and 12-16 bits deep (and hence usually, though not always, stored as two bytes per pixel), then we all know that the file is going to contain 256*256*2=131072 bytes of pixel data at the end of the file. If the file is say 145408 bytes long, as all GE Signa 3X/4X files are for example, then you need to skip 14336 bytes of header before you get to the data."

Many vendors, including Siemens, Philips, General Electric, Toshiba, Hitachi, Imatron, and many others, have developed their own proprietary formats [16]. Although they differ in varying degrees from the standard formats, these proprietary formats generally utilize many of the same concepts as the standard formats [16].

34

2.2.2 Magnetic Resonance Imaging

Magnetic Resonance Imaging (MRI) is a medical diagnostic technique that creates images of the body using the principles of nuclear magnetic resonance. A versatile, powerful, and sensitive tool, MRI can generate thin-section images of any part of the body—including organs, bones, and ligaments—from any angle and direction, without surgical invasion and in a relatively short period of time.

The principles of MRI take advantage of the random distribution of protons, the nuclei of abundant hydrogen atoms, which possess fundamental magnetic properties [43,47,62]. Once the patient is placed in the cylindrical magnet, the diagnostic process follows three basic steps. First, MRI creates a steady state within the body by placing the body in a steady magnetic field that can be over 30,000 times stronger than the earth's magnetic field [60,62]. Then the MRI scanner stimulates the body with radio waves to change the steady-state orientation of the protons [26,28,47]. After terminating the radio signal, a short-wave radio antenna detects, at a pre-selected frequency, the electromagnetic transmissions emitted by the hydrogen nuclei [26,28,47]. The transmitted signal is used to construct internal images of the body using principles similar to those developed by computed tomography, or CT scanners [28,47].

2.2.3 Computed Tomography

The Computed Tomography (CT) scanner, an intricate extension of the conventional X-ray device, offers clear views of any part of the anatomy, including soft organ tissues. Used without the need for injected dyes, the full body scanner rotates 180°

35

around a patient's body, sending out a thin X-ray beam at hundreds of different points [56,58]. Detectors, usually solid-state crystal or Xenon gas, positioned at the opposite points of the beam detect and record the absorption rates of the varying densities of tissue and bone [56]. The density of the scanned object determines the quantity of the emitted X-ray beam that passes through the object, and thus the intensity of the grayscale image at that location [56]. These data are then relayed to a computer that converts the information into a picture.

2.2.4 Ultrasound Scanning

Ultrasound is a sound wave having a frequency higher than the upper limit of the human audible range, 20 kHz [60]. Ultrasound Scanning (US) is a non-invasive diagnostic medical imaging technology that uses these high frequency sound waves to form an image of body tissues that can be viewed for medical diagnosis [5,6,60]. The sound waves are recorded and can be displayed as a real-time visual image or simply as a still image. As the sound waves pass through the body, echoes are produced that can be used to identify how far away an object is, its size, and its uniformity [5].

The ultrasound transducer functions as both a generator of sound and a detector. When the transducer is pressed against the skin, it directs the inaudible, high frequency sound waves into the body [60]. As the sound echoes from the body's fluids and tissues, the transducer records tiny changes in the pitch and direction of the sound [5]. These echoes are instantly measured and interpreted by a computer, which in turn creates a real-time picture on the monitor [5].

36

2.3 3-D Reconstruction For Medical Imaging

A major problem that has been studied for decades in the medical industry is the three-dimensional reconstruction of body parts from parallel cross sections, such as those produced by MRI, CT and US scans [25]. Three-dimensional models are used for surgery planning, prosthesis fabrication, radiation therapy planning, and volumetric measurement [25]. Also, in the preparation of complex bone surgery, it has become a common practice to make solid models of the bone structures for visualization purposes [25].

The challenge of creating three-dimensional models in the medical and biological industries has been studied for over a century [24]. The book by Gaunt and Gaunt [24], whose citations of previous reconstruction research date as far back as the mid-nineteenth century, details the pre-computer techniques of three-dimensional reconstruction, known as serial reconstruction. Serial reconstruction is a procedure by which the three-dimensional representation is developed by stacking plates on top of one another. Each of these plates, which were made of wax, wood, tin foil, cardboard, or many other types of material, had been shaped by a two-dimensional cross-section of the part in much the same way as the medical imaging or laser scanning technologies of today organize their data. They describe several other methods of reconstruction, such as graphical reconstruction, solid reconstruction, cinematography, stereo-photography, and holographic reconstruction [24].

The utilization of computer graphics technologies in order to visualize, analyze and reproduce the human body has become crucial to the present medical field [25].

37

Two-dimensional data generated by medical imaging systems such as CT, MRI, and US are often not comprehensive enough for the surgeons to analyze the conditions of their patients practically [1,25,30].

Three-dimensional reconstruction techniques rebuild a computer model of the object that has been reduced to slices by the imaging method [42]. The advantage of a three-dimensional reconstruction is that a global view of the structure is obtained, eliminating the need for a physician to attempt to reconstruct the object from multiple cross-sections by inaccurate estimation [60]. Potamianos, et al. [51] cite six benefits that three-dimensional models can provide:

- "quantitative morphological description of patient anatomy"

- "pre-operative planning and simulation of surgical approach"

- "biomechanical modeling of joints with or without implants"

- "intra-operative registration of patient with 3-D data set and precise navigation of surgical tools, in conjunction with computer assisted surgery"

- "development of knowledge base"

- "manufacturing of precise physical models and implants"

The need for accurate three-dimensional reconstruction has inspired its own rapidly growing field of study within the computer science and engineering fields [42]. In addition to the hundreds of research papers and conference presentations by researchers all around the globe, there are at least 78 software packages (commercial and

38

otherwise) available for three-dimensional reconstruction of MRI, CT, confocal, and serial-section data for medical and life science imaging [42].

Despite the advantages it provides, the representation of a three-dimensional volume on a two-dimensional screen does not necessarily provide physicians with a complete awareness of the patient's problem [51]. In order to extract three-dimensional information from the picture, surgeons must learn to interpret on-screen displays [51]. While noting the validity and advantages of viewing a three-dimensional representation on a two-dimensional screen, Potamianos, et al. [51] discuss four visualization issues that are not resolved by computer models.

- "2-D screen displays do not provide an intuitive representation of 3-D geometry"

- "Unusual or deformed bone geometry may be hard to comprehend on-screen"

- "The integration of multiple bone fragments is hard to visualize on-screen"

- "Planning complex 3-D manipulations on the basis of 2-D images is difficult"

As such, significant research has been performed to develop cohesiveness between the medical industry and rapid prototyping technologies, so much that conferences are now being held solely to further research interests in this topic. Hundreds of journal articles and conference presentations have discussed the implementation of rapid prototyping technologies into medical arenas, and many

39

software programs, specifically MedCAD™ by Materialise, have successfully bridged the gap from medical imaging data to rapid prototyping fabrication.

2.3.1 Rapid Prototyping

In manufacturing, rapid prototyping provides the means to dramatically reduce the lead-time required to produce a semi-functional physical prototype. Simply stated, rapid prototyping (RP) is the process of producing an actual physical model from a CAD drawing. The ability to produce these models in a matter of hours is possible due to techniques that implement an additive fabrication process. While most traditional manufacturing techniques use subtractive or formative processes, RP techniques build the model, one layer at a time, from bottom to top [31]. This additive nature provides cohesiveness with the data types created by medical imaging technologies, as well as the data generated by laser scanning reverse engineering systems, as they are created in sliced intervals as well. The opportunity for physicians to obtain a physical model of the patient's anatomy has led to considerable research and development focusing on the integration of medical imaging data sets and rapid prototyping fabrication [31,51].

RP techniques can be broadly classified into three major categories based on the pre-fabricated material used: liquid, solid, and powder [31].

Liquid based RP systems became the first RP processes available to the public. In 1988, 3D Systems, Inc. introduced stereolithography, which utilizes laser beams to solidify photo-curable resin. The stereolithography apparatus (SLA) has become a benchmark for the RP industry, and epitomizes liquid based RP systems. The SLA

40

consists of a vat containing the photo-curable resin, a low-powered ultraviolet laser beam (usually helium-cadmium or argon ion), and an elevator that moves a support structure vertically as each layer is created [11]. Because the part is built with an additive process, the elevator begins positioned near the surface of the liquid resin. The laser beam traces the desired pattern for the current layer of the part in the x-y plane. The resin instantly solidifies and the elevator is then lowered one layer thickness and the same process proceeds on the remaining layers until the entire part is completed [31]. Finally, due to the toxic nature of the resin, a finishing process rinses the product in a solvent and cures the remaining resin in an ultraviolet oven [31]. Other less popular liquid based RP systems exist, the most common of which is Cubital's Solid Ground Curing process.

Solid based RP systems are vastly different from liquid based systems, as well as each other. In general, these systems use solids as the material to create the prototype. Among many other processes, two technologies stand out as the most commonly used systems, Fused Deposition Modeling and Laminated Object Manufacturing.

Fused Deposition Modeling (FDM), developed by Stratasys, Inc. is generally more intuitively understood than the previous techniques. In short, the process builds a part layer by layer using a nozzle that extrudes a soft plastic that hardens quickly after set in place [31]. The FDM contains two nozzles for material extrusion, one for the part model and the other for any necessary support structures. After the FDM head melts the solid material, the nozzles expel very fine layers of the plastic, and the semi-liquid material is extruded through the head using a precision volumetric pump [31]. The molten material heats and fuses with the previous layer, and quickly solidifies [31]. Once

41

the head traces the path of each layer, the support material is peeled off to reveal a completed part without a need for further refinement. Various finishing techniques such as polishing or painting can be used for esthetical purposes as well.

The second common solid based technique is Laminated Object Manufacturing (LOM), developed by Helisys, Inc. This process glues together layers of very thin sheets that have been cut to the desired shape by a carbon dioxide laser beam [31]. The apparatus consists of a platform that supports and moves the fabricated part in the vertical direction, a feeder device that replenishes the sheet material, and a laser apparatus that cuts the part's cross sectional contours [11]. A heated laminating roller provides the pressure to glue together the successive layers [31]. The laser cuts those areas of the sheet not lying within the part's contour into small tiles, thus converting the excess into necessary support structures [31]. Once all the layers are completed, the extraneous material is easily broken away. Various gluing mechanisms may be utilized. The most common method consists of pre-coating the entire foil with glue [11]. However, removing the extraneous tiles becomes difficult, a disadvantage of this method. To rectify this problem, the process of selective gluing was established. The entire foil is pre-coated with heat-sensitive glue. The heat of the laser activates the heat sensitive glue by tracing those areas that fall within the part's cross-section. The disadvantage of this process arises in a large increase in fabrication time and energy expended.

Powder based RP systems are generally very similar to liquid based systems in that they usually use a laser beam to harden the original material, which in this case is a

42

powder. The most common techniques are Selective Laser Sintering and Three-Dimensional Printing.

Selective Laser Sintering (SLS) was one of the initial RP techniques developed [31]. The process is similar to that of the SLA, but in this case an infrared laser beam is used to fuse powdered thermoplastic material layer by layer [31]. To start, the powder is spread evenly with a roller mechanism across the work surface. The sintering chamber is cleansed with an inert gas, typically nitrogen, and heated to nearly the powder's melting temperature [11]. Scanning mirrors are used to redirect the laser beam and fuse the powder along the exterior of the contour [31]. This process is repeated for each layer. The powder that is not fused and remains in place serves as support material for any possible overhangs in the part, and once the model is complete, is wiped free from the part [11].

The Three-Dimensional Printing (3DP) technique produces each layer in a manner similar to an ink jet printer but uses a powder deposition process [11]. The powdered material and a binder material are deposited layer by layer using a feeder system that crosses the work volume along one axis [11]. The feeder system needs to make only one pass per layer across the surface, and prints each layer until the part is finished.

2.3.2 Reconstruction Algorithms

Three-dimensional reconstruction can be thought of as the rebuilding of an item that has been torn apart. In this case, when data is obtained via laser scanning or medical

43

imaging techniques, the item has been torn apart into numerous cross-sectional planes, or slices, usually less than a millimeter thick. Several algorithms have been developed to accomplish this rebuilding objective, each having their own advantages and shortcomings.

In order to begin study on reconstruction algorithms one must understand some standard geometric constructions. Amenta, et al. [4] describe the important concepts succinctly:

> "Given a discrete set S of sample points in R^d, the *Voronoi cell* of a sample point is that part of R^d closer to it than to any other sample. The *Voronoi diagram* is the decomposition of R^d induced by the Voronoi cells. Each Voronoi cell is a convex polytope, and its vertices are the *Voronoi vertices*; when S is nondegenerate, each Voronoi vertex is equidistant from exactly $d+1$ points of S. These $d+1$ points are the vertices of the *Delaunay simplex*, dual to the Voronoi vertex. A Delaunay simplex, and hence each of its faces, has a circumsphere empty of other points of S. The set of Delaunay simplices form the *Delaunay triangulation* of S. Computing the Delaunay triangulation essentially computes the Voronoi diagram as well."

The importance of the Delaunay triangulation has been further described in a more understandable manner by Lambert [36]. The Delaunay triangulation, in two dimensions, is a network of non-overlapping triangles in which the circumscribing circles of any triangle enclose no points. A circumscribing circle of a triangle is a circle that has all three vertices of the triangle on its circumference. Thus, a Delaunay triangulation connects points to their natural neighbors. Delaunay triangulation has important applications in the representation and analysis of special phenomena. The distribution of a set of points in a plane can be presented using many discrete structures. Delaunay triangulation is among the most efficient and usable techniques available.

44

The Delaunay triangulation and Voronoi diagrams are important because these tools are the most often used in surface reconstruction algorithms; it is difficult to find an algorithm that does not utilize these geometric tools. All of the algorithms described below have been developed based on either Voronoi diagrams or Delaunay triangulation, or both.

The algorithm put forth by Hoppe [27] is targeted toward three-dimensional data with no particular organization, which is not necessarily true for the data with which this study is concerned. Nevertheless, the algorithm is important to consider. This algorithm begins by determining the topological type of the surface, and produces an initial estimate of its geometry. Then, using an optimization algorithm, the process reduces the number of "faces" on surface shell and improves the fit to the data points. And finally, the surface image is changed from a piecewise linear representation to a piecewise smooth representation. The disadvantage of such a method, as Amenta, et al. [4] explains, is that algorithms such as this produce approximating rather than interpolating meshes.

Another algorithm of the same nature put forth by Curless and Levoy [18] is specifically dedicated to data obtained via laser scanning and optical triangulation. The implementation of their algorithm, which is capable of managing exceptionally large amounts of data, is especially fast and robust.

Bernhard and Ioannides [25] propose a reconstruction algorithm based upon Delaunay triangulation that they call Delaunay Reconstruction. Advantageous properties of this algorithm include its compatibility with rapid prototyping machinery, automatic

45

treatment of complicated objects presenting multiple contour branching and holes, and considerable data reduction compared to other volume-oriented methods.

Amenta, et al. [3,4] developed an algorithm for the reconstruction of surfaces from unorganized sample points based on the three-dimensional Voronoi diagram and Delaunay triangulation. The authors claim that this algorithm was the first solution with provable guarantees. Given a good sample of data from a smooth surface, the output is guaranteed to be topologically correct and convergent to the original surface as the sampling density is increased.

2.4 Methodology Development

To facilitate the use of a highly technical machine such as the laser scanner for someone who is inexperienced and uncomfortable with its use, a structured methodology is essential. Many medical researchers that unnecessarily use medical imaging techniques to obtain geometric data of skeletal system body parts do so simply because they do not know they have an alternative, or are not knowledgeable enough with the operations of the alternatives. By developing a strict methodology to perform tasks the researchers require, an unnecessary burden of learning the operations of the machine is lifted. Also, significant savings of time and resources will be realized, as the researchers will not have to experience delays resulting from unsuccessful scans and reparation of poor-quality scans.

Ostrofsky [48] indicates that the need for structured processes in large-scale design processes has been magnified in the technology-driven twentieth century. He

notes that the growth of technology has led to complexities in modern planning that have affected the efficiency of the resulting activities. Although the focus of his volume is on larger scale design processes, some of his theory can be applicable to this research. He observes that the presence of a structured methodology does not guarantee a successful system of design for a number of reasons. Most importantly, decisions made by the designers or planners are almost always made with incomplete data, inadequate information, or other uncertainties associated with randomness. These limitations usually exist at each stage of the process and thus compound at each stage of the methodology. Therefore, he claims, any process can produce results that, at best, minimize the risks associated with decision made under uncertainty. Or in other words, the decision structure of any methodology cannot guarantee successful results but can offer a structure that results in efficient use of the time and resources available to the designer or planner.

Siddal's [61] book on engineering design describes that in order to present a process for an improved procedure, a theory requires the following components.

- Taxonomy: the identification of standard elements

- Morphology: the identification of the steps or components of the process

- Creativity: the explanation of the creation process of the procedure

- Decision Making: procedures for deciding on the best configurations and proper specifications

47

Parallels may be drawn to this process with respect to this research problem. In order to develop a thorough methodology for researchers to follow, each of the steps listed above must be addressed.

2.5 The Human Musculoskeletal System

The human body parts on which this methodology concentrated are taken from the human musculoskeletal system. The most important function of this system is to allow movement of the body in its parts or as a whole. In addition, the musculoskeletal system provides support and protection for the entire body and for its other organ systems [57]. The functional effectiveness of the system is important because the tasks of everyday life require integration of activity within the system [57]. For instance, a torn ligament in the knee not only impairs the function of that joint but also impairs the entire leg.

The functional unit of the musculoskeletal system is the joint with its associated structures. In this unit, bones acting as levers are held together by specialized connective tissues and are set into motion in relation to one another through muscle action. The system is composed of skeletal muscle tissue and various types of connective tissue, such as bone, cartilage, tendons, and ligaments [57]. The focus of this project was human bones, tendons, and ligaments.

Tendons and ligaments are similar structures. Tendons attach muscle to bone and ligaments attach bone to bone. Both represent a form of dense connective tissue that is both flexible and offers great resistance to a pulling force [57]. Tendons and ligaments

48

consist primarily of thick bundles of collagen fibers packed closely and parallel with one another. The primary difference in the structure of a tendon and a ligament is that fiber bundles are less regularly arranged in the ligament. Also, ligaments contain more amounts of loose connective tissue than tendons [57].

Cartilage acts as a material that retains the shape of organs, such as the ear, nose, and trachea. It is able to resist compression and bending forces to a considerable extent. As such, it is located on the articular surfaces of practically all joints where its resiliency protects the bone from direct compression and permits smooth movement of skeletal pieces against each other [57].

Bones of the skeleton are discrete organs consisting of several tissues. Most bones are hollow and contain marrow cells in the hollowed portion. The skeleton is divided into two regions: the axial skeleton and the appendicular skeleton. The axial skeleton consists of the skull, the vertebral column, the sternum, and the ribs. The appendicular skeleton consists of the bones of the limbs. The bones of the axial skeleton are flat or irregularly shaped and are built of a spongy bone invested by a cortex of compact bone. Most of the bones in the appendicular skeleton are made up of a long, narrow shaft and two expanded ends [57].

2.6 Testing and Validation

For users to believe the results of this project are accurate, and not based simply on objectivity or personal experience, the results must be proven to be accurate. Ostrofsky [48] states that testing is used not only to resolve questions concerning

physical reliability but also to verify performance. He notes that testing is "the verification of attributes of the system and, as such, is the means of reducing the designer-planner's risks when the system becomes operational." Although testing does not eliminate risks, it does increase the information base upon which performance estimates are made for operations. He further states that testing is used to verify hypotheses, generate new information, expose overlooked shortcomings, and improve the concept being studied.

Ostrofsky [48] also addresses the need for astute understanding of statistics relating to curve fitting, regression analysis, testing of hypotheses, and factorial analysis, as well as the various disciplines necessary to provide the technological awareness of the project, for verification of the validity of the obtained results.

2.6.1 Fractional Factorial Design of Experiments

In order to develop a methodology for others to follow, each item must be scanned several times to determine the best possible configuration and parameter settings. Each of the several parameters has various possible settings and the part may be oriented an infinite number of ways. Because each scanning procedure lasts several hours, the manner in which the experiments are constructed is terribly important so that each variable (factor) and variable setting (level) may be appropriately considered. Rather than perform a scanning procedure for every combination of factors and levels, which would require excessive experiment time, an intelligent statistical design of experiments

50

can limit the number of experiments while still providing sufficient information to determine the appropriate parameter settings.

Montgomery [41] describes that as the number of factors and levels in a factorial design increases, the number of experiments required to produce a complete replication of the factorial design grows exponentially. If the researcher can reasonably assume that higher-order interactions are insignificant, then information on the main effects and lower-order interactions may be acquired by administering only a fraction of the complete factorial experiment. In return, the statistician loses the ability to collect information about the higher order interactions between the factors. These fractional factorial designs are among the most extensively used types of designs for process improvement. He further describes that the use of fractional factorial designs is based upon three primary ideas.

- "Sparsity of effects principle": when there are several variables, the system or process is likely to be driven by the main effects and lower-order interactions rather than by higher-order interactions

- "Projection property": fractional factorial designs can be projected into larger designs in the subset of significant factors

- "Sequential experimentation": it is possible to combine two or more fractional factorial experiments to assemble a larger design to estimate the factor effects and interactions of interest

The designs are constructed using well-defined methods and the results of the fractional factorial experiment are analyzed using analysis of variance (ANOVA).

51

2.6.2 Analysis of Variance

Neter, et al. [46] defines analysis of variance (ANOVA) models as versatile statistical tools for studying the relationship between a response variable and one or more explanatory or predictor variables. They observe that these models do not require any assumptions about the nature of the statistical relationship between the response and explanatory variables, nor do they require that the explanatory variables be quantitative.

In essence, ANOVA determines whether observed differences can be attributed to chance or to changes in the input, or independent, variables. Assuming the data has been obtained through a well-designed controlled experiment, if the ANOVA determines that the differences can be attributed to the input variables, further analysis of the results pinpoints which of the input variables are responsible [23]. This fact differentiates the ANOVA from a significance test, which determine whether or not differences are too large to be attributed to randomness, but cannot determine the cause of the differences [23].

ANOVA is the conventional tool used to analyze the results of fractional factorial experimental designs such as that developed for this research [41]. These analyses show statistically those variables, such as the many scanning parameters and part orientation, that contribute to the improvement or deterioration of the outcome, such as scan quality and scan duration. Such results statistically verify the procedures advocated by the methodologies developed by this research.

52

3.0 RESEARCH METHODOLOGY

The research has been divided into the following three phases: taxonomy development, methodology development, and reconstruction algorithm research. Each phase has also been further subdivided into several work packages, which will be detailed as each phase is presented.

3.1 Taxonomy of Human Body Parts

In accordance with the engineering design methodology presented by Siddal [61], the research project began by developing a thorough taxonomy of human body parts from the musculoskeletal system. This taxonomy does not base its classifications on the functionality of the tissues, although similar functioning parts are in fact classified together in many instances. Rather, classifications were determined by the following geometric similarities, all of which may affect one or many scanning parameters.

- Size

- Shape

- Texture

- Tissue type

- Flexibility

- Fragility

- The presence of holes (such as vertebrae)

- Curvature

53

- The presence of any other areas needing specific attention or focus

The taxonomy is limited to the following elements of the musculoskeletal system.

- Axial Bones – bones from this portion of the skeleton are generally odd-shaped. The logical classification of these bones will be vital for the successful completion of this study so that a separate methodology will not need to be developed for each axial bone.

- Appendicular Bones – bones from this portion of the skeleton are generally shaped similarly, although their sizes vary greatly.

- Tendons – these tissues differ greatly from other tissues in terms of texture, flexibility, curvature, etc. even though their shape may resemble that of a ligament or appendicular bone.

- Ligaments – these tissues, similar to the tendons, may differ from the other tissues in many ways, even though the shape and size may be similar.

Each anatomical element was vigorously researched and observed before any scanning procedures were performed.

3.2 Development of Scanning Methodologies

Upon completion of the taxonomy, the research turned to the development of strict methodologies for each anatomical classification developed by the taxonomy. For each classification, a fractional factorial experimental design was planned using either two or three levels within the following factors.

54

- Anatomical part (when feasible) – number of levels depends on the number determined by the taxonomy, and availability of scan-able parts

- Coating – the type of material used to coat the part for maximum reflectivity – at least two levels, white paint (if allowed by part donor) and a talc/alcohol mixture (easily washed off)

- Minimum Horizontal point spacing (coupled with the Maximum Horizontal Point Spacing) – the smallest horizontal distance between measured points, can never be larger than maximum point spacing – three levels, dependent upon the size of the elements in the classification and complexity of their shapes

- Maximum Horizontal point spacing (coupled with the Minimum Horizontal Point Spacing) – the largest horizontal distance between measured points, can never be smaller than minimum point spacing – three levels, dependent upon part size and complexity

- Vertical point spacing – the vertical distance between measured planes – two levels, dependent upon the size of the elements in the classification. This factor may require several additional levels because certain parts may require more precision at certain portions of the scan than at others. The point spacing may be altered during a scan. Thus, several additional levels become possible for this factor.

- Edge detection method – during the laser scanning procedure, an edge may be detected in two ways, either an automatic mechanism or by a

55

defined delta value. If the automatic option is selected, an edge is detected when the laser falls off the surface of the part. In the manual mode, an edge is detected by a defined delta value set by the user. Part orientation and mounting – three levels for each classification considered, dependent upon the shape and geometric complexities of the items in the classification

The dependent variable measured was the scan quality. The quality measure is simply the percentage of horizontal levels that do not require editing or reconstruction at the end of the scan. So, a measure of one (1.00) would be a perfect scan that required no editing, while a measure of zero (0.00) would be a scan whose performance was so poor that it was discarded. In addition, a determination of the factors which reduce the scan duration was also considered, however this determination was secondary to the optimization of scan quality, the primary advantage of using laser scanning technology.

A scanning procedure was performed for each of the experiments deemed by the fractional factorial experimental design. Although the fractional factorial design for each of the several classifications is identical in structure, these experimental designs differed slightly for each classification because the aforementioned factors and levels differed for each classification.

An analysis of variance was performed to determine the variables that are most responsible for improvement in the scan quality and procedure duration variability. From these results, the optimal parameter settings can be determined and implemented into a structured methodology.

56

Invariably, some of the input parameters inversely affected the two possible output considerations, quality and time. For example, a lesser setting for the horizontal or vertical point setting parameter will inevitably improve the scan's quality because more points will be taken at each level or at more levels. However, the additional point acquisition will adversely affect the scan duration for obvious reasons. Thus, once the experiments were performed, special notes were inserted into the scanning methodologies that allow the user to make a determination that best suits their application.

3.3 Repair Algorithms

Next, the research turned to the reconstruction of imperfect data files from the laser scan. Concurrently with the above portion of the proposed research, a goal of this research project was to determine how and why these imperfect data files occur. Conceivably, the evidence could be found as a result of the scanning methodologies, for the cause of the imperfections often lie in the scanning parameters. By analyzing the properties of the part at the time of the imperfect scan, trends or similarities between events of imperfection became evident and were noted in the accompanying scanning methodologies.

Unfortunately, if the preventative forecasters fail or do not exist, the researcher will often be left with an imperfect scan to repair. Therefore, because the parameters being studied may not always be the source of imperfection, a study was conducted to develop a set of algorithms that facilitate the imperfect scan repair process and to determine the feasibility of implementing interpolation algorithms into the laser scanning

57

software. For example, often, there is considerable doubt whether a point is accurate or astray. At present, the operator determines visually, and sometimes erroneously, if the point is accurate. This portion of the study would examine the possibility that the computer be able to detect and make the user aware of possible stray points based on built-in estimation algorithms, or through a stand-alone program that analyzes and has the ability to alter the ASCII data from the laser scanning file. Several algorithms have been developed for use in three-dimensional reconstruction programs that use interpolation for surface reconstruction in the absence of data points. Intuitively, it seems that these three-dimensional applications could easily be altered to suit a two-dimensional applications such as this.

Validation of the effectiveness of these algorithms is presented for each step in the set of algorithms. Rather than verify the effectiveness of an all-inclusive algorithm at its completion, each step of the algorithm set is verified individually for effectiveness. First, raw data obtained from the laser scanner was filtered through each algorithm in the set developed. Important data points, or sets of data points, that should have been altered by the algorithm were initially noted and the changes verified at the completion of each component of the set of algorithms.

4.0 TAXONOMY OF HUMAN TISSUES AND STRUCTURES

The first challenge of this study will be to develop a thorough taxonomy of human body parts based on traits such as shape, texture, tissue type, and curvature, all of which may affect the scanning parameters. The human tissues on which this methodology will concentrate will be taken from the human musculoskeletal system. The most important function of this system is to allow movement of the body in its parts or as a whole. This taxonomy was not based on part functionality, although similar functioning parts are in fact classified together in many cases. Although two human body parts may be functionally very different, they may have similar characteristics with respect to scanning parameters and thus will be scanned in very similar ways. As such, the guidelines for a medical researcher to follow need not be customized to each body part, but rather to each classification.

4.1 Tissue Taxonomy Overview

The human tissues on which this methodology will concentrate will be taken from the human musculoskeletal system. The most important function of this system is to allow movement of the body in its parts or as a whole. In addition, the musculoskeletal system provides support and protection for the entire body and for its other organ systems [40]. The functional effectiveness of the system is important because the tasks of everyday life require integration of activity within the entire system [40]. For instance, a torn ligament in the knee not only impairs the function of that joint but also impairs the entire leg, as well as the movement of the rest of the body.

59

The functional unit of the musculoskeletal system is the joint with its associated structures. In this unit, bones acting as levers are held together by specialized connective tissues and are set into motion in relation to one another through muscle action. The system is composed of skeletal muscle tissue and various types of connective tissue, such as bone, cartilage, tendons, and ligaments [40]. The focus of this project will be to examine bones, tendons, and ligaments.

Tendons and ligaments are similar structures. Tendons attach muscle to bone and ligaments attach bones to other bones. Both represent a form of dense connective tissue that is flexible and offers great resistance to a pulling force [40]. Tendons and ligaments consist primarily of thick bundles of collagen fibers packed closely and parallel with one another. The primary differences in the structure of a tendon and a ligament are that fiber bundles are less regularly arranged in the ligament, and ligaments contain more amounts of loose connective tissue than tendons [40].

Bones of the skeleton are discrete organs consisting of several tissues. Most bones are hollow and contain marrow cells in the hollowed portion. The skeleton is divided into two regions: the axial skeleton and the appendicular skeleton. The axial skeleton consists of the skull, the vertebral column, the sternum, and the ribs. The appendicular skeleton consists of the bones of the limbs. The bones of the axial skeleton are flat or irregularly shaped and are built of a spongy bone invested by a cortex of compact bone. Most of the bones in the appendicular skeleton are made up of a long, narrow shaft and two expanded ends [40].

60

This research begins by developing a thorough taxonomy of human body parts from the musculoskeletal system. This classifications developed through this taxonomy are not based on functionality, although similar functioning parts are in fact classified together at times. Rather, the geometric similarities and the resulting orientation and mounting methods that these geometric similarities require determine the classifications. The following are the structural and geometric characteristics that were evaluated:

- Size

- Shape

- Texture – in general, smooth surfaces appear on bone surfaces were cartilage exists, and thus, are areas where bones articulate. Conversely, those areas where soft tissues such as ligament and tendon tissue attach to the bone surface produce a rough texture.

- Tissue type – two types of bone tissue, compact and spongy. In general, most bones of the human body contain the densely packed compact bone tissue at their periphery. The spongy bone tissue is located in the interior layers of the bone and usually would not be exposed to the scanning device unless the bone is dismantled to expose its interior layers.

- Flexibility

- Fragility

- The presence of holes (such as in the spinal vertebrae)

- Curvature

- The presence of any other areas needing specific attention or focus

61

Table 4-1 Overview of Category Attributes

Class Shape	Size	Texture & Tissue Type	Flexibility & Fragility	Holes & Curvature	Other Features
Flat	Variable	Rough and Dense	Rigid	Variable	Some Protrusions
Long	Variable (>3:1 Aspect Ratio)	Smooth and Dense	Rigid	None	Dual Head
Short	Small (<3:1 Aspect Ratio)	Variable	Rigid	Rarely	Extremely Variable Geometries
Curved	Variable	Smooth and Moderately Dense	Moderate	Semi-Circular	Protrusions
Concave	Fairly Large	Smooth and Dense	Rigid	Numerous	Typically Rough Edges
Vertebral	Medium	Extremely Dense	Extremely Rigid	Always	Multiple Protrusions and Holes
Int. Facial	Small	Smooth, thin and flaky	Extremely Inflexible, Weak	Always, but randomly	Multiple Protrusions and Holes
Soft Tissue	Small	Soft, smooth, and very strong	Extremely Flexible and Strong	None	None

Experience and expert guidance has confirmed that the most important variable in obtaining high quality scan data is proper part orientation and mounting. Thus, classification of the tissues is based primarily on part orientation and mounting requirements, and secondarily on similarities needed in the scanning parameters.

As such, due to the similarities of their geometric qualities, tendons and ligaments are grouped together and classified in the "Soft Tissue" category. The bones will be grouped into seven categories, or part families, based upon the required part orientation,

similarities in part mounting, and common geometric characteristics. They are identified by their typical shape.
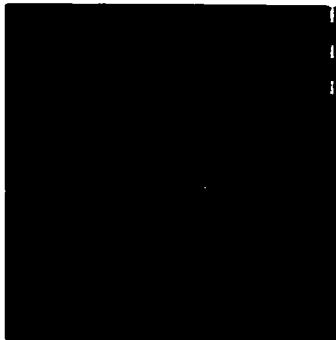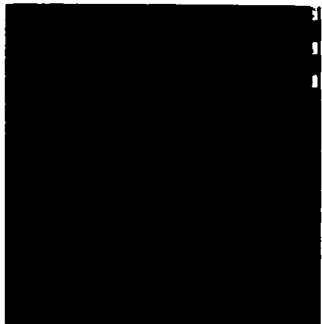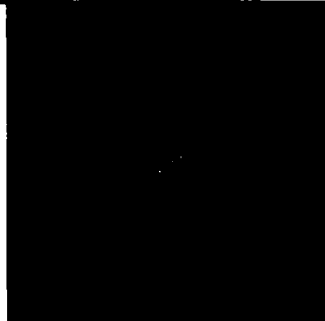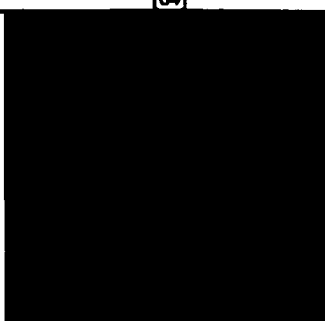
4.2 Flat Bones

The bones in this classification have the simplest of forms, thin and flat in two planes and rounded or oval in the other, typically without protrusions in any direction, although an exception appeared in this category in the form of the scapula bone, which includes a protrusion from the flat surface but may still be scanned in the same manner as the other flat bones as long as the correct orientation is applied. Examples: sternum, patella. The bones of this category maintain similar surface and shape features but also share an additional scanning requirement. For each bone of this category, the proper orientation is essential for obtaining accurate scan data due to each bone's special circumstance, such as the scapular process and the holes of the sacrum and coxa.

Figure 4-1 Example of the Flat Bone category

[64]

Table 4-2 Members and characteristics of the Flat Bone category

Bone (Os)	Size and Shape	Texture, Tissue Type	Flexibility, Rigidity	Connections	Other	Picture
Sternum (1)	Long, slender, and flat. 3 components: manubrium (triangular, articulates with clavicles), body (tongue-shaped, extends inferiorly along the midline), and xiphoid process (smallest part, attaches to interior of body).	Smooth along flat surface. Rigid protrusions along each edge from the insertion of the rib bones.	Before age 25, the fusion of the bone is incomplete. Before fusion, an impact or strong pressure can more easily cause a break between the bone fusion points.	None along the frontal or rear faces. None of any scanning significance.	None	[64]
Coxal (Hip) (2)	Consists of three bones fused together: ilium, pubis, and ischium. The ilium makes up the superior portion forming a broad curved surface, and provides the basis for the inclusion of the coxa into the flat category. Remaining portions extend downward and fuse at the bottom to create the insertion point for the femur.	Smooth, dense bone along all faces. Texture becomes rough near the anterior portions of the pubis and ischium, and on the ilium near the sacrum.	The coxal bones have a sturdy build. To withstand the stresses involved in weight bearing and locomotion, the bones of this region are quite massive.	The top portion of the ilium forms a curved surface that provides an extensive area for the attachment of muscles, tendons, and ligaments. Near the middle and bottom portions of the coxa, the flatness of the ilium gives way to the obturator foramen, the insertion point for the femur.	The tibial insertion point creates a hole, and generally requires special measures during the scanning process.	[64]

64

Bone (Or)	Size and Shape	Texture/Tissue Type	Flexibility		Other	Picture
Sacrum (1)	Consists of the fused components of five sacral vertebrae. Flat anterior surface tapers in width toward the bottom.	Strong, dense bone tissue with fairly smooth surface. The posterior surface is moderately rough in texture with sacral crests and sacral hiatus.	Very strong tissue allows for very little fragility.	Has a convex curved posterior surface. The anterior surface is flat but develops a concave curve near the coccyx.	The sacral foramina pose numerous scanning problems that must be accounted for through appropriate orientation.	[64]
Patella (2)	Broad, circular base. Thin width.	Rough convex anterior surface and smooth anterior surface.	Very strong tissue allows for very little fragility.	Posterior surface presents two concave facets for articulation with the medial and lateral condyles of the femur.	None.	[64]
Scapula (2)	The anterior surface forms a broad, flat triangle. The head of the scapula forms a broad process that supports the cup-shaped glenoid cavity.	Smooth surface surrounding the entire shape of the bone.	Strong, but thin bone tissue along the spine of the scapula create possible fragile surface along the scapular process.	The coracoid process along the top portion of the anterior face creates a concavity along the anterior of the structure.	Spine of the scapula formed by the acromion process poses scanning problems and requires using the appropriate orientation.	[64]

4.3 Long Bones

The bones in this classification are the most common of forms, long and slender in two planes and rounded, or circular, in the third, such as the bones in the limbs. Typically, they have a protrusion of varying shape and size at each extremity of the bone, which facilitate the movement within the joint. The dimensions of the bones in this

65

classification vary greatly, as the size factor does not adversely alter the scanning parameters necessary for this group. One characteristic, a large aspect ratio, or ration of length to width, remains constant throughout the classification. For each member of this classification, the length to width ratio exceeds three to one. Examples: humerus, metacarpal, femur.

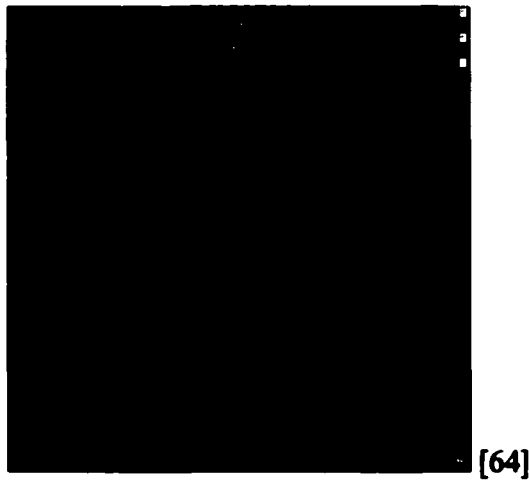**Figure 4-2 Example of the Long Bone category**

[64]
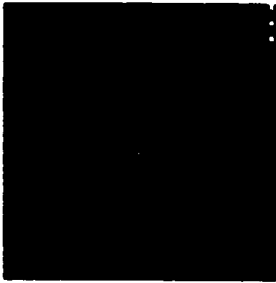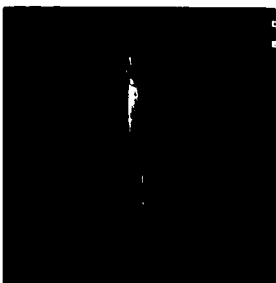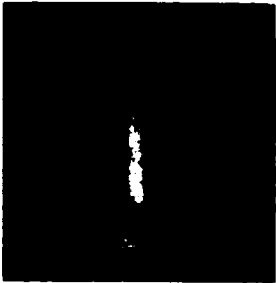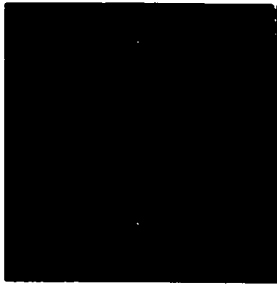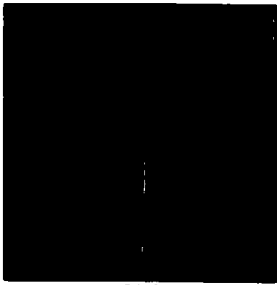
Table 4-3 Members and characteristics of the Long Bone category

Bone (12)	Shape	Texture/Lesion	Fragility			
Clavicle (2)	S-shaped bones. From the roughly pyramidal sternal end, it curves laterally and dorsally until it articulates with the acromion of the scapula.	The superior surface of the clavicle is smooth, while prominent lines and tubercles mark the inferior surface of the acromial end.	Clavicles are relatively small and fragile, and fractures are common.	The clavicle curves along its main axis laterally and dorsally.	None.	[64]

66

Bone (Qty)	Size and Shape	Texture Lesion Free	Flexibility/Fragility	Curvature	Other	Picture
Humerus (2)	The proximal shaft of the humerus is round in section and the humerus maintains the general shape of a long bone.	Smooth surface that becomes rough at each end, both the head and condyle ends.	The humerus is generally strong, but often fractures at the narrow surgical neck just beneath the surface of the head.	No curvature that would be considered atypical to the long bone category.	None.	[64]
Radius (2)	The disc-shaped radial head articulates with the capitulum of the humerus. A narrow neck extends from the radial head to the radial tuberosity. The distal end of the radius, which is wider and flatter than the shaft, articulates with the bones of the wrist.	Smooth surface that becomes rough at each end.	By themselves, both the ulna and radius are relatively fragile bones.	No curvature that would be considered atypical to the long bone category.	None.	[64]
Ulna (2)	When viewed in cross-section, the shaft of the ulna is roughly triangular. Near the wrist, the ulnar shaft narrows before ending at a disc-shaped head that bears a short styloid process.	Smooth surface that becomes rough at each end.	By themselves, both the ulna and radius are relatively fragile bones.	No curvature that would be considered atypical to the long bone category.	None.	[64]
Metacarpal (10)	Although significantly smaller than other members of the long bone category, the metacarpal retains all other important geometric features associated with the category.	Smooth surface that becomes rough at the articulation points at each end of the bone.	Moderately fragile with little flexibility.	No curvature that would be considered atypical to the long bone category.	None.	[64]

67

Bone (Qty)	Size and Shape	Texture/Tissue Type	Flexibility/Function	Curvature	Other	Factor
Femur (2)	Longest bone in the body. The head of the femur protrudes at an angle of approx. 125°. As it approaches the knee joint, the linea aspera divides into a pair of ridges that continue to the medial and lateral epicondyles.	Each projection from the femur is smoothly rounded, as is the thick shaft.	The heaviest bone in the body, the femur is very strong and dense.	No curvature that would be considered atypical to the long bone category.	None.	[64]
Tibia (2)	The anterior surface of the tibia near the condyles bears a prominent, rough tibial tuberosity. A ridge begins at the tibial tuberosity extends distally along the anterior tibial surface. As it approaches the ankle joint, it broadens to the medial malleolus.	Smooth surface that becomes rough at the articulation points at each end of the bone.	The large, heavy bone is very strong and inflexible.	No curvature that would be considered atypical to the long bone category.	None.	[64]
Fibula (2)	Slender bone. The fibular head articulates with the tibia at an articular facet.	Smooth surface that becomes rough at the articulation points at each end of the bone.	The thin shaft is fairly strong for its limited size but its slender size produces common fractures. Forceful movement of the foot outward and backward can often fracture the lateral malleolus.	No curvature that would be considered atypical to the long bone category.	None.	[64]

68

Bone (Type)	Size and Shape	Texture/Tissue Type	Flexibility Type	Curvation	Other	Picture
Metatarsal (10)	Although significantly smaller than other members of the long bone category, the metatarsal retains all important geometric features associated with the category.	Smooth surface that becomes rough at the articulation points at each end of the bone.	Moderately fragile with little flexibility.	No curvature that would be considered atypical to the long bone category.	None.	[64]

4.4 Short Bones

The bones of this classification are also very common, but have a much smaller aspect ratio, or ratio of length to width, than those bones of the "Long" class. In this category, each member's aspect ratio is less than three to one. Typically, they are very short in height, and appear box-like in shape. The obvious exception to this quality is the inclusion of the maxilla bone into this category. However, although shape appearance is dissimilar to other elements of the category, the scanning variables are similar. The maxilla requires the same orientation, horizontal and vertical point spacing, and mounting techniques as the rest of the components of this classification.

The bones of this category typically have smooth surfaces and, with the exception of the facial bones in the category, are extremely strong. Many aspects of the scanning methodology of this category will mirror those of the "Long" category. However, the compact size of the "Short" category structures will require substantial care in the mounting and orientation phases of the scanning process, as well as finer horizontal and vertical point spacing. Examples: carpals, tarsals.

69

Figure 4-3 Example of the Short Bone category

[64]
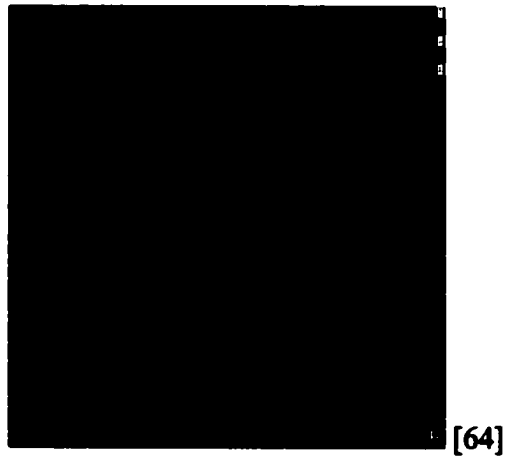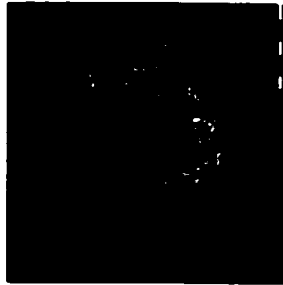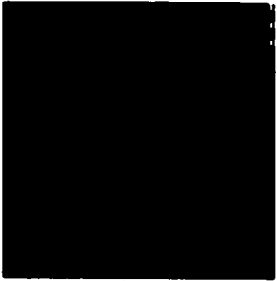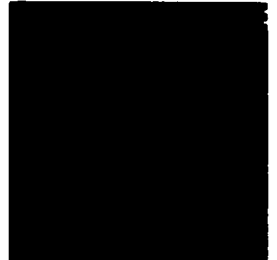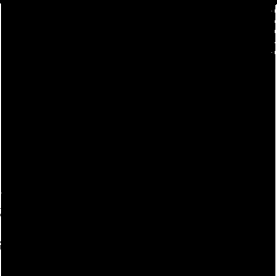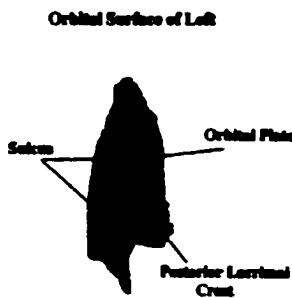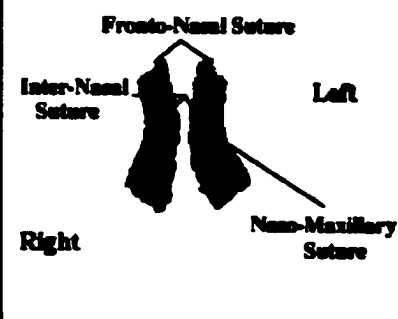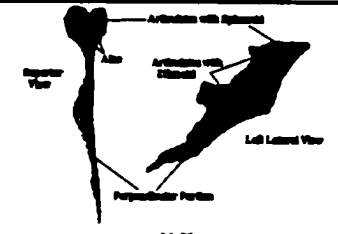
Table 4-4 Members and characteristics of the Short Bone category

Bone (Qty)	Size and Shape	Texture/Tissue Type	Flexibility/Durability	Curvature	Other	Picture
Carpal (16)	Relatively equal in size, each of these bones differs slightly in shape. Most are small and round, like small rocks, but the lunate bone is comma-shaped and the triangular bone has the shape of a small pyramid.	All of the carpal bones are fairly rough in texture, with the exception of smooth facets for articulation with other carpal and arm bones.	Greatly inflexible, they are very strong due to their primary function.	Most of the carpals are have a rounded exterior, but no curvature that would require special attention.	None.	[64]
Phalanx (hand) (28)	Small, narrow bones that widen at each end. They vary in width and height, but their aspect ratios are sufficiently small.	Very smooth in texture.	Greatly inflexible, they are weaker than other members of the category but sufficiently durable, so considered strong.	All of these bones have increased width at each end, slightly less so than their counterparts in the foot.	None.	[64]

70

Bone (#)	Size and Shape	Texture / Tissue Type	Flexibility / Fragility	Curvature	Other	Picture
Tarsal (14)	Seven different small bones in each foot make up the tarsals. Four have typical box-like shape, while the three cuneiform bones have wedge shape.	All of the tarsal bones are fairly rough in texture, with the exception of smooth facets for articulation with other tarsal bones and the tibia.	Greatly inflexible, they are very strong due to their primary function of transmitting the weight of the body.	No curvature that would affect scanning parameters.	None.	[64]
Phalanx (foot) (28)	Small, narrow bones that widen at each end. They vary in width and height, but their aspect ratios are sufficiently small.	Very smooth in texture.	Greatly inflexible, they are very strong due to their primary function of transmitting the weight of the body.	All of these bones have increased width at each end.	None.	[64]
Inferior Nasal Conchae (2)	Small, scroll-shaped bone attached to the lateral wall of the nasal cavity.	Rough texture, but smooth at articulations points with the ethmoid, maxillary, palatine, and lacrimal bones.	Extremely fragile, non-weight bearing bone that displays little flexibility.	Increased width at the center of the major axis, but not significant curvature for scanning parameter change.	None.	[64]
Lacrimal (2)	The smallest of the facial bones. A vertical ridge, the posterior lacrimal crest divides the lateral or orbital surface into two parts. In front of this crest is the lacrimal sulcus, a longitudinal groove.	Smooth texture on the side that forms the medial wall of orbit. Rough texture on remainder of surface.	The most fragile bone in the facial skeleton.	Increased width at the center of the major axis, but not significant curvature for scanning parameter change.	None.	Orbital Surface of Left Sulcus Orbital Plate Posterior Lacrimal Crest [15]

71

Bone (Qty.)	Size and Shape	Texture, Tissue Type	Flexibility/Fragility	Curvature	Other	Picture
Nasal (2)	Each of the nasal bones is a small, thin rectangular bone that together forms the bridge of the nose.	Smooth anterior and posterior surfaces. Rough edges at articulation point with each other.	Inflexible bone is very thin and fragile. Fractures common along bridge of the nose.	Slight curvature around the nasal cavity.	None.	[15]
Coccyx (1)	A vestigial set of bones equivalent to the tail of many mammals. It is the set of fused, tapered, rounded bones, 4-5 in number, which articulate with the sacrum.	Uneven, bumpy texture. Deep ridges at fusion points of the rounded bones.	Strong, inflexible bone at the thickest portion of the bone; strength decreases in the lower portions. Fractures common in the lowest portion of the bone.	Tapered shape with deep ridges at fusion points, but no significant curvature.	Two projections, called cornu project upward from the top face of the coccyx.	[70]
Vomer (1)	Small in height and extremely thin in width, forms the inferior portion of the nasal septum.	Smooth, relatively soft bone tissue across the entire geometry of the bone.	Relatively flexible but extremely fragile due to the very thin structure.	Little curvature along main axis, split alae create heart-shaped curvature at the top of the bone.	None.	[15]
Maxilla (2)	The oddly shaped bone forms the inferior lateral rim, the lateral margins of the external nares, the upper jaw, and most of the hard palate. The frontal process, a superior projection, protrudes along the nasal cavity and orbital, and the	The exterior surface of the maxilla maintains a very smooth texture. The interior surface texture is significantly rough and jagged. Along the lower edge the surface becomes jagged at the insertion points of the upper teeth.	Each maxilla is basically hollow, which gives the bone is moderate fragility.	Significant curvature along the exterior face of the bone and several protrusions from the sides and rear of the bone geometry.	The teeth present possible scanning obstacles if they are intact during scanning. Finer point spacing will be required to capture and differentiate the surfaces of the teeth and maxilla bone.	[15]

72

Bone (Cat.)	Size and Shape	Texture Tissue Type	Flexibility Location	Curvature	Other	Picture
	zygomatic process protrudes from the cheek area.					

4.5 Curved Bones
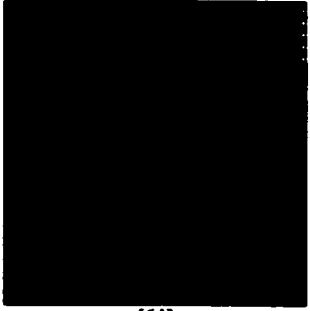
The bones in this classification are long and slender like the bones of the "Long" class, but are curved in a semi-circular shape. The sizes, functions, and surface details of these bones are less important to the scanning parameters than will be the irregular shape, which dramatically alters the scanning operation. Thus, bones of vastly different function have been included in this category strictly based upon this characteristic, i.e. mandible and rib. Several other bones that have curvatures within their shapes are not included in this category, such as the clavicle. Only those structures whose shapes are nearly semi-circular need be included in this category due to the additional precautions that need to be taken as a result of the irregular shape. Examples: ribs, mandible.
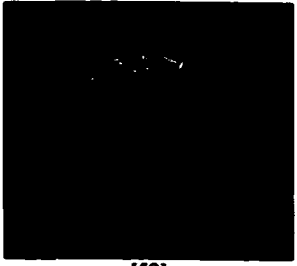
Figure 4-4 Example of the Curved Bone category

[64]

73

Table 4-5 Members and characteristics of the Curved Bone category

Bone (ID)	Size and Shape	Texture/Tissue Type	Flexibility/Fragility	Curvature	Other	Picture
Rib (24)	The ribs are elongate, curved, flattened bones. The vertebral end of the rib articulates with the vertebral column at the capitulum. An interarticular crest divides the surface of the head into superior and inferior articular facets.	Smooth surface that becomes rough at the articulation points at each end of the bone.	The ribs can bend and move to cushion shocks and absorb blows, but severe and sudden impacts can cause fractures.	The bend, or angle, of the rib is the site where the tubular body, or shaft, begins curving toward the sternum. The internal rib surface is concave, and a prominent costal groove along its inferior border marks the path of nerves and blood vessels.	None.	[64]
Mandible (1)	The mandible is flat, nearly semi-circular, and contains several abnormal protrusions. The mandibular body supports the teeth, is the attachment site for several muscles, and maintains the insertion point for the salivary gland. Also, the coronoid and condylar processes protrude from each end of the bone to articulate with the skull and the major muscles of the jaw.	The mandibular body maintains a smooth surface along its frontal and rear faces. The insertion points for the teeth create a rough texture along the top face.	The mandible is a strong, inflexible bone. However, fractures can easily occur along the coronoid and condylar processes.	The nearly semi-circular shape can be more accurately described as a rounded angular shape. The curvature of the mandible aligns the bone very easily with the other elements of the "Curved" category.	The teeth present possible scanning obstacles if they are intact when the mandible is scanned. Finer point spacing will be required to capture and differentiate the surfaces of the teeth and mandible bone.	[64]

74

Bone (C)	Size and Shape	Exterior Tissue Type	Durability Fragility	Curvature	Other	Picture
Hyoid (1)	The semi-circular hyoid bone maintains a very curved body and the greater and lesser cornua. The lesser cornua are simply protrusions from the bone to attach to the stylohyoid ligaments.	The surface of the hyoid is relatively smooth throughout the surface. Its roughest areas are in the body portion of the bone and serve as an attachment site for muscles of the larynx, tongue, and pharynx.	The small bone is thin and fragile. It displays some moderate flexibility but can be easily broken with minimal force.	The body of the hyoid has a more rounded shape and resembles a semi-circle more than any other member of the "Flat" category.	Special attention may be required to guarantee the data acquisition of the lesser cornua at the edges of the body.	[59]
Palatine (2)	The superior surface, concave from side to side, forms the back part of the floor of the nasal cavity. The inferior surface, slightly concave and rough forms, with the corresponding surface of the opposite bone, the posterior fourth of the hard palate.	The interior surface is rough while the exterior and orbital processes maintain a smooth surface. A transverse ridge lies along the posterior portion for the attachment of part of the aponeurosis of the Tensor veli palatini.	The small bone is thin and fragile. It displays some moderate flexibility but can be easily broken with minimal force.	The curvature, although semi-circular according to that definition provided for this category when the two are joined together, maintains distinct angles between the horizontal and perpendicular plate, as well as convex angles at each end to produce the orbital process.	When separated, the palatine bones remain in the "Curved" classification because the methodology for scanning "Curved" bones may be applied with little alteration. Special attention will need to be placed on the orbital process at the end of each perpendicular plate.	[15]

4.6 Concave Bones

These bones, found in the cranial or facial regions, exhibit many of the same characteristics as the "Flat" class, but are concave along what would be the flat plane. The existence of the concavity affects the manner by which the bone is mounted for the scanning procedure, and thus requires an additional class of structures. This class

75

consists solely of bones of the skull, the interior of which accounts for the concavity of each bone. Examples: frontal (skull), maxilla.
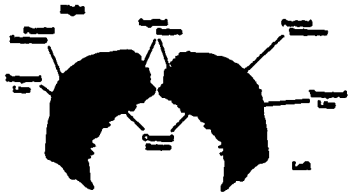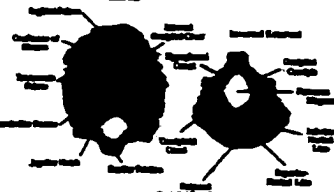
Figure 4-5 Example of the Concave Bone category
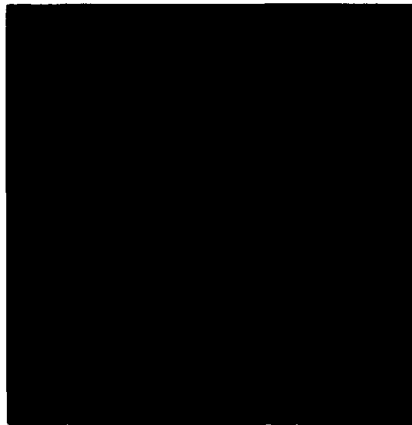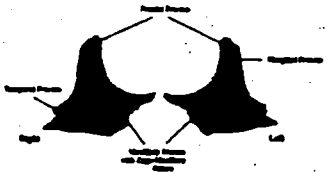
[64]

Table 4-6 Members and characteristics of the Concave Bone category

Bone (Other)	Size and Shape	Texture Tissue Type	Flexibility Properties	Curvature	Other	Picture
Frontal (1)	The bowl-shaped bone forms the anterior surface of the cranium and the roof of the orbits. Were the bone flat, its shape would be nearly rectangular.	Both the interior and exterior surfaces of the frontal bone maintain very smooth texture. Along the edge surface the texture becomes significantly rough and jagged except along the orbits where the surface remains smooth. The frontal sinus is very thin and rough.	The base of the bone is very sturdy and inflexible. Along the outside edges the bone can be brittle and small fragments can easily break apart from the base. The orbital surface is smooth and strong but the frontal sinus causes that portion of the orbital surface to be very brittle.	The bone maintains a concave surface along its base. The orbits and sinus cavities present curvatures that generally require special attention.	The sinus cavities are extremely brittle and oddly shaped, presenting random concavities and rough texture that require significant special attention.	[15]

76

Bone (Qty)	Size and Shape	Texture (Tissue Type)	Flexibility (Density)	Curvature	Other	Picture
Parietal (2)	The bowl-shaped bone forms part of the superior and lateral surfaces of the cranium. Were the bone flat, its shape would be nearly rectangular.	Both the interior and exterior surfaces of the parietal bone maintain very smooth texture. Along the edge surface the texture becomes significantly rough and jagged.	The base of the bone is very sturdy and inflexible. Along the outside edges the bone can be brittle and small fragments can easily break apart from the base.	The bone maintains a concave surface with no additional curvatures that affect scanning parameters.	None.	[15]
Temporal (2)	The bowl-shaped bone forms part of the lateral walls of the cranium and zygomatic arch. The external face contains the zygomatic process, a long protrusion that is part of the cheekbone. The interior surface presents several irregularities and protrusions.	Both the interior and exterior surfaces of the temporal bone maintain somewhat smooth texture. Along the edge surface the texture becomes significantly rough and jagged.	The base of the bone is very sturdy and inflexible. Along the outside edges the bone can be brittle and small fragments can easily break apart from the base. The zygomatic process is narrow and can easily be fractured.	The bone maintains a concave surface with the zygomatic and styloid processes protruding from the surface.	In addition to the two processes that protrude from the surface, there are several holes that require significant special attention. The internal acoustic canal and the external auditory canal are the most significant of these holes as they have the most critical depth to width ratio.	[15]
Occipital (1)	The bowl-shaped bone forms the posterior and inferior surfaces of the cranium. The large hole, or foramen magnum connects the cranial cavity with the spinal cavity, which is enclosed by the vertebral	Both the interior and exterior surfaces of the occipital bone maintain very smooth texture. Along the edge surface the texture becomes significantly rough and jagged.	The base of the bone is very sturdy and inflexible. Along the outside edges the bone can be brittle and small fragments can easily break apart from the base.	The bone maintains a concave surface with no additional curvatures that affect scanning parameters.	The large hole, the foramen magnum presents an obstacle deserving special attention. However the width of the hole greatly exceeds its depth, which allows scanning to proceed	[15]

77

Bone class	Size and Shape	Texture, Lesion, Type	Durability, Density	Concerns	Other	Picture
	column.				with few, if any, adjustments.	
Zygomatic (2)	The bowl-shaped bone forms part of the zygomatic arch and contributes to the rim of the orbits. The frontal process protrudes upward along the side of the orbit.	Both the interior and exterior surfaces of the zygomatic bone maintain very smooth texture. Along the edge surface the texture becomes significantly rough and jagged.	The base of the bone is very sturdy and inflexible. Along the outside edges the bone can be brittle and small fragments can easily break apart from the base.	The bone maintains a concave surface with only the frontal processes and orbital geometry requiring special attention for the scanning parameters.	None.	[15]

4.7 Vertebral Bones

This class contains only those bones found in the spinal vertebral column. The irregular shape and spinal column through the middle of the bone insist that these be reverse engineered with a different process than the previous classes. Each vertebra consists of three basic parts: a body, a vertebral arch, and articular processes. The body transfers weight along the axis of the vertebral column, and therefore these bones are typically dense and strong. The vertebral arch forms the posterior margin of each vertebral foramen. Together, the vertebral foramina enclose the spinal canal. The existence of the spinal column creates multiple scanning obstacles that are difficult to rectify under any methodology. However, if the ratio of the depth of the hole created by the spinal column and the width of the column is small, the laser will be able to find normal sightlines through the hole to obtain accurate data points.

78

Figure 4-6 Example of the Vertebral Bone category

[64]

Table 4-7 Members and characteristics of the Vertebral Bone category

Bone Class	Size and Shape	Texture Tissue Type	Flexibility Fragility	Curvature	Other	Picture
Cervical (7)	Smallest of the vertebrae, they are oval and have curved faces. The superior surface is concave from side to side. The spinous process is relatively stumpy, generally shorter than the diameter of the vertebral foramen. The tips of the processes bear a prominent notch. The transverse processes are large, providing surface area for muscle attachment.	Relatively smooth texture throughout the surface of the cervical vertebrae. Becomes rough in texture on the surfaces of the body.	Dense, strong bone tissue surrounds the vertebral foramen, becoming less strong at the thin spinous process. The cervical vertebrae support only the weight of the head, causing the vertebral body to be relatively small and light.	The cervical vertebrae are nearly triangular from a top-down view. The split spinous process provides a curvature that requires special attention. Also, the body has concave upper and lower faces. However, the curvature of the foramen requires the most significant attention.	In addition to the large vertebral foramen, the cervical vertebrae have prominent, round, transverse foramen.	[64]

79

Bone (code)	Size and Shape	Texture/Tissue Type	Visibility/Projections	Curvature	Other	Picture
Thoracic (12)	The thoracic vertebrae have a distinctive heart-shaped body, a smaller vertebral foramen than the cervical vertebrae, and a long, slender spinous process projecting posteriorly and inferiorly. The transverse processes are relatively thick, and they contain transverse costal facets for rib articulation.	Each thoracic vertebra articulates with ribs along the dorsolateral surfaces of the body, which creates rough texture along the transverse processes. The surface of the body is extremely rough in texture, and the remaining surfaces of the thoracic vertebrae are relatively smooth in texture.	The heart-shaped body is more massive than that of cervical vertebrae, due to its weight-bearing nature, creating a much stronger bone than the cervical vertebrae. In addition, the spinous and transverse processes are larger and stronger than in the cervical vertebrae.	The thoracic vertebrae have three distinct protrusions from the body and foramen base, creating curvature between each protrusion. However, the curvature of the vertebral foramen requires the most significant attention.	Narrowing vertebral foramen creates difficulties in scanning when the width of the hole is less than the depth.	[64]
Lumbar (5)	The largest of the vertebrae, the body is thicker than that of thoracic vertebrae and the superior and inferior surfaces are oval rather than heart-shaped. The slender transverse processes project dorsolaterally. The stumpy spinous processes project dorsally.	Lumbar vertebrae have neither whole facets nor demifacets on the body, and the transverse processes do not have costal facets. The surface of the body is rough on all edges, as well as the surfaces of the spinous process.	The lumbar vertebrae bear the most weight, creating the most rigid and strongest of the vertebral bodies, and the spinous processes are massive.	The thoracic vertebrae have five distinct protrusions from the body and foramen base, creating curvature between each protrusion. However, the curvature of the vertebral foramen requires the most significant attention.	Smallest vertebral foramen creates difficulties in scanning when the width of the hole is less than the depth.	[64]

80

4.8 Interior Facial Bones

These bones have the most irregular of shapes and require nearly unique scanning procedures for both members of the class. They are found in the interior portion of the facial region and have multiple scanning obstacles to negotiate. Their textures are highly brittle, and the irregular surface patterns and multiple openings and cavities cause accurate scanning to be highly unlikely, even under the most rigorously followed methodology. Development of scanning methodologies for this group must be performed on an application-specific basis and rarely will result in usable data.

Figure 4-7 Example of the Interior Facial Bone category

[64]

Table 4-8 Members and characteristics of the Interior Facial Bone category

Bone (1)	Standard Shape	Internal Features	Texture	Openings	Danger	Picture
Sphenoid (1)	Extremely oddly shaped, almost like a butterfly or bat. The hollow body forms the central axis of the sphenoid bone, while the greater wings extend	Both the interior and exterior surfaces of the sphenoid bone maintain smooth texture away from the edges. Along the edge the surface the texture becomes significantly	The base of the bone is somewhat sturdy and inflexible. Along the outside edges the bone is brittle and small fragments can easily	Many curves are present that are very difficult to negotiate, including the curves formed as a result of the lesser wings, pterygoid	Sphenoidal sinus, optic canal, superior and inferior orbital fissures, foramen rotundum, foramen ovale, foramen spinosum, and foramen lacerum	[15]

81

Bone Name	Size and Shape	Texture/Tissue Type	Fragility Density	Curvature	Other	Picture
	laterally. Vertical extensions of each wing contribute to the posterior wall of the orbit. The lesser wings extend horizontally anterior to the sella turcica, a bony enclosure on the superior surface of the body.	rough and jagged.	break apart from the base.	plates, and sphenoidal sinus.	together make the development of effective scanning methodologies nearly impossible.	
Ethmoid (1)	The cribriform plate forms the floor of the cranium and the roof of the nasal cavity while the crista galli is a bony ridge that projects superior to the cribriform plate. The lateral masses contain the ethmodial sinuses, and the superior and middle nasal conchae are delicate projections of the lateral masses. The perpendicular plate forms part of the nasal septum.	Most of the interior and exterior surfaces of the ethmoid bone maintain smooth texture away from the edges. Along the edge surface the texture becomes significantly rough and jagged.	This bone is extremely brittle, as thin as paper in many areas. Small fragments can easily break apart.	Nearly random curvature and holes are prevalent throughout the surface of the ethmoid.	With the dozens of holes and common sightlines to interior sections of the bone, scanning this bone for accurate geometry will be impossible.	[64]

82

4.9 Soft Tissues

In dense regular connective tissue, the collagen fibers are arranged parallel to each other, packed tightly, and aligned with the forces applied to the tissues [40]. Tendons are cords of dense regular connective tissue that attach skeletal muscles to bones [40]. The collagen fibers run along the longitudinal axis of the tendon and transfer the pull of the contracting muscle to the bone [40]. Ligaments resemble tendons but connect one bone to another. The soft tissues require their own category within this taxonomy for two major reasons:
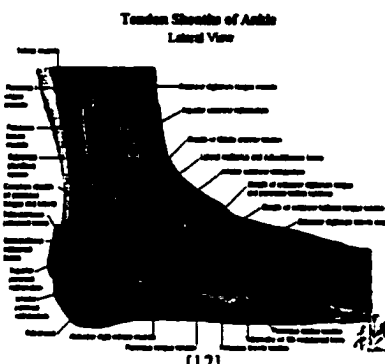
- Flexibility – the infirmity of the connective tissue requires that the structure be mounted from both ends in order to be scanned accurately

- Surface Texture – the rough, detailed collagenous exterior requires that the structure be scanned at much greater detail than the categories of bone

Figure 4-8 Example of the Soft Tissue category

Tendo Calcaneus

Anterior Talofibular Ligament

Calcaneo-Fibular Ligament

[35]

83
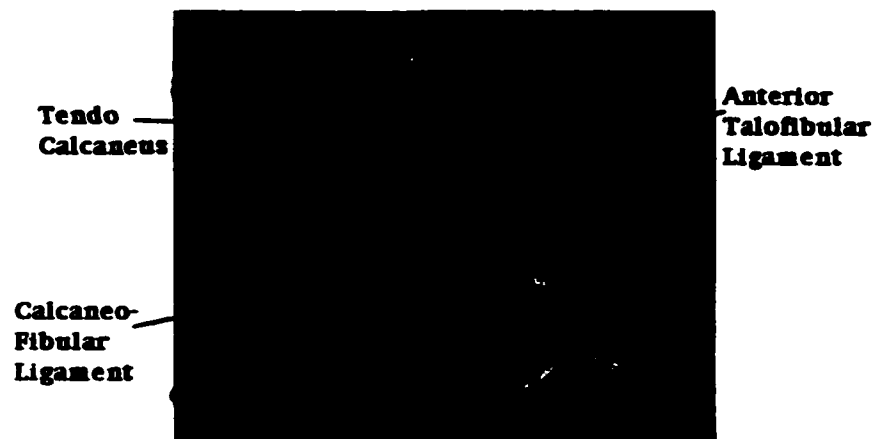
Table 4-9 Members and characteristics of the Soft Tissue category

Bone (OIS)	Size and Shape	Texture Tissue Type	Flexibility Fragility	Curvature	Other	Picture
Tendon (All)	Tendons are cords of dense regular connective tissue, where collagen fibers are arranged parallel to each other, packed tightly, and aligned with the forces applied to the tissue. The collagen fibers run along the longitudinal axis of the tendon and transfer the pull of the contracting muscle to the bone.	Tendons are made up of almost entirely collagen fibers. The collections of parallel collagen fibers are wound together like the strands of a rope creating a rough texture around the perimeter of the tendons.	Very flexible tissue, but very strong. The collagen fibers, which tendons are almost consisted of, are stronger than steel when pulled from either end.	Generally long and slender, there is no curvature that would affect scanning parameters. However, due to the tissue's flexibility, curvature can arise simply from the force of gravity.	None.	Tendon Sheaths of Ankle Lateral View [12]
Ligament (All)	Ligaments are cords of either dense regular connective tissue, where collagen fibers are arranged parallel to each other, packed tightly, and aligned with the forces applied to the tissue, or, less frequently, elastic fibers, which are branched and wavy.	Some ligaments are made up of almost entirely collagen fibers like the tendon, and are arranged in a similar manner.	Very flexible tissue, but very strong. Elastic tissue has a springy, resilient nature so it has the ability to stretch and rebound to its initial position. Collagen fibers in ligaments retain the same properties as those in tendons.	Generally long and slender, there is no curvature that would affect scanning parameters. However, due to the tissue's flexibility, curvature can arise simply from the force of gravity.	None.	Knee - Cruciate and Collateral Ligaments Right Knee in Extension [12]

84

5.0 SCANNING METHODOLOGIES

Upon completion of the taxonomy, the research turned to the development of strict methodologies for each anatomical classification developed by the taxonomy. These methodologies detail the best manner in which the parts may be scanned, including the optimal scanning parameters and part configuration, with respect to the scan quality and speed, while also detailing potential trouble areas that may lead to poor scan quality or speed. Once the experiments were completed, the data was evaluated to determine the appropriate scanning parameters. For each classification, a fractional factorial experimental design was planned using several levels within the following factors: horizontal and vertical point spacing, coating material, edge detection method, mounting apparatus, and part orientation. From these conclusions, the methodology for each class of parts was derived. The dependent variable measured was the scan quality. The quality measure is simply the percentage of horizontal levels that do not require editing or reconstruction at the end of the scan. In addition, a determination of the factors which reduce the scan duration was also considered, however this determination was secondary to the optimization of scan quality, the primary advantage of using laser scanning technology over existing medical imaging technologies.

5.1 Methodology Development

The completion of the taxonomy of human structures leads the research to the development of meticulous methodologies for each anatomical classification developed by the taxonomy. For each classification, five factors were expected to contribute to the

85

measurable variables, scan quality and duration, which will be further defined below. These factors were selected based on information provided by experts in the use of laser scanning and other reverse engineering equipment, and are widely considered to be the most important variables in obtaining high-quality scan data.

- Coating – the type of material used to coat the part for maximum reflectivity – two levels, a talc/alcohol mixture (easily washed off) and white paint (difficult to remove). These levels may be further expanded to differentiate between glossy and matte paint. Experience has proven that improper coating invariably leads to substandard scan quality due to the essential requirement of maximum reflectivity of the laser beam, however there have been no previous studies that suggest improved performance from any particular coating method.

- Minimum Horizontal Point Spacing – the smallest horizontal distance between measured points, always less than the Maximum Point Spacing – two levels, dependent upon the size of the elements in the classification and the complexity of the geometry. The operator sets these two parameters together, and thus they are set as a pairing in the scanning design of experiments. The two parameters can, and usually are set equal to one another. However, in some experimental designs, the parameters were set at different levels to assess the benefits or drawbacks associated with unequal values.

86

- Maximum Horizontal point spacing (coupled with the Minimum Horizontal Point Spacing as stated above) – the largest horizontal distance between measured points, can never be smaller than minimum point spacing – two levels, dependent upon part size and complexity.

- Vertical point spacing – the vertical distance between measured planes – two levels, dependent upon the size of the elements in the classification. This factor provides the exceptional flexibility of adding several additional levels at selected areas of interest. Because certain parts may require more precision at certain portions of the scan than at others, the Vertical Point Spacing may be altered during a scan without the need to stop the scanning procedure. Thus, several additional levels become possible for this factor if necessary.

- Edge detection method (a proprietary measure, but its influence on scanning results is undocumented) – during the laser scanning procedure, an edge may be detected in two ways. If the automatic option is selected, an edge is detected when the laser falls off the surface of the part. In the manual mode, an edge is detected by a defined delta value set by the user. In this mode, a series of course horizontal or vertical moves are made with Maximum Horizontal spacing. If the two measured range values exceed the defined the Delta value, the system then switches to a finer search mode. The system then makes moves with the Minimum Horizontal step

87

spacing, searching for a range measurement difference of less than the Delta value to determine the final edge location.

- Part orientation and mounting – the position of the piece during the scanning procedure and the manner in which it is held in this position – two levels for each classification considered, dependent upon the shape and geometric complexities of the items in the classification. Experience and expert opinion has shown that this factor represents the single most important factor in obtaining effective scanning results. In many cases, with all other variables constant, a simple change in orientation can lead to vastly improved scan quality. However, due to the infinite number of mounting and orientation possibilities, the manner by which alternatives were selected for this research is largely a subjective process and is often the result of simple trial and error of several iterations.

The dependent variable measured is the scan quality. The quality measure is simply the ratio of horizontal levels that do not require additional manual editing at the completion of the scan to the total number of cross-sectional levels in the scan. So, a measure of one (1.00) would be a perfect scan that required no manual editing, while a measure of zero (0.00) would be a scan whose performance was so poor that it was discarded.

88

5.2 Design of Experiments and Scanning Experimentation

In order to obtain valid and objective initial conclusions about the scan data, a statistically significant experimental design is necessary. Because the availability of the scanning equipment is somewhat limited, and the biological tissues in question are time-sensitive due to their propensity for losing their natural moisture, thus causing a change in their shape and surface characteristics, the manner in which the experiments are constructed is exceedingly important so that each variable and variable setting may be appropriately considered in the available time frame. Rather than perform a scanning procedure for every combination of the factors and levels, which would require excessive experiment time, an intelligent statistical design of experiments can limit the number of experiments while still providing sufficient information to determine the most important main effects on appropriate parameter settings.

In this case, there are five factors to consider: orientation and mounting, horizontal point spacing, vertical point spacing, coating material, and the edge detection protocol. Each of these factors has two levels, as outlined above, three of whose levels are different for each classification. A complete factorial design would consist of 32 scans, or runs, for each category. Rather, because it was safe to assume that high-order interactions are negligible, and there was limited experimental capacity, a one-quarter fractional factorial design was considered.

The experimental design, as detailed by Montgomery [41], that was utilized in this research is outlined below. A positive or negative sign denotes the levels of each factor in each experiment within the design.

89

Table 5-1 2^{5-2}_{III} Experimental Design

Experiment	Vert. Pt. Spacing	Coating	Orientation	Horiz. Pt. Spacing	Edge Det.
1	−	−	−	+	+
2	+	−	−	−	−
3	−	+	−	−	+
4	+	+	−	+	−
5	−	−	+	+	−
6	+	−	+	−	+
7	−	+	+	−	−
8	+	+	+	+	+

The Flat Bone category was the first considered, and the sample bone studied was the scapula. The following table outlines the values of the factor levels for this experiment.

Table 5-2 Experimental Design Factor Levels for Flat Bone Category

Factor	−	+
Vert. Pt. Spacing	0.75 mm	1.0 mm
Coating	Powder	Paint
Orientation	Horizontal	Vertical
Horiz. Pt. Spacing (Min/Max)	0.75 mm/0.75 mm	1.0 mm/1.0 mm
Edge Detection	Auto	Delta

Each of the factor levels given above has been previously explained in detail with the exception of the terms provided for the orientation factor. These terms that describe the general manner by which the scapula was mounted refer to the direction of the scapula's major axis during the scanning procedure. Thus, the "Horizontal" orientation depicts the scapula lying on its side edge, with its longest axis nearly parallel to the

90

surface of the scanning plate and the "Vertical" orientation describes the scapula standing

upright on the scanning plate.

5.3 Analysis of Variance

Each of the eight runs of the experiment was performed and the parameters used

for each run of a fractional factorial design of experiments are best analyzed using an

analysis of variance [41]. The data results are as follows.

Table 5-3 Summary Results for the Flat BoneCategory Data

Horizontal Point Spacing (HPS)	Vertical Point Spacing (VPS)	Orientation (ORIEN)	Coating Type (COAT)	Edge Detection Algorithm (EDGE)	Scan Quality
1.0 mm	0.75 mm	Vertical	Powder	Auto	0.475
0.75	1.0	Vertical	Powder	Auto	0.536
0.75	0.75	Vertical	Paint	Delta	0.624
1.0	1.0	Vertical	Paint	Delta	0.568
1.0	0.75	Horizontal	Powder	Delta	0.435
0.75	1.0	Horizontal	Powder	Delta	0.478
0.75	0.75	Horizontal	Paint	Auto	0.577
1.0	1.0	Horizontal	Paint	Auto	0.535

Outlined below are the results obtained through the use of a statistical software

package for the "Flat" category design given above.

91

Table 5-4 Analysis of Variance Results for the Flat Category

ANALYSIS OF VARIANCE TABLE FOR QUALITY

SOURCE	DF	SS	MS	F	P
VPS (A)	1	1.800E-05	1.800E-05	0.28	0.6513
COAT (B)	1	0.07220	0.07220	1110.77	0.0009
ORIENT (C)	1	0.01584	0.01584	243.72	0.0041
HPS (D)	1	0.02040	0.02040	313.88	0.0032
EDGE (E)	1	1.620E-04	1.620E-04	2.49	0.2552
ERROR	2	1.300E-04	1.620E-04		
TOTAL	7	0.10875			

CASES INCLUDED 8 MISSING CASES 24

This analysis of variance shows three of the five variables having a significantly low p-value, which leads one to reject the standard null hypothesis that the factor level means are equal. These results demonstrate credible evidence that the variability witnessed in the scan quality was largely the result of the change in coating type, horizontal point spacing, and part orientation. Further, the change in values of the vertical point spacing and edge detection method does not significantly affect the quality of the resultant scan data. This finding makes sense intuitively, as the vertical point spacing simply changes the distance between cross-sectional scans and the edge detection algorithm changes only the manner by which edge points are initially discovered. Neither of these variables changes the manner by which data is acquired along a given cross-section, like the other three variables.

Although these findings demonstrate the importance of the three influential variables, and satisfy the need sought in this research, additional experimentation of a more precise nature would more closely identify the specific affects of each variable. Multiple replications of scans of a single structure, or multiple scans of many of the same

92

kinds of structures, will enable more specific conclusions to be developed for each independent variable and each structure.

Further replications of this experimental design, using alternative scan subjects, such as the humerus bone from the "Long" bone category yield similar results. In each case, substantial evidence exists to suggest that the three aforementioned factors contribute most to the change in quality.

As a result, upon observing similar repeated results from the experimental design, in conjunction with the knowledge that the time available to scan each specimen was limited, the design of experiments was altered to focus more closely on those significant variables. Therefore more specific conclusions could be drawn with respect to these three variables based on more subtle variations in their factor levels, most specifically with the orientation and mounting of the scan parts.

5.4 Scanning Results and General Conclusions

The results obtained through the experimental design indicated that three variables contributed most to the improvement in scan quality: horizontal point spacing, coating type, and part orientation. These three variables most affect the procedure by which data is collected on a given cross-section, so, intuitively, it makes sense that these would be the variables that most affect the overall scan quality. In contrast, the two variables deemed inconsequential to the quality outcome deal only with the number of cross-sections inspected (vertical point spacing) and the manner by which the device identifies its target (edge detection approach).

93

Within these three factors deemed most important to the success of the scan, it is clear that a more dense point cloud, or smaller horizontal point spacing, produces a more accurate scan with fewer imperfections. However, the increase in density of the point cloud often leads to additional minor editing of the data, all of which are easily solved using repair algorithms contained within this text. Never does the increase in point cloud density lead to algorithmically unsolvable data problems that would not have existed with a less dense data set. The converse is often true, however. Occasionally a low-density data set will exhibit data imperfections, such as a hole of missing points, which a high density set will eliminate through its more defined search for data.

Even more apparent is the advantage observed from using a dull, matte white paint, rather than the talcum powder or even a glossy paint, as the part coating material. Initially, the research focused on the perceived advantage of using white paint as a coating substance, rather than the talcum powder that is typically used when scanning manufactured pieces. As the results from the analyses of variance showed unmistakable evidence that the quality resulting from the use of white paint was obviously better than that resulting from the use of the powder, due to the excretion of moisture from the biological tissues, further experimentation was performed to determine the best type of white paint for these application. This analysis strongly indicated that a dull, matte paint coating led to increased scan quality. Just by observing the scan procedure take place, one can see the reflection of the laser beam was more focused when using a matte paint, the alternative of which would lead to possibly unnecessarily missing findable points.

94

However, the variable that most affects the quality of a scan, regardless of the results that a self-defined quality measure presents when substantial effort was spent providing high quality in both levels of the factor, is the part mounting and orientation. Any gains in quality seen as a result of optimizing the other variable settings can quickly be lost when improperly orienting the specimen. Furthermore, a subtle alteration of a part's orientation can lead to a substantial increase or decrease in scan quality. Often, in cases of extremely odd-shaped parts, a small number of iterations of orientations can lead to a considerable improvement in quality. Some observations for improving scan quality through part mounting and orientation are given below.

- Whenever possible, the part should be mounted so that as little surface area as possible directly faces the rotating plate and the ceiling. Because the laser only moves in the X and Y directions, important geometries can be lost along the top and bottom faces of the part.

- For the same reason, concavities and holes should never be faced directly up or down unless is has been determined that obtaining their geometric data is unnecessary.

- Often there is a specific region of interest along the geometry of the part. In these cases, ensure that the laser has an unobstructed sight line to all faces of this region of interest.

- If the geometry of a hole is a region of interest, ensure that the hole faces the laser at an angle between 30° and 45° from vertical. This enables the laser to have a direct line of sight to the interior faces of the hole and will

95

minimize the loss of points. Note, however, that the internal geometries of holes are very difficult to obtain because the line of sight to one edge of the hole is often blocked by the other edge.

- If the geometry of a deep concavity is a region of interest, ensure that the hole directly faces the laser. This will give the laser a line of sight to gather any information it can from the deep concavity. Unfortunately, these obstructions are extremely difficult geometries to obtain and are often impossible.

- All mounting devices within the scan radius should be painted black whenever possible. The sensors of the laser scanner will be unable to collect point data at these locations.

- When using mounting devices, if the devices contact the part within the scan radius, ensure that the devices contact the part in locations where it will be easy to determine the location of missing points by simply observing several adjacent layers. For example, along the shaft of a long bone the geometry does not change a great deal from one layer to the next. In such cases, the resulting data holes can be easily filled through interpolation.

Unfortunately, despite the substantial insight it provided, the quality measure that served as the dependent variable in the analysis of the design of experiments proved to be unable to tell the whole story of the quality of a scan. It is possible for an unusable scan to receive a fairly high quality score according to this standard. In these cases, a large

96

majority of cross-sections collect perfect data, while a small percentage of cross-sections collect very poor data that must be discarded. This poor data collection always occurs at oddly shaped, and thus usually important, regions of the item.

This unfortunate phenomenon should not discard the findings of the design of experiments, which became even more apparent as further testing outside the original design was performed. Rather, these observable facts demonstrate more clearly the importance of correct mounting and orientation of items. As a result, the remainder of the experimentation was spent determining the best mounting and orientation methods for each item. The horizontal point spacing continued to be varied based on the size, complexity, and detail required for each part.

Thus, for each of the bone categories, the following settings should be used:

- Coating – the original design of experiments and additional experimentation confirmed that a dull, matte, white paint is the best coating substance for bony structures. If unavailable, a glossy white paint produces acceptable, but inferior results.

- Edge Detection protocol – the design of experiments confirmed that this proprietary setting had little or no effect on the quality of the scan. Experience and observation showed that the default "automatic" setting led to slightly faster scan duration, and is therefore the recommended setting.

- Vertical Point Spacing – the design of experiments confirmed that a change in this variable did not affect the output quality of the scan.

97

However, it is obvious to see that this setting changes the density of collected points, an important element when developing a lifelike model. Thus, this setting should continue to be altered based on the size of the item in question. Good results were obtained with slice intervals as small as 0.35 mm, but anything smaller than this produced erratic data collection. Typically a setting of 0.5 mm is sufficiently small to obtain precise data of any size part. For large parts whose geometry is simple, a slice layer of up to 1.0 mm captures enough detail to create a meticulous surface model. Setting recommendations are given for each of the specific classifications below.

- Horizontal Point Spacing – in much the same way as the Vertical Point Spacing setting, this setting may continue to be altered by classification. Good results were observed for settings as low as 0.4 mm, but for larger less detailed items a value of between 0.75 mm and 1.0 mm produced acceptable results. Furthermore, an advantage to the user is that there are two settings for this variable (minimum and maximum). In cases where the data obtained symptomatically contains holes throughout the scan, and other orientations and mounting options have been exhausted, setting these values unequal to each other often helps improve the scan data. This occurs because the scanner is not forced to obtain a point at a specific location, but rather is permitted to search through a small range to obtain a

98

point. Setting recommendations are given for each of the specific classifications below.

- Part Mounting and Orientation – the most volatile of variables, this setting often requires a small number of iterations before excellent results are obtained. The guidelines given above serve as a starting point for developing this setting, but usually the setting can be classification-specific. Only in rare instances, such as the scapula in the Flat category, does the setting require an application-specific mounting and orientation. Rather, the classification setting usually requires only application-specific adjustments to the common setting.

5.4.1 Flat Bones Specific Conclusions

The flat bone category contains bones that are either very easy to scan or very difficult to scan, and often require application-specific mounting and orientation due to extensive part complexity. The following variable settings can be uniformly set, as there are no elements whose size would dictate a change in parameter values.

- All of the elements may be scanned using the recommended matte white paint, provided that the surface of the bone has been sufficiently dried.

- The Vertical Point Spacing is best set between 0.5 and 0.75 mm, depending on the user's need for data.

- The Horizontal Point Spacing should also generally be set between 0.5 and 0.75 mm. If the appropriate circumstances arise, it is acceptable to set the

99

minimum and maximum values unequal to each other to allow the machine to select a point within a range rather than at an exact location.

- The orientation of the part should be such that its longest axis sits nearly vertically on the rotating plate, with a long, thin rod of any sort balancing the upper portion along an easily interpolated, or unimportant face of the bone. Generally, parts are mounted not on the rotating plate itself, but rather on a block of wood that is glued to the plate. Therefore, two nails hammered through the wood from the opposite side can elevate the portion of the bone resting on the wood. This eliminates the need to glue the bottom portion to the wood, which distorts the representation of the lower geometry.

- When mounting the sacrum, ensure that it rests is close to vertical as possible.

- When mounting the coxal, try to ensure that the femur insertion hole faces 30° to 45° toward the ceiling to capture as much of the interior surface of the hole as possible.

- When mounting the scapula, one should not rotate the bone in the manner depicted below in Figure 5-1, in which important elements of the bone's geometry face the turntable or ceiling. Rather, if the bone is rotated in the opposite direction, so that the important protrusions rest vertically, more elements of the odd geometry will be captured. This is a difficult bone to capture, and many iterations of the orientation may be required.

100

Figure 5-1 Improper angle for mounting scapula
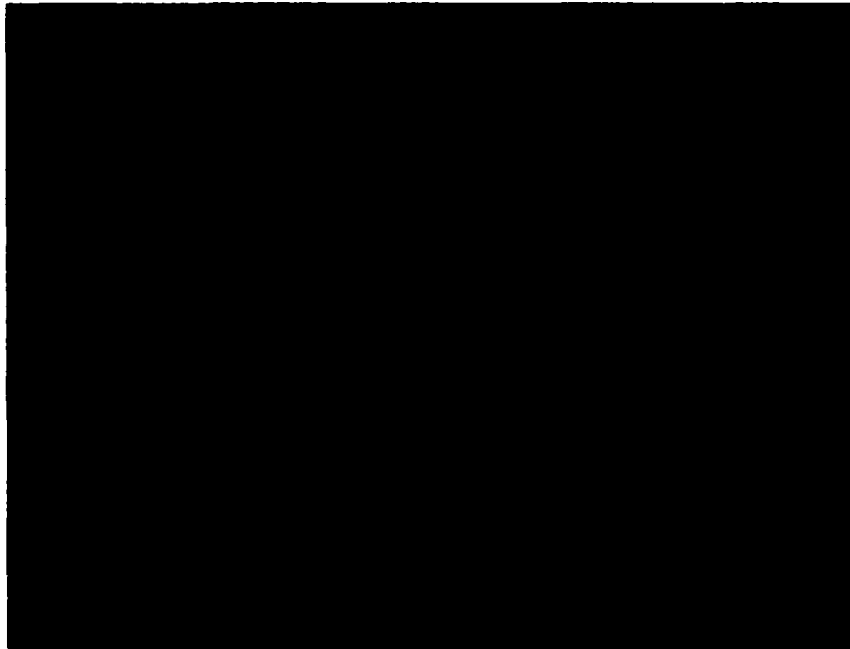
5.4.2 Long Bones Specific Conclusions

The bones of this category follow a very simple set of instructions, as each element has extremely similar shape. As a result, three alternative orientations are presented so that users may select the method that best suits their applications.

- All of the elements may be scanned using the recommended matte white paint, provided that the surface of the bone has been sufficiently dried.

- The Vertical Point Spacing is best set between 0.5 and 0.75 mm, depending on the user's need for data. However, if there are additional

101

time constraints, a value of 1.0 mm can be used on the larger bones of the class without substantial loss of quality.

- The Horizontal Point Spacing should also generally be set between 0.5 and 0.75 mm. Along the shaft portions of the bones, the point spacing may be relaxed to 1.0 mm if the data along this region does not have to be as dense.

There are several effective ways to mount and orient members of the Long bone category.

- The first method of orientation is a very flat, nearly horizontal orientation, as depicted in Figure 5-2. This method is only effective, and should only be used when the geometry of one end is the only important geometry. In this case, the bone rests on two thick posts at the top end and two nails drilled through the wood on the bottom end. The scan radius should only include the area of the important head. This minimizes the lost data at the top of the scan to a small surface area. In Figure 5-2, the top face of the geometry comes nearly to a single point. The draw back to such a method is a significant loss of data along one face of the shaft and at the opposite end of the bone.

Figure 5-2 Horizontal method of mounting Long bones.
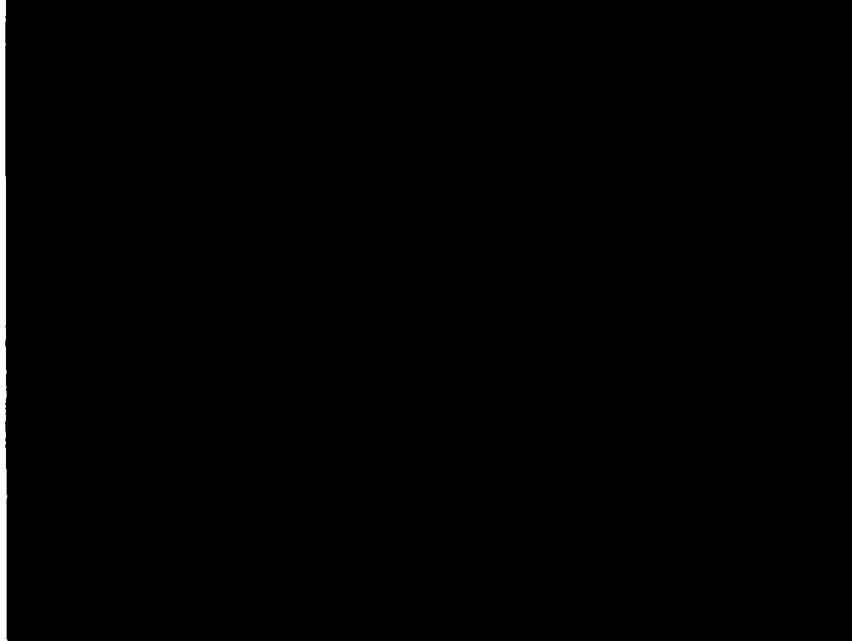
- The next method of mounting a long bone, as depicted in Figure 5-3, rests the shaft of the bone on two long posts (chopsticks work well) at an angle of approximately 30° from vertical and the bottom of the bone rests on nails that have been hammered through the wood base. The need for this orientation arises when the geometry of both ends are important. It minimizes the total lost data at the top and bottom faces.

103

Figure 5-3 Angular chopsticks method of mounting Long bones.
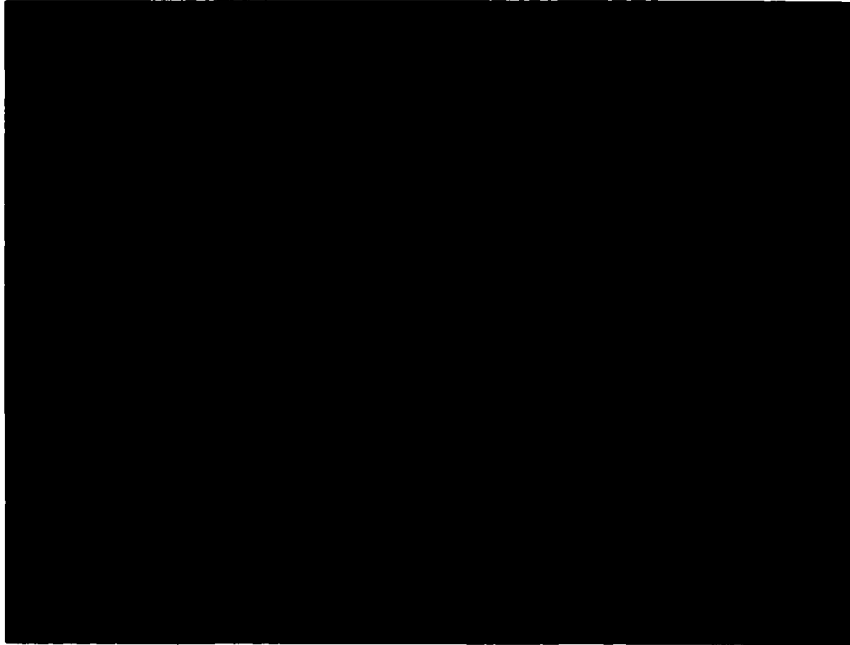
- The final method of mounting long bones is to drill a hole at one end and stand the bone upright on a mounted post, as in Figure 5-4. This method produced the highest quality of data along the shaft and at the top end. At the bottom, the data quality is good with the exception of the area of drilling. However, if this area is small, this orientation tends to perform the best of any of these possibilities.

104

Figure 5-4 Vertical method of mounting Long bones.
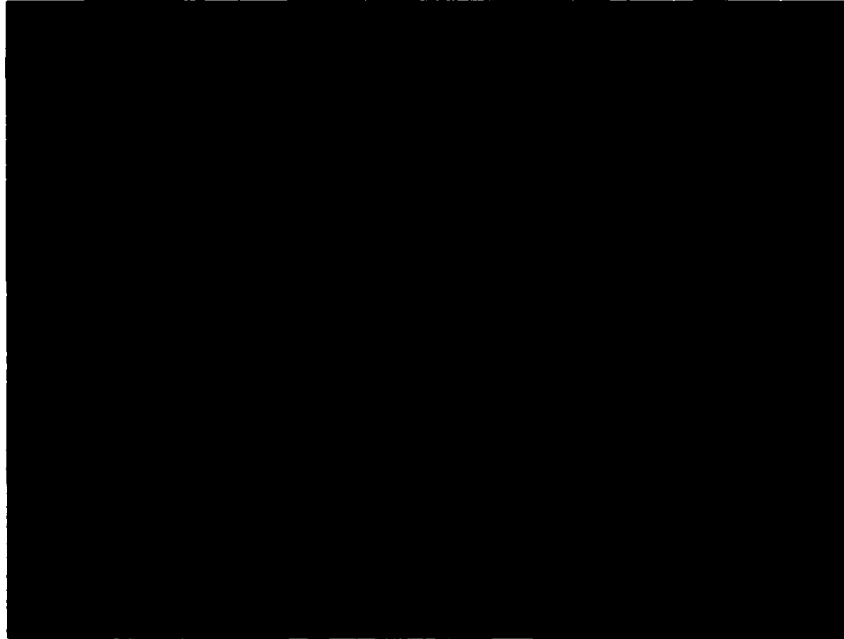
5.4.3 Short Bones Specific Conclusions

The bones of this category also follow a very simple set of instructions, as each element has a small, compact shape. However, due to the size limitations, the ways in which these bones need to be scanned are also limited.

- All of the elements may be scanned using the recommended matte white paint, provided that the surface of the bone has been sufficiently dried.

105

- The Vertical Point Spacing is best set at 0.5 mm or below, depending on the user's need for data. The size of the bones, and their typical fine detail nature require a very dense cloud of points.

- The Horizontal Point Spacing should also generally be set at or near 0.5 mm. If the appropriate circumstances arise, it is acceptable to set the minimum and maximum values unequal to each other to allow the equipment to select a point within a range rather than at an exact location.

- To mount the short bones, use a 1/16" drill bit to drill a small hole in a region of the bone where data loss is minimized, such as at a pointed end. Mount the bone by placing the end of a toothpick into this hole and into the base block of wood. Hot glue may be used to secure the toothpick in the wood.

Figure 5-5 Toothpick method of mounting Short bones.

106

5.4.4 Curved Bones Specific Conclusions

Bones of this class should be scanned using the same parameter settings as the Flat category, with the notable exception of insisting that the concave surface face the laser directly. In addition, it is important to make sure that the top or bottom faces of the concave surface do not cover any portion of the interior of the concavity, thus blocking the line of sight from the laser.

- All of the elements may be scanned using the recommended matte white paint, provided that the surface of the bone has been sufficiently dried.

- The Vertical Point Spacing is best set between 0.5 and 0.75 mm, depending on the user's need for data.

- The Horizontal Point Spacing should also generally be set between 0.5 and 0.75 mm. If the appropriate circumstances arise, it is acceptable to set the minimum and maximum values unequal to each other to allow the machine to select a point within a range rather than at an exact location.

- The orientation of the part should be such that its longest axis sits nearly vertically on the rotating plate, with a long, thin rod of any sort balancing the upper portion along an easily interpolated, or unimportant face of the bone.

5.4.5 Concave Bones Specific Conclusions

Bones of this class should be scanned using the same parameter settings as the Long category, with the notable exception of insisting that the curvature face the laser

107

directly, so that while sitting on the plate the bones look as close to the letter "C" as possible. In addition, it is important to make sure that the top or bottom heads of the bone do not cover any portion of the interior of the curvature, thus blocking the line of sight from the laser.

- All of the elements may be scanned using the recommended matte white paint, provided that the surface of the bone has been sufficiently dried.

- The Vertical Point Spacing is best set between 0.5 and 0.75 mm, depending on the user's need for data.

- The Horizontal Point Spacing should also generally be set between 0.5 and 0.75 mm. Along the shaft portions of the bones, the point spacing may be relaxed to 1.0 mm if the data along this region does not have to be as dense.

- The orientation of the part should be such that its longest axis sits nearly vertically on the rotating plate, with a long, thin rod of any sort balancing the upper portion along an easily interpolated, or unimportant face of the bone.

- An alternative to this orientation, which is an easier method to set up, is to set the curvature so that the bone looks like the letter "U" with both ends of the curvature facing upwards. The curved ends of the bones are held upright by two posts and two nails protruding from the wood base elevate the curvature. This method should be used when the ends of the bone are the important elements of the geometry.

5.4.6 Vertebral Bones Specific Conclusions

The bones of this class are very difficult to scan effectively due to the foramen and irregularities of the shapes. As previously stated, when a hole is present, as is in each of these cases, it is best to mount the part at a slight angle so that points of the interior faces of the hole may be seen by the laser.

- All of the elements may be scanned using the recommended matte white paint, provided that the surface of the bone has been sufficiently dried.

- The ideal Vertical Point Spacing is at most 0.75 mm. The intricate irregularities in the shapes require a very dense cloud.

- The Horizontal Point Spacing should generally be set between 0.5 and 0.75 mm. It is recommended to set the minimum and maximum values unequal to each other to allow the machine to select a point within a range rather than at an exact location.

- When orienting bones from the Vertebral category, mount them such that the transverse axis is mounted vertically on the scanning plate. As always when negotiating a hole in the part, the bone should be slightly leaned so that the laser may have lines of sight into the interior of the hole. However, in these cases, be sure that the angle of lean is very small, i.e. very close to vertical, due to the great depth of these holes.

109

5.4.7 Interior Facial Bones Specific Conclusions

The bones of this class are poor applications for this type of data acquisition method. The multiple layers of thin bony tissue and random holes along these several planes would be impossible for a laser which moves along a single plane to negotiate. A different method of data acquisition, such as MRI digitization, is recommended despite the excessive time requirements of the process.

5.4.8 Soft Tissue Specific Conclusions

Initially perceived as a poor application to the laser scanning technology as well, the data acquisition of the soft tissue category can perform moderately well. However, there are several limitations to the use of this method for a soft tissue application. First, the nature of soft tissue is such that if the tissue is not kept sufficiently moist, the loss of moisture will cause a significant change in geometry in a very short period of time, a matter of only minutes. As a result, scanning could only take place in a period of three to five minutes, which drastically limits the scan area. Usually no more than five or six cross-sections can be scanned at a time.

- Because the item must be kept so moist, it is impossible to use a coating substance to maximize the reflective beam. Thus, unless the tissue is completely white, as it is in many cases, there will be a significant loss of data. Further, the translucent nature of the soft tissue often results in an inaccurate reflective beam, which in turn results in inaccuracy.

110

- The Vertical Point Spacing is best set at 0.5 mm or below, depending on the user's need for data. The size of the bones, and their typical fine detail nature require a very dense cloud of points.

- The Horizontal Point Spacing should also generally be set at or near 0.5 mm. If the appropriate circumstances arise, it is acceptable to set the minimum and maximum values unequal to each other to allow the equipment to select a point within a range rather than at an exact location.

- To mount the soft tissue, a mounting apparatus was built. This apparatus consisted of two binder clips, one glued to a base block of wood, and the other glued to a metal strip, which is attached to long rod that is screwed into the turntable plate. Figure 5-6 depicts the apparatus holding a ligament in place. A strip of black electrical tape was placed around the metal rod at the height that the scanning was to take place. Thus, the scanner will not find data points along this rod.

111

Figure 5-6 Soft tissue mounting apparatus.

- When scanning soft tissue, only a handful of cross-sections may be digitized at a time. After which, the tissue must be removed and soaked in saline to preserve its shape. Thus, in order to scan the entire item from top to bottom, the laser scanner must be paused every four to five minutes so that the part may be moistened. When moistening, it is important that the location of the part is not altered by touch. Extreme sensitivity is essential.

112

6.0 REPAIR ALGORITHMS

The final element of the research is the development of an algorithm, or set of algorithms, capable of the reconstruction of imperfect data files from the laser scan. In tandem with the methodology development portion of the proposed research, a goal of this research project is to determine how and why these imperfect data files occur. Often the evidence is found as a result of the scanning methodologies, for the cause of the imperfections often lies in the scanning variables and the manner in which these variables are administered. In these cases, preventative information has been built into the scanning methodologies.

Unfortunately, if the preventative forecasters fail or do not exist, researchers are often left with an imperfect scan to manually repair. Therefore, because the parameters being studied may not always be the source of imperfection, the development and implementation of interpolation algorithms into a self-contained algorithm was explored. A typical example of an editing decision that this algorithm automatically resolves is the choice of whether to alter the location of a stray point, given that there is doubt whether a point is accurate or astray. At present, the operator determines visually, and sometimes erroneously, if the point is accurate. This portion of the research determined that the computer has the ability to detect and make the user aware of possible stray points based on built-in estimation procedures.

113

6.1 Editing Tasks

Three types of errors occur during the laser scanning process: stray points, data holes, and split or crossed contours. The most difficult of these errors to repair manually is the split or crossed contours, a relatively common occurrence among laser scanning data, typically arising from oddly shaped parts or poor part orientation. Manually, however, the most difficult error to repair proved to be the elimination of data holes. Significant research has been performed with the intent to develop solid models of specific human bones. In many instances, researchers have shown the ability to transform a Computed Tomography scan into point data that can be further manipulated to produce a solid model. To do so, they fit closed contours to the perimeter points obtained from the individual cross-sections, and then lofted these contours to develop the three-dimensional model. The closed contours are fitted using a Bernstein Basis Function network, an adaptive approach to determining a small number of control points that enables a closed Bezier curve to be constructed from the measured points. The weights of the neural network represent the control points of the defining polygon net used to generate the closed Bezier curves.

This procedure should also be followed in a step of the process of repairing imperfect scan data from reverse engineering equipment as well. The data obtained using the laser scanning equipment is very similar to the exterior surface data obtained by extracting point data from a CT scan. Thus, in the case of a faultless scan, no modifications to the previously researched method would be necessary. This method would have the capability of transforming the laser scan data into a solid model. The

114

algorithms developed herein are designed to complement that of Knopf [34] and Al-Naji [2] for reverse engineering applications.

6.1.1 Algorithm Requirements

Research and expert opinion [50] revealed that all errors that can occur during the laser scanning process can be classified into three core error groups: contour misrepresentation, stray points, and data holes. Proprietary software programs for laser scanning equipment provide the tools essential for manually editing the data files to correct these errors, but no software performs these tasks automatically. Rather, the proprietary software packages provide only data smoothing features to repair scan data without human intervention. As a result, an experienced user of the equipment and associated software perform these editing tasks manually. This series of algorithms will mimic the standard thought process that these skilled users employ at each step during the editing procedure to automatically repair the data that meet its user-defined criteria.

Undoubtedly, the scanning error easiest to notice and rectify is contour misrepresentation. In this case, the scanning software either erroneously connects two non-adjacent data points, usually on opposite sides of the part surface creating two contours when there should actually be only one, or the software erroneously connects two or more contours together into one. The former scenario is extremely common while the latter is rare. To solve these types of errors, the repair algorithm will contain a boundary-tracking algorithm that will properly link adjacent edge points in sequence, which will properly order the points along the boundary of the contour. To do this, the

115

algorithm must first have the capability of deciphering the accurate number of contours in a given cross-section, and then have the ability to determine the order in which each point within the contour should be connected.

The least common of the core errors to repair is the stray point, a relatively infrequent occurrence among laser scanning data, typically arising as a result of improper coating, extraneous material along the surface of the part, poor part orientation, or simply random error. However, in general, if the laser-scanning machine locates a point, the point it finds is accurate. If the scanner suggests that a data point appears to be stray, it was probably caused by either extraneous matter attached to the scan item or by translucence of the item, which often leads to a poor reflective beam. By evaluating an error value of each cross-sectional contour point from the Bezier curve calculated by the Knopf/Al-Naji method [2,34], this algorithm will mimic the manual editing operation by determining a point to be stray if it exceeds a threshold error value from the expected contour edge. In such a case, a software user should be informed that the point should be eliminated from the contour and the curve should then be re-evaluated.

Data holes will also be repaired after the process of constructing the Bezier curves has been completed. The algorithm will replace the missing data along the cross-sectional Bezier curve at the point spacing interval provided by the user at the start of the scan. Data holes vary in width, from a single missed point to losses of over half of the cross-sectional perimeter, and everything in between. It is widely believed that the scanning method that the user employs during the set-up procedure contributes directly to the elimination of these types of errors. As such, by following the methodologies

116

previously presented, a user will reduce considerably the loss of data through data holes. Small data holes are very common and easy to correct because the perimeter of the cross-section is obvious in these cases. The cause of such cases are usually poor part coating, deep concavities, or the blocking of laser's line of sight to the part surface by either the mounting device or another portion of the part itself. Larger data holes occur for the same reasons as small data holes, but usually result from a poor part orientation, which causes the blockage of the laser's line of sight to a substantial portion of the part surface. These variations must be treated differently, from requiring only the addition of a single or few points along the obvious shape of the contour to the deletion of the entire contour.

In the case of only a few missing points along the contour perimeter, the points may be simply replaced along the Bezier curve, whose shape will not be distorted from a small number of missing points. However, in the case of a data hole missing a more influential number of consecutive points, the shape of the constructed Bezier curve would be slightly different. Thus, following the logic of experienced editors of data files, the algorithm will repair the hole by comparing the nearest neighbor data points on adjacent cross-sectional layers and placing a point at a linearly interpolated location in the current layer.

In the case of a hole that is missing an excessive number of data points the contour should be eliminated. In these cases, it is deemed that the contour has lost so significant an amount of data that any attempt to reconstruct the contour is counterproductive. Following the methodology developed for the structure significantly reduced this possibility.

117

Naturally, these cutoff points between the three classifications of data holes may be altered based on the preference of the user and the point spacing of the scan. However, for the purposes of the validation of the algorithms, these limits were set at three percent and fifteen percent of the total number of points in the layer, respectively. In other words, if there are 200 points in a given cross-section, a hole that should contain six or fewer additional data points is considered to be a small hole and is repaired without the need to validate their location by examining adjacent layers, and a hole that should contain seven to thirty additional data points is considered a larger hole and is repaired with the aid of the adjacent layer inspection. Holes of more than thirty data points represent such a significant loss of data that the contour is discarded.

6.2 Additional Background Information

To repair the three core scanning errors, and then allow the user to verify the correctness of the automatic repairs, six steps are actually needed: contour clustering, contour sequencing, contour fitting, stray point elimination, data hole filling, and user verification. Once the tasks of repairing an imperfect data file were identified, additional research was necessary to determine the tools required to solve these tasks.

6.2.1 Neural Networks – Kohonen Self-Organizing Map

The field of neural networks has developed several methods whose goal is to classify an input signal into output categories, or into clusters. Methods have been

118

developed that incorporate supervised learning, when target values are available for training patterns, and unsupervised learning, when training data is unavailable [22].

"During the self-organizing process, developed by Kohonen, the cluster unit whose weight vector matches the input pattern most closely (typically, the square of the minimum Euclidean distance) is chosen as the winner. The winning unit and its neighboring units update their weights [22]." The architecture and algorithm of the network can then be used to cluster a set of continuous-valued vectors into a finite set of clusters.

These neural networks have been applied to various problems including character recognition, clustering, and even the traveling salesman problem [22].

6.2.2 Traveling Salesman Problem

The traveling salesman problem is a classical combinatorial optimization problem that is easy to state but very difficult to solve. The problem is to determine the shortest path through a set of vertices so that each vertex is visited exactly once. Several algorithms have been developed in the fields of operations research and neural networks to solve this problem [52].

The exact algorithms, designed to find the optimal solution, are typically derived from an integer linear programming formulation or a branch and bound algorithm [38]. The formulation for an integer linear programming method is as follows [52]:

119

Minimize $\sum_i \sum_j d_{ij} x_{ij}$

Subject to: $\sum_j x_{ij} = 1, \qquad i = 1,...,N$

$\sum_i x_{ij} = 1, \qquad j = 1,...,N$

$(x_{ij}) \in X$

$x_{ij} = 0 \text{ or } 1,$

where d_{ij} is the distance between vertices i and j and the x_{ij}'s are the decision variables: x_{ij} is set to 1 when arc(i,j) is included in the tour, and 0 otherwise. $(x_{ij}) \in X$ denotes the set of subtour-breaking constraints that restrict the feasible solutions to those consisting of a single tour.

Potvin [52] notes that problems with a few hundred vertices can now be routinely solved to optimality, which allows this procedure to apply directly to this application.

Alternative solution methods have more recently been applied to this problem in the area of neural networks. Although the quality of solutions obtained via neural networks is lower than those obtained through the classical solutions of operations research, the neural network technology provides a means to solve these problems at great speeds [52].

6.2.3 Bezier Curves and Bernstein Basis Functions

Bezier curves, named for Pierre Bezier, are parametrically defined curves that can be expressed mathematically as a weighted average of a set of points, called control

120

vertices, which are connected in sequence to form an open or closed control polygon [8]. The end points of the curve and the endpoints of the polygon are coincidental, although the curve does not necessarily coincide with any of the interior vertices [8]. As such, to define a closed contour using a Bezier curve, the first and last control points must be equal.

Barsky [8] describes the evaluation of the Bezier curve as follows:

"A particular point on the curve corresponds to a specific set of weights applied to these control vertices. As the values of these weights are varied, the curve is then traced out. Each weighting factor is a function of a parameter. Thus, the connection between the value of the parameter and a point on a curve is established by evaluating each of these weighting functions at the particular value of the parameter and then computing the corresponding weighted average."

He further explains that the Bezier curve is constructed in the following manner [8]:

Consider a control polygon V=[V_0, ..., V_i, ..., V_d]. A Bezier curve of degree d, denoted by $Q_d(u)$ is defined by:

$$Q_d(u) = \sum_{i=0}^{d} V_i B_{i,d}(u), \ u \in [0,1]$$

where $B_{i,d}(u)$ is the ith Bernstein polynomial of degree d

$$B_{i,d}(u) = \binom{d}{i} u^i (1-u)^{d-i}, \ i=0,...,d.$$

This definition will be used to insert missing points along the path of the constructed Bezier curve. As previously mentioned, Al-Naji [2] showed that a Bezier curve is easily fit through a set of data points collected from the surface of bony tissue. This data was obtained from a computed tomography scan and manipulated to only

121

contain the edge data points. Further, Lancaster [37] presents a method to calculate the shortest distance from a point to a Bezier curve, which will be used to determine if a point exceeds the user-defined error threshold for determining whether a point is stray and should be deleted.

6.2.4 Shape Description

Three simple shape descriptors, and the manner in which they change throughout the cross-sectional layers of the scan data, will be provided to the user to evaluate the effectiveness of the scan and its automatic repair. The first descriptor is the data centroid, a measure of the center of the data on each two-dimensional cross-section. This value is calculated by simply determining the average value of the X and Y coordinates for each layer. The second descriptor is the elongatedness, a simple measure of the area within the contours of the cross-section. This value will be calculated by the ratio between the length and width of the region-bounding rectangle. The final descriptor is the sum of the perimeter path values, obtained from the traveling salesman problem that will be performed to obtain the correct sequence of data points in each contour, for each cross-section.

The values obtained for all layers of the scan data can be plotted on the same graph to show any change in pattern between levels, which will provide the user with an opportunity to examine the effectiveness of the automatic repair process.

122

6.3 Algorithm Construction

The algorithm assumes that the bottom and top layers of the scan have been manually edited. This detail becomes necessary during the data hole filling subroutine and this logic will become more apparent at that time. Once the first layer is manually edited, or confirmed to have no imperfections, the algorithm begins to reconstruct the layers from the bottom up.

The first task is to identify the number of contours on the current layer, and then sequence each of these contours according to the traveling salesman solution. This will provide the shortest tour of the data perimeter, invariably providing the accurate sequence, and always eliminating the primary obstacle of the contour misrepresentation error, the split or crossed contour. Other heuristics, such as the nearest neighbor algorithm, routinely produce incorrect tours, especially in the cases of imperfect data.

Once the appropriate sequence of each contour on the current cross-section is determined, a Bezier curve is fit to each contour in the manner detailed by Al-Naji [2] and Knopf [34]. At this point, the remaining two core errors may be edited. First, the data holes may be filled, and then stray points can be deleted.

The algorithm proceeds through the same stages for each of the cross-sectional layers. Upon completion, the final stage of the algorithm allows the user to observe the summary statistics that will identify any obvious distortions in the data, and allow the user to determine whether these distortions are accurate.

123

6.3.1 Conceptual Algorithm

This algorithm ties together the five sub-algorithms in the appropriate sequence. The sequence was determined through experience, expert user interviews, and simple logic. It performs each of the five algorithms on each cross-sectional layer of data and then executes the adjacent layer comparison algorithm for the user's benefit.

IMPERFECT DATA RECONSTRUCTION ALGORITHM

Step 0.   Obtain imperfect scan data.

- Laser scan piece

- Export data in X, Y, Z text format

- Data will be sorted by Z value, obtaining cross-sectional slices

Step 1.   Select lowest Z value cross-section that has not been fit by the "Imperfect Data Reconstruction Algorithm."

Step 2.   Apply "Clustering Algorithm" to determine the number of contours within this cross-sectional layer.

Step 3.   For each contour in the cross-section, apply the "Edge Tracking Algorithm" to link the edge points into the appropriate sequence.

- Ordered edge points stored in real coordinate values expressed in metric units

Step 4.   Apply the "Contour Fitting Algorithm" as proposed by Al-Naji [2] and Knopf [34] to each contour of the current cross-section.

124

Step 5.   Apply "Stray Point and Hole Repair Algorithm" to each contour in the cross-section.

Step 6.   Apply the "Adjacent Layer Comparison Algorithm."

Step 7.   Save the fitted cross-section. Are there any remaining unfitted cross-sections?

- If Yes, proceed to Step 1.

- If No, Done. These contours may be lofted to create a solid model.

6.3.2 Clustering Algorithm

This algorithm utilizes the Kohonen self-organizing map algorithm presented by Fausett [22] and is easily solved using neural network software packages such as NeuralWorks™. In this algorithm, the points are clustered together without the need for training data. Other neural network algorithms are available that require training data if available. These algorithms tend to produce better results in a timelier manner, but the need for training data requires additional steps that may not be desired by users of this methodology.

CONTOUR CLUSTERING ALGORITHM (As presented by Fausett [22])

Step 0.   Randomly initialize weights, w_{ij}, unless some information is available concerning the distribution of clusters.

Set the parameters for the radius of the neighborhood, R, and the learning rate, α.

125

Step 1. While stopping condition is false, do Steps 2-8.

Step 2. For each input vector X, do Steps 3-5.

Step 3. For each j, compute $D(j) = \sum_i (w_{ij} - x_i)^2$.

Step 4. Find index J such that D(J) is a minimum.

Step 5. For all units j within a specified neighborhood of J, and for all i:

$$w_{ij}(new) = w_{ij}(old) + \alpha[x_i - w_{ij}(old)].$$

Step 6. Update learning rate.

Step 7. Reduce radius of neighborhood at specified times.

Step 8. Test stopping condition.

6.3.3 Edge Tracking Algorithm

This algorithm is simply the integer programming formulation, which searches for the minimum distance, or tour, around a set of points. In this application, the goal of this algorithm is to eliminate the crossed or split contours that erroneously occur through the scanning process. Because the scan data points are always less than one millimeter apart, except in cases involving data holes, the optimal tour is always the perimeter of the contour. Only in rare hypothetical cases, and in no instance using actual scan data during the validation process, was the optimal tour not the perimeter tour of the contour.

126

EDGE TRACKING ALGORITHM

Minimize $\quad \sum_i \sum_j d_{ij} x_{ij}$

Subject to: $\quad \sum_j x_{ij} = 1, \qquad i = 1,...,N$

$$\sum_i x_{ij} = 1, \qquad j = 1,...,N$$

$$(x_{ij}) \in X$$

$$x_{ij} = 0 \text{ or } 1,$$

where d_{ij} is the distance between vertices i and j and the x_{ij}'s are the decision variables: x_{ij} is set to 1 when $\text{arc}(i,j)$ is included in the tour, and 0 otherwise. $(x_{ij}) \in X$ denotes the set of subtour-breaking constraints that restrict the feasible solutions to those consisting of a single tour.

6.3.4 Contour Fitting

As previously indicated, this algorithm fits a Bernstein-Bezier curve to the scan data. Developed at the University of Western Ontario, this method was developed to transform data obtained from a CT scan into a solid model. An intermediate step in this process produced a data set similar to those obtained through the laser scanning process. It is at this point where the following algorithm begins to construct a curve through the data points.

127

CONTOUR FITTING ALGORITHM (As presented by Al-Naji [2])

Step 0.   Set the parameter values required for the desired output as follows:

- Set the initial desired degree of curve n, (where number of control points is n+1)

- Set the average error to a desired accuracy, E_2.

- Set the maximum number of cycles through the training to equal k_{max}.

Step 1.   Assign a parametric value $u_{t,j}$ to each edge data point, $p_{t,j}$, using the centripetal parameterization algorithm.

The parameter value $u_{t,j}$ assigned to the tth data point in slice j is given by:

$$u_{t,j} = u_{t-1,j} + \frac{\| p_{t,j} - p_{(t-1)j} \|^{1/2}}{\sum_{t=1}^{T-1} \| p_{(t+1)j} - p_{t,j} \|^{1/2}}, \text{ where } u_{1,j} = 0, \ u_{T,j} = 1, \ \|.\| \text{ is the}$$

distance metric, and $p_{t,j}$ is the tth data point.

Step 2.   For the first cross-section, initialize the weights, $w_{i,1}$, to small random values taken around the centroid of the data set $[P_1]$. For all other cross-sections, j>1, initialize the weights to the converged weight values obtained from the previous cross-sectional plane, $w_{i,j-1}$.

Step 3.   To ensure C^0 continuity for the closed Bezier curve, set the weight values $w_{0,j} = p_{1,j}$ and $w_{n,j} = p_{T,j}$.

Step 4.   While the stopping condition is false, do Steps 5-10.

Step 5.   Randomly select a training pair $(u_{t,j}, p_{t,j})$ from the current contour.

128

Step 6. Determine the output of the basis function neurons in layer 1 by computing the Bernstein basis functions at $u_{t,j}$ using

$$\phi_{i,n}(u_{t,j}) = \frac{n!}{i!(n-1)!} u_{t,j}^{i}(1-u_{t,j})^{n-1}.$$

Step 7. Determine the response of the neurons in the output layer by calculating the Bezier curve coordinate values at $u_{t,j}$ using $S_{xy}(u_{t,j}) = \sum_{i=0}^{n} \phi_{i,n}(u_{t,j})w_{i,j}$.

Step 8. Calculate the error for each output neuron in layer 2 by

$$e_{xt} = x(u_{t,j}) - x_{i,j}$$

$$e_{yt} = y(u_{t,j}) - y_{i,j},$$

where the error vector is given by $e_t = [e_{xt}, e_{yt}]$.

Step 9. Update the weights for $i = 1,2,...,n-1$ according to

$w_{i,j}(k+1) = w_{i,j}(k) + \alpha(e_t\phi_{i,n}(u_{t,j}) + \Delta w_{i,j}(k))$, where the momentum

term is $\Delta w_{i,j}(k) = w_{i,j}(k) - w_{i,j}(k-1)$.

Step 10. While considering 1st order continuity, update both second and second to last weights, $i = 1$ and n -1, according to $w_{i,j}(k+1) = w_{i,j}(k) + \beta(\Delta G)$

where $\beta = 0.01$, and the slope at the polygon end-points is given by

$$\Delta G = (w_{n,j}(k) - w_{n-1,j}(k)) - (w_{1,j}(k) - w_{0,j}(k)).$$

Step 11. Calculate the mean-squared error by $MSE_j = \frac{1}{T}\sum_{t=1}^{T} e_t e_t^{T}$, where T is the total number of data points, and T is the vector transpose.

129

Step 12.   Test for stopping conditions:

- If $MSEj \leq E_2$ then Stop.

- If $MSEj > E_2$ and $k < k_{max}$ then go to Step 4.

- If $MSEj > E_2$ and $k = k_{max}$, then:

  o Add a desired number of control points to the total number of control points used in order to improve the curve fit accuracy.

  o Reset the number of iterations to $k = 1$.

  o If the number of control points is greater than maximum number allowed for computations then Stop, otherwise go to Step 2.

6.3.5 Stray Point Elimination and Hole Repair

This algorithm repairs the remaining two core errors based on the Bezier curve previously constructed. As indicated, the algorithm determines the severity of the holes to be filled by calculating the distance between the hole's endpoints and comparing this distance to the average horizontal point spacing. If the hole is determined to be small (as is most typical of data holes), it is filled simply be adding points along the Bezier curve. Larger holes are filled through the linear interpolation of the nearest X-Y point in the layer below, which is why the bottommost layer must be manually altered initially, and the nearest X-Y neighbor in the nearest five layers above the current layer. Five layers must be considered above the current layer because typically large holes repeat themselves in adjacent layers. Thus, if five layers are considered, the hole is not expected

130

to exist at all five layers. If it does exist in all five of the examined layers, the scan was poorly executed and a change in part orientation is needed.

STRAY POINT AND HOLE REPAIR ALGORITHM

Step 1.   Are there any data holes missing less than three percent of the total number of data points in the contour?

- If Yes, proceed to Step 2.

- If No, proceed to Step 3.

Step 2.   Fill these small holes by defining points along the fitted Bezier curve at neighbor distances equal to the average Horizontal Point Spacing. Proceed to Step 3.

Step 3.   Are there any data holes missing less than 15 percent of the total number of data points in the contour?

- If Yes, proceed to Step 4.

- If No, proceed to Step 6.

Step 4.   Define an estimate point clockwise along the constructed Bezier curve at a distance equal to the average Horizontal Point Spacing from the endpoint of the hole. Using linear interpolation, move this point between the nearest X-Y neighbor in the layer immediately below the current layer and the nearest X-Y neighbor in the nearest five layers immediately above the current layer. Proceed to Step 1.

131

Step 5. Are there any data holes missing more than 15 percent of the total number of data points in the contour?

- If Yes, proceed to Step 6.

- If No, proceed to Step 7.

Step 6. Prompt user to delete this contour.

- If Yes, delete all points from this current contour.

- If No, proceed to Step 4.

Step 7. Are there any points X_i whose normal distance from the fitted Bezier curve is greater than the user-defined error value E_1?

- If Yes, proceed to Step 8.

- If No, proceed to Step 9.

Step 8. Inform user that this point should be deleted.

- If agreed, delete this point X_i, and proceed to Step 9.

- If not agreed, proceed to Step 9.

Step 9. Are there any unfitted contours remaining at this level?

- If Yes, set the next contour as the "current" contour and proceed to Step 3.

- If No, Done. Return to "Imperfect Data Reconstruction Algorithm."

132

6.3.6 Adjacent Layer Comparison

This algorithm calculates three summary statistics for user verification.

ADJACENT LAYER COMPARISON ALGORITHM

Step 0.   Obtain complete scan data set.

Step 1.   Calculate the centroid, elongatedness, and obtain the traveling salesman

              solution for the optimal tour of the perimeter.

Step 2.   Graph each of the variables separately, connecting the values of adjacent

              layers.

Step 3.   Display each graph so that the user may determine the effectiveness of the

              scan and automatic repair process.

6.4 Validation

The sub-algorithms defined above were evaluated and their effectiveness verified. The primary focus of the validation effort was based on the algorithms' applicability to a given problem. To show the applicability of this set of algorithms, they are put to the test of editing a scan of a scapula bone, which are very difficult to scan effectively and result in several imperfections, often many on a single cross-section. The three dimensional view of the unedited scan is below.

133

Figure 6-1 3-D representation of scapula with noticeable errors
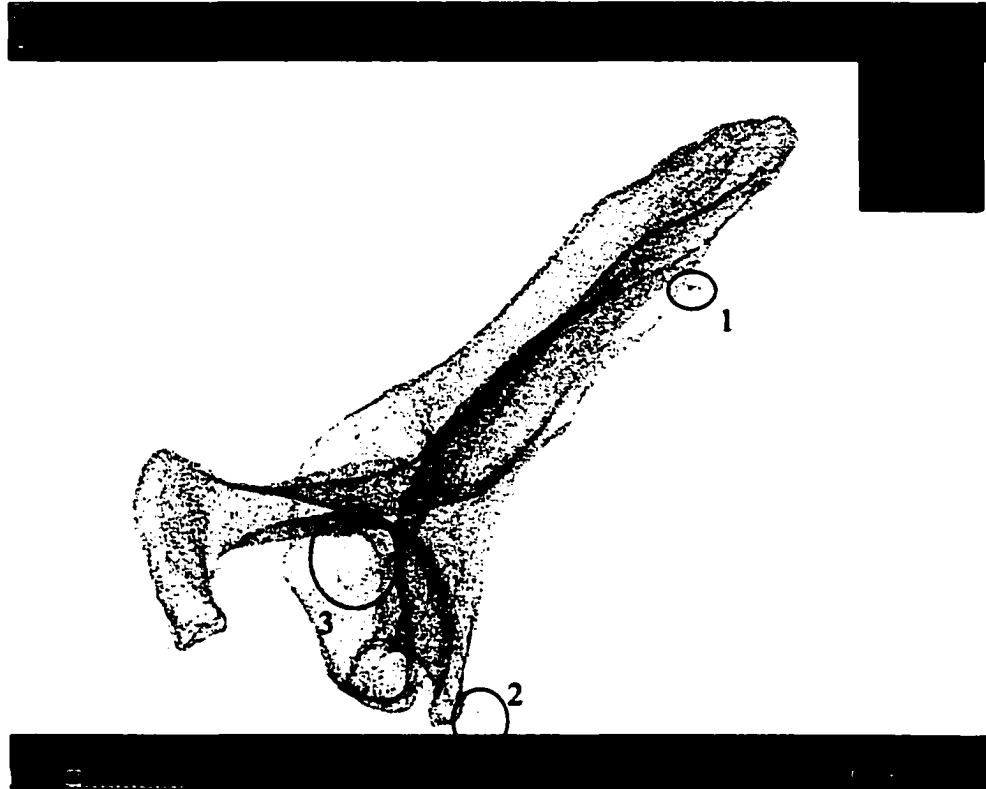
This three-dimensional image indicates that the scan data, for the most part, is good. Evidence of stray data points arising from the mounting apparatus exist in Circles 1 and 2 and evidence of a data hole exists in Circle 3. As one looks closer at each cross-section however, glaring imperfections exist, specifically near the protruding regions and in the point sequencing throughout the scan.

134

Figure 6-2 Z Level 124 - Sequencing and Holes


Figure 6-2 Z Level 124 - Sequencing and Holes
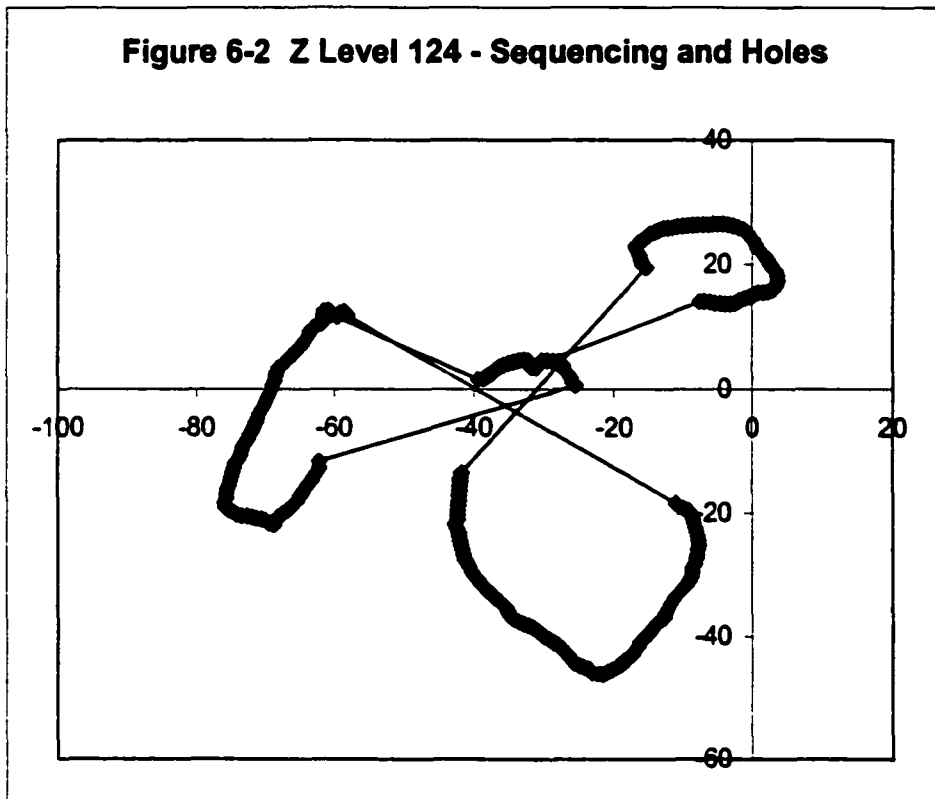
Clearly the cross-section from cross-section 124 (of 165) requires substantial editing. There are clearly three contours, each of which has at least one large hole. As the verification process proceeds, cross-sectional examples will be provided to illustrate the effects of each routine.

The primary algorithm, which calls upon the five sub-algorithms for its data, is best verified subjectively. The algorithm is structured such that its processes mimic those of expert users of laser scanning systems. For each cross-section, these users visually identify the number of contours, and then properly sequence the data points within them before filling any data holes and removing any stray points. Further, the order in which the subroutines are called follow a logical progression. Before any work can begin on a cross-section, the number of contours must be known. If, for example, this routine was

135

called after the ordering routine, traveling salesman algorithm would be performed on the entire cross-section of data, and the optimal tour would inaccurately join two contours into one. Also, because the reconstruction of data holes and stray points requires the knowledge of the Bezier curve, this algorithm must be called after the contour fitting routine. Thus, the proposed order in which the primary algorithm calls its subroutines is most efficient.

The clustering algorithm was verified using the NeuralWorks™ software package, which has the ability to use the Kohonen self-organizing mapping technique described above. Using a learning rate of α=0.25,the Kohonen structure was able to correctly cluster all of the cross-sectional layers into the appropriate number of contours, except for those contours with two or more larger holes within the contour. However, cases such as these are rare if the appropriate steps are taken in the scanning procedure. In the following example, as in nearly all of the cross-sections, the network correctly identified the two clusters without error.

Figure 6-3 Z Level 134 - Clustering

136
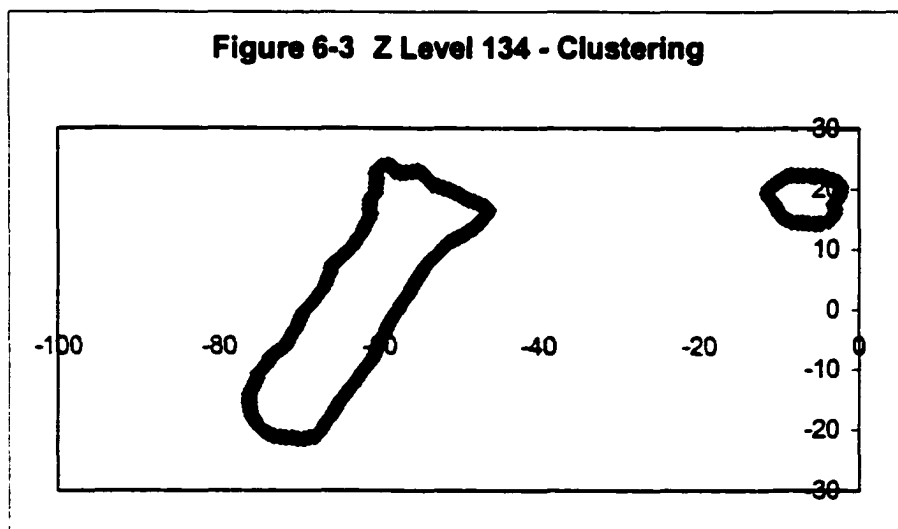
The next step in the algorithm calls the traveling salesman algorithm for data sequencing. The focus of this research is not to argue the effectiveness of the different methods of obtaining the optimal tour, but rather to show that the traveling salesman problem itself is the correct approach to sequencing surface data obtained by a laser scanner. The validation of these algorithms has been demonstrated many times in the past. In fact, every contour tested for this validation was sequenced correctly. The following before and after diagram is an example of alterations seen through this process.

Figure 6-4a Z Level 147 - Before Sequencing

Figure 6-4b After Sequencing
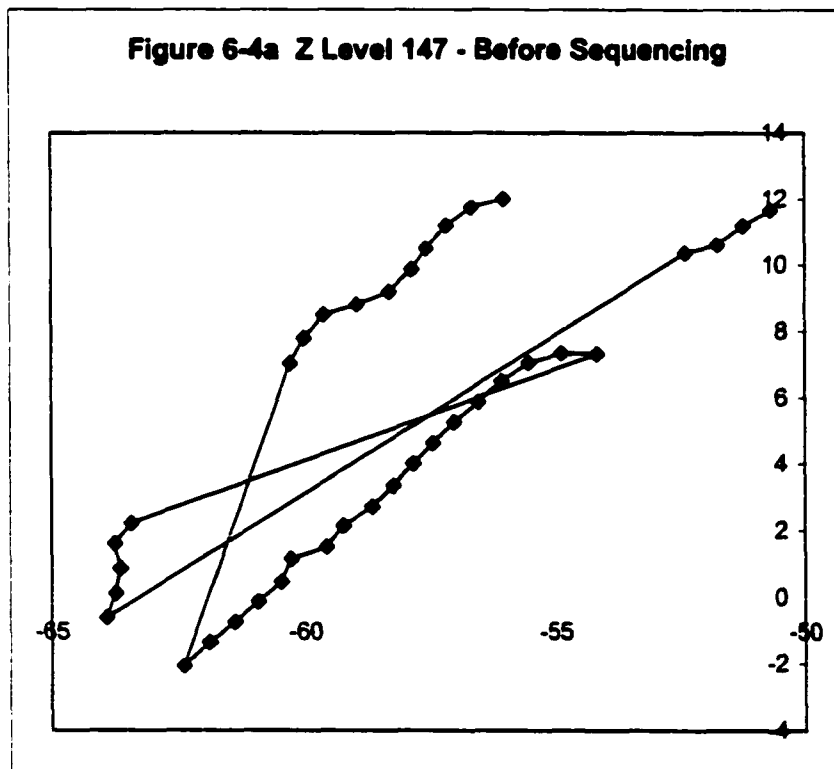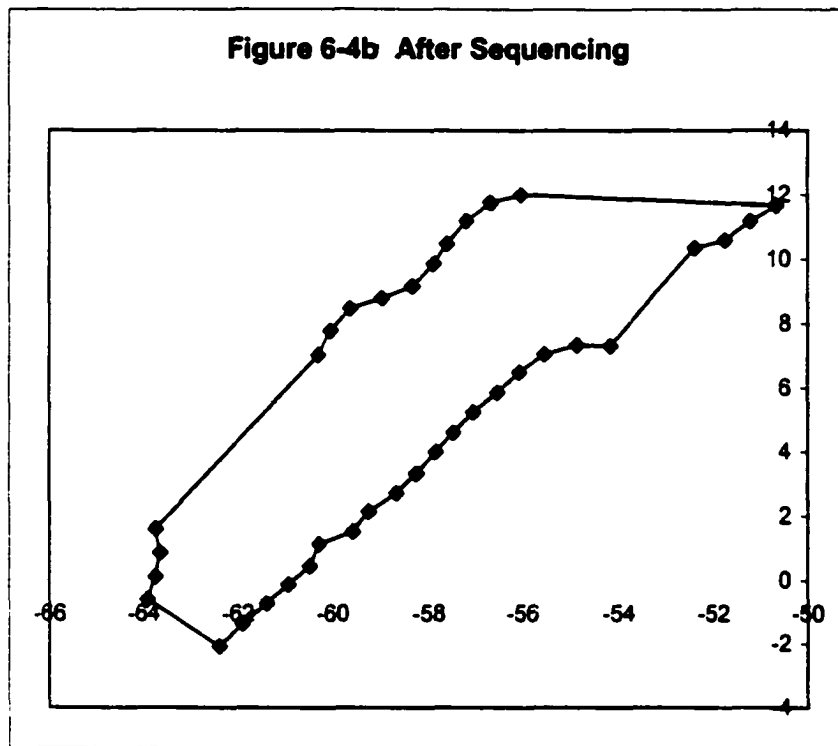
After the contours are appropriately identified and sequenced, thereby editing the contour misrepresentation core error, the Bezier curve must be constructed so that the remaining core errors can be edited. Al-Naji [2] has already shown the applicability of this technique and validated its results. Consider the following example that shows a layer of data (with tick marks at point locations) and its adjacent layers (without tick marks). Notice the hole at the bottom of the plot.

138

Figure 6-5 A data hole in a single scapula cross-section
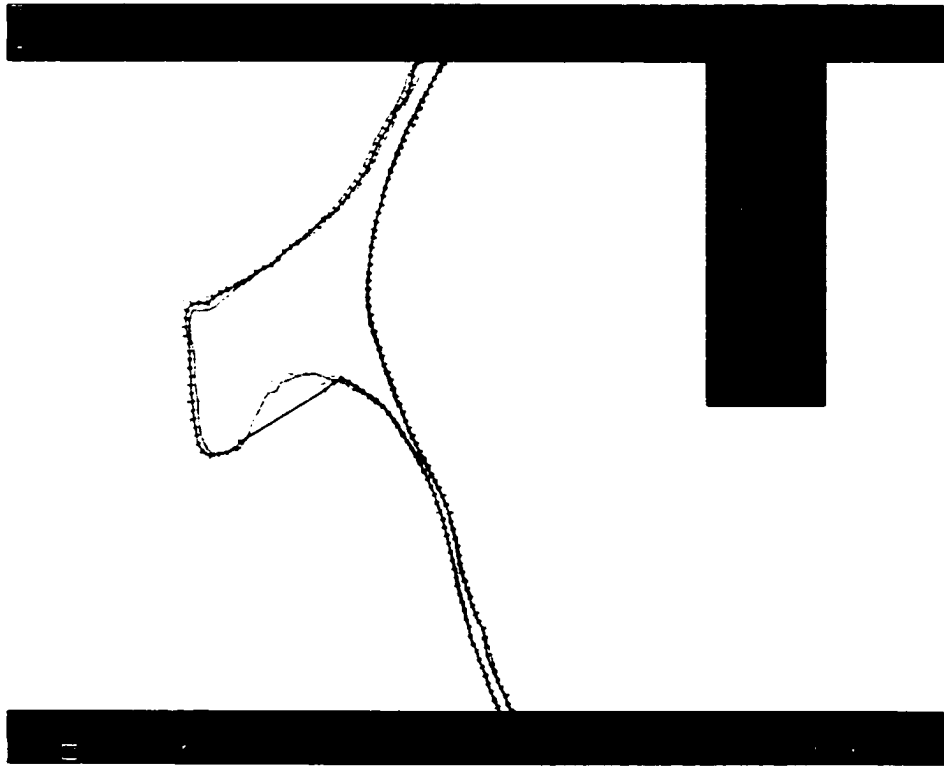
If this hole is calculated to be small, and knowing the Bezier curve equation from the Al-Naji algorithm, points can be easily defined along this curve using well-known equations. In the case of the larger hole, once the points are defined along the curve, they are further manipulated to interpolate the distance between the lower and upper layers. In a similar manner, once the Bezier curve has been defined, stray points can be eliminated by calculating their distance from the Bezier curve using well-known equations. If the distance exceeds a user-defined threshold limit, the point should be eliminated. Finally, by plotting the summary statistics of the scan data, the user determine if there are any cross-sections whose data appear abnormal.

139

After performing each of these steps manually, the three-dimensional representation below reveals a smoother appearance without the obvious errors and the resulting solid model obtained through a rapid prototyping technology showed a very refined, smooth, and accurate structure.

Figure 6-6 Edited 3-D representation of scapula
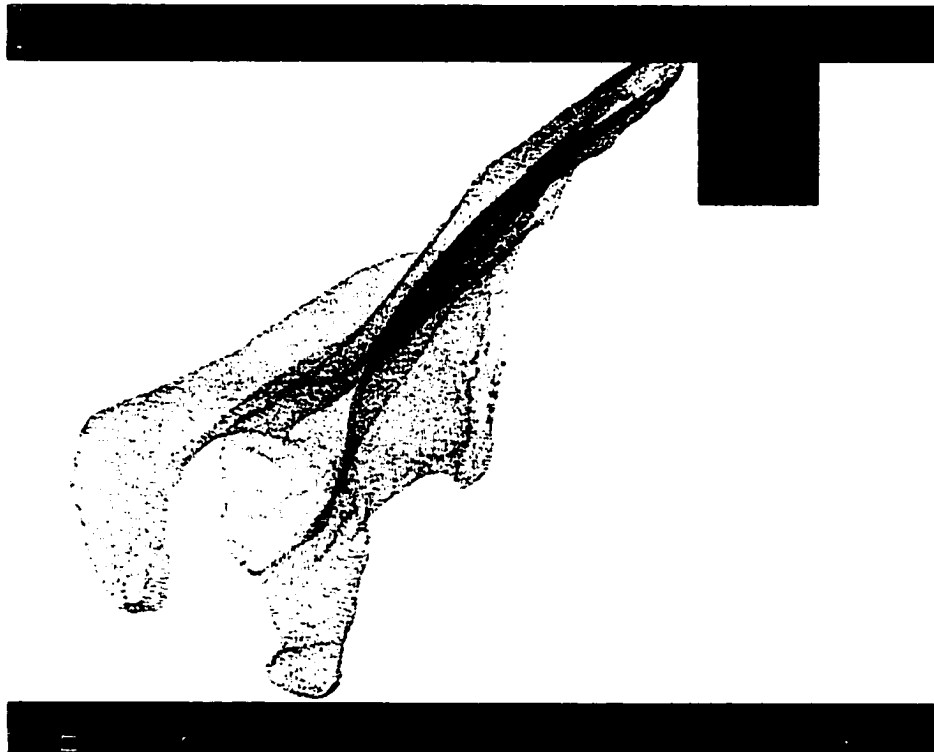
7.0 SUMMARY

7.1 Conclusions

This research has seen successful conclusions but has also identified areas that will require further research to fully understand. The objectives of this research were to standardize and automate the reverse engineering process in the medical and orthopaedic research arena. To achieve this objective, a detailed, structured methodology for obtaining super-accurate geometric data has been developed for all classifications of the human musculoskeletal system. In so doing, this research has led to the further conclusion that the reverse engineering process can be facilitated through the use of group technology, by utilizing part families. And finally, a conceptual algorithm was developed to repair the inevitable imperfect data obtained through this process.

In general, the development of the scanning methodologies was very successful. Clear evidence was obtained that demonstrates that substantial improvement in scan quality can be obtained by utilizing the appropriate scanning parameter settings, and more significantly, by orienting the item correctly. The traditional mentality that suggests that scanning methods, and specifically orientations, should be determined on a case-by-case basis is inaccurate and unnecessary. Although some parts have notable obstacles that may require alterations to a scanning methodology, there is no question that most structures can be classified into part families that have similar, if not identical requirements for reverse engineering.

141

Further, the development of the set of algorithms laid a foundation for further research along this topic. The "parent" algorithm that calls upon the five sub-algorithms is very sound. The approach that it follows mirrors that of every expert user of laser scanning systems and their software editors. Additionally, by bringing into the process the traveling salesman algorithm and the Bezier curve fitting methodology, the basis for future improvement of the algorithm is developed. The general structure and many of the sub-algorithms appear to fit well within the context of this application. Further research should be performed to perfect each of the subroutines so that the algorithm's results approach those of expert users.

7.2 Future Research

Additional work needs to be done perfecting the algorithm developed within. As it currently operates, the quality of this algorithm's editing does not compare to that from expert users of the system because the algorithm does not currently have the ability to make probabilistic decisions. The need for these kinds of decisions becomes noteworthy during the point insertion, or data hole repair. There is a need for a probabilistic point insertion algorithm that takes into account all of the surrounding point cloud rather than the nearest neighbors in adjacent layers.

The natural extension to the work described herein is to apply the same principles to the contact scanning technology. The contact scanning machines are able to produce more accurate data in a faster time frame, but have limitations in its abilities to scan over five axes. However, with a rotating fixture, such as that of the laser scanner, these

142

limitations could be reduced. Currently, the best results in terms of accuracy and quality of surface finish are obtained using contact reverse engineering systems. Contact systems have several fundamental advantages over non-contact systems [9]:

- Treatment of surfaces to prevent reflections is not required

- Vertical faces can be accurately scanned

- Data density is not fixed and is automatically controlled by the shape of the component

- Time-consuming manual editing of the data to remove stray points is not required

- Post processing for cutting can be faster as surface offsetting may not be required

- Very tiny detail can be accurately replicated

This would provide the possibility of further improving the goals of this research, to develop better quality data files at a faster and more cost-effective rate.

Further, as new technologies arise and existing technologies improve, this research must be adapted to keep pace. To date, the new and improved technologies have already substantially improved, and will continue to improve upon the scanning rate, or speed, the primary focus of the current reverse engineering community. New technology has implemented a method of spreading the laser beam across the entire scanning cross-section to collect data points at a rate nearly a hundred times the rate of point range technology. Moreover, the use of multiple laser sources within a scanning apparatus could increase this rate further. Because the scan duration was only a secondary

143

consideration of this research, the conclusions developed herein remain valid. Improved quality will always be of primary importance to reverse engineers and manufacturers alike, as improved scan quality inevitably leads to a healthier bottom line.

A second natural extension of this research would be to branch out the scanned items to include manufactured parts. Many of the same obstacles that face the medical researcher have existed for some time in manufacturing industries as well. The existence of structured methodologies for reverse engineers to digitize manufactured parts by part family rather than through application-specific methodologies would reduce the learning curve associated with instructing new users as well as provide a framework for consistency and repeatability.

In addition, this research provides a framework to expand the orthopaedic research of reverse engineering technologies. For example, orthopaedic researchers may desire the ability to distinguish between rough and smooth texture of a tissue simply by viewing a data file of a part that they have never seen or touched. To determine the methodology and scanning protocol required to obtain such precise data would facilitate the distribution of data throughout the community.

BIBLIOGRAPHY

BIBLIOGRAPHY

1. Adachi, J., et al., "Surgical Simulation Using Rapid Prototyping," *Proceedings of the Fourth International Conference on Rapid Prototyping*, University of Dayton, Ohio, 1993, pg. 135.

2. Al-Naji, Rasha, "Reconstruction of bone geometry for the manufacture of customized radial head implants," Unpublished M.S. Thesis, Department of Mechanical and Materials Engineering, School of Engineering Science, The University of Western Ontario, May, 1998.

3. Amenta, Nina, and Marshall Bern, "Surface Reconstruction By Voronoi Filtering," *14th Symposium on Computation Geometry*, June 1998.

4. Amenta, Nina, Marshall Bern, and Manolis Kamvysselis, "A New Voronoi-Based Surface Reconstruction Algorithm, *SIGGRAPH '98*, Orlando, Florida, July 19-24, 1998, web.mit.edu/manoli/www/crust/sigcrust.pdf.

5. American College of Radiology, "Radiology Resource," http://www.radiologyresource.org, Feb. 4, 2001.

6. Baker, Joan, Bellevue Community College, Ultrasound Program, http://facweb.bcc.ctc.edu/jbaker, July 7, 2000.

7. Baribeau, R. and M. Rioux, "Influence of Speckle on Laser Range Finders," *Applied Optics*, 30(20), July 1991, pg. 2873-2878.

8. Barsky, Brian A., "Parametric Bernstein/Bezier Curves and Tensor Product Surfaces," *ACM/SIGGRAPH '90 Course 25*, Dallas, Texas, August 7, 1990.

9. Bidanda, B., S. Motavelli, and K. Harding, "Reverse Engineering: An Evaluation of Prospective Non-Contact Technologies and Applications in Manufacturing Systems," *International Journal of Computer Aided Manufacturing*, Vol. 4, No. 3, 1991, pg. 145-156.

10. Bidanda, Bopaya and Yasser A. Hosni, "Reverse Engineering and Its Relevance to Industrial Engineering: A Critical Overview," *Comput. Ind. Eng.*, Vol. 26, No. 2, 1994, pg. 343-348.

11. Bidanda, Bopaya, Vivek Narayanan, and Richard Billo, *Handbook of Design, Manufacturing, and Automation*, Ch. 48, "Reverse Engineering and Rapid Prototyping," John Wiley & Sons, Inc., New York, 1994.

12. Borromeo, Renee, Physical Therapist Assistant Program, Pennsylvania State University, "PT 384: Kinesiology – Anatomy Pictures," http://www.ma.psu.edu/~pt/384anat.htm, Mar. 17, 2000.

13. Bracewell, Ronald N., *Two-Dimensional Imaging*, Prentice Hall, Englewood Cliffs, New Jersey, 1995.

14. Butson, Matthew and Waguih H. El Maraghy, "Evaluation of Reverse Engineering Techniques," *Autofact '96: Rapid Design and Manufacturing Conference Proceedings*, Detroit, 1996, pg. 48-64.

15. California State University at Chico, Department of Anthropology, "The Skull Model," http://www.csuchico.edu/anth/Module/skull.htm, May 1, 1999.

16. Clunie, David, Medical Image Format FAQ, http://www.dclunie.com/medical-image-faq/html, May 8, 2001.

17. Curless, Brian, "New Methods for Surface Reconstruction from Range Images," Ph.D. Dissertation, Department of Electrical Engineering, School of Engineering, Stanford University, June 1997.

18. Curless, Brian, and Marc Levoy, "A Volumetric Method for Building Complex Models from Range Images," *SIGGRAPH '96 Proceedings*, July 1996, pg. 303-312.

19. Curless, Brian, and Marc Levoy, "Better Optical Triangulation Through Spacetime Analysis," *International Conference on Computer Vision '95*, http://graphics.stanford.edu/papers/spacetime/paper_2_levels/paper.html, Sept. 5, 1996.

20. Digibotics, Inc., "Accurate and Automatic 3D Laser Digitizing Systems," http://www.digibotics.com, Oct. 14, 1999.

21. Dorsch, R.G., G. Hausler, and J.M. Herrmann, "Laser Triangulation: Fundamental Uncertainty in Distance Measurement," *Applied Optics*, 33(7), March 1994, pg. 1306-1314.

22. Fausett, Laurene, *Fundamentals of Neural Networks: Architecture, Algorithms, and Applications*, Prentice Hall, Upper Saddle River, New Jersey, 1994.

23. Freund, John E., *Mathematical Statistics*, 5th Ed., Prentice Hall, Inc., Englewood Cliffs, New Jersey, 1992.

24. Gaunt, W. A. and P. N. Gaunt, *Three Dimensional Reconstruction in Biology*, University Park Press, Baltimore, Maryland, 1978.

25. Geiger, Bernhard and Marinos Ioannides, "Reverse Engineering and Rapid Prototyping Techniques in Medicine," *International Conference on Medical Physics and Biomedical Engineering*, University of Cyprus, 1994, Vol 1, pg. 48-52.

26. Heart Imaging, http://www.heartimaging.com/faqs/faqs3.htm, Aug. 27, 2000.

27. Hoppe, Hugues, "Surface Reconstruction from Unorganized Points," Ph.D. Dissertation, Department of Computer Science and Engineering, College of Engineering, University of Washington, 1994.

28. Hornak, Joseph P., "The Basics of MRI," http://www.cis.rit.edu/htbooks/mri/, July 14, 1999.

29. Ingle, Kathryn A., *Reverse Engineering*, McGraw-Hill, Inc., New York, 1994.

30. Jacob, A., et al., "First Experience in the Use of Stereolithography in Medicine," *Proceedings of the Fourth International Conference on Rapid Prototyping*, University of Dayton, Ohio, 1993, pg. 121.

31. Kai, Chua Chee and Leong Kah Fai, *Rapid Prototyping: Principles and Applications in Manufacturing*, John Wiley & Sons, New York, 1997.

32. Kaisto, I. et al., "Laser Range Finding Techniques in the Sensing of 3-D Objects, Sensing and Reconstruction of Three-Dimensional Objects and Scenes," *SPIE-The International Society for Optical Engineering*, Santa Clara, Feb. 1990, pg. 122-133.

33. Kappelman, John, Timothy Ryan, and Myriam Zylstra, "The Digital Library as a Platform for Studying Anatomical Form and Function," *D-Lib Magazine*, Vol. 5, No. 9, September 1999, http://www.dlib.org/dlib/september99/kappelman/09kappelman.html.

34. Knopf, G. K., and X-G. Guo, "Bernstein Basis Finctions (BBF) Network for surface reconstruction," *Applications of Artificial Neural Networks in Image Processing*, SPIE 3030-16, San Jose, California, February 9-14, 1997, pg. 116-124.

35. Lahr, Steven, "Lateral Ankle," Ithaca College, http://www.ithaca.edu/faculty/lahr/LE2000/ankle%20pics/2posterolatankle-new.jpg, June 21, 2001.

36. Lambert, Tim, "Realizing a Delaunay Triangulation," *Information Processing Letters*, Vol. 62(5), June 13, 1997, pg. 245-250, http://www.cse.unsw.edu.au/~lambert/java/realize.

37. Lancaster, Don, "The Guru's Lair," http://www.tinaja.com/glib/bezdist.pdf.

38. Laporte, G., "The Traveling Salesman Problem: An Overview of Exact and Approximate Algorithms," *European Journal of Operational Research*, Vol. 59, No. 2, 1992, pg. 231-247.

39. Louderback, Jeff, "Area labs make strides in high-tech health care," *Dayton Business Journal*, http://dayton.bcentral.com/dayton/stories/1999/01/18/focus3.html, Jan. 18, 1999.

40. Martini, Frederic H., *Fundamentals of Anatomy and Physiology*, Prentice Hall, Inc., Upper Saddle River, New Jersey, 1998.

41. Montgomery, Douglas C., *Design and Analysis of Experiments*, 4th Ed., John Wiley & Sons, New York, 1997.

42. Montgomery, Kevin, National Biocomputation Center, "3-D Reconstruction," http://biocomp.stanford.edu/3dreconstruction, May 13, 2001.

43. Morgan, Christopher J. and William R. Hendee, *Introduction to Magnetic Resonance Imaging*, Multi-Media Publishing, Inc., Denver, 1984.

44. Musculoskeletal Research Center, University of Pittsburgh, Department of Orthopaedics, http://www.pitt.edu/~msrc, June 14, 2001.

45. National Collegiate Athletic Association, Injury Surveillance System, "Spring study shows many baseball, softball injuries occur on base path," http://www.ncaa.org/news/2000/20000925/active/3720n13.html, Sept. 25, 2000.

46. Neter, et al., *Applied Linear Statistical Models*, 4th Ed., McGraw Hill Companies, Inc., Chicago, 1996.

47. Oldendorf, William and William Oldendorf Jr., *Basics of Magnetic Resonance Imaging*, Martinus Nijhoff Publishing, Boston, 1988.

48. Ostrofsky, Benjamin, *Design, Planning, and Development Methodology*, Prentice-Hall, Inc., Englewood Cliffs, New Jersey, 1977.

49. Penn State College of Medicine, "Department of Radiology," http://www.xray.hmc.psu.edu/.

50. Personal Communication with Russ Beck, Digibotics Inc., University of Pittsburgh, Pittsburgh, PA, February 19, 1999.

51. Potamianos, P., et al., "Rapid Prototyping For Orthopaedic Surgery," *Proc. Instn. Mech. Engrs.*, Vol 2112, Part H, 1998, pg. 383-393.

52. Potvin, Jean-Yves, "The Traveling Salesman Problem: A Neural Network Perspective," *ORSA Journal on Computing*, Vol. 5, No. 4, Fall 1993, pg. 328-348.

53. Qinghang Li, et al., "The affecting factors on the application accuracy of image guided surgical localization systems," Wayne State University, Department of Neurological Surgery, http://www.neurosurg.wayne.edu/cas/pub/accuracy.html, Mar. 1, 2001.

54. Renishaw, Inc., http://www.renishaw.com, Aug. 2, 2000.

55. Renishaw, Inc., Instructional Presentation, University of Pittsburgh, Pittsburgh, PA, July 6-7, 2000.

56. Romans, Lois E., *Introduction to Computed Tomography*, Williams & Wilkins, Baltimore, 1995.

57. Rosse, Cornelius, and D. Kay Clawson, *The Musculoskeletal System in Health and Disease*, Harper and Row, New York, 1980.

58. Seeram, Euclid, *Computed Tomography: Physical Principles, Clinical Applications, and Quality Control*, W. B. Saunders Co., Philadelphia, 1994.

59. Shanahan, Donal, Anatomy and Clinical Skills Centre, The Medical School, University of New Castle, "The Hyoid," http://www.fmcc.org.uk/~nds4/tutorials/larynx/text/hyoid.html, Aug. 12, 2001.

60. Shung, K. Kirk et al., *Principles of Medical Imaging*, Academic Press, Inc., New York, 1992.

61. Siddall, James N., *Optimal Engineering Design: Principles and Applications*, Marcel Dekker, Inc., New York, 1982.

62. Sigal, Robert et al., *Magnetic Resonance Imaging: Basis for Interpretation*, Springer-Verlag, New York, 1988.

63. Stone, Kevin R., The Stone Foundation for Sports Medicine and Arthritis Research, http://www.stoneclinic.com, Feb. 15, 2001.

150

64. The eSkeletons Project, "The Human Skeleton," http://www.eskeletons.org, Aug. 10, 2001.

65. The Johns Hopkins University Medical Institutions, "Better Burn Mask," http://www.hopkinsmedicine.org/healthnewsfeed/hnf_846.htm, April 26, 2001.

66. True Sport, "NCAA Injury Statistics," http://www.rocketarm.com/injury-stats.html, Feb. 15, 2001.

67. Tumer, Irem, "University of Texas Reverse Engineering Internet Web Site," http://shimano.me.utexas.edu/~irem/rev_eng, Apr. 17, 1999.

68. Wood, Kristin L. and Kevin N. Otto, "A Reverse Engineering Design Methodology," http://madlab.me.utexas.edu/papers/reverse/reverse_1992/rev1.htm, Aug. 26, 2001.

69. Wood, Kristin L. and Kevin N. Otto, "Reverse Engineering and Redesign," http://madlab.me.utexas.edu/papers/reverse/reverse_1996/dtm1523/rev2.htm, Aug. 26, 2001.

70. Yu, Zhao, The Stanford Visible Female, Stanford Medical School, "Information Frames – Pelvic Bones," http://k-2.stanford.edu/~yuzhao/Pelvis-Infoframes/frames/coccyx.html.